An Evaluation and Development of Bonding Technologies for Rapid Disassembly of Automotive Vehicles

By Yuchen Lu

Oxford Brookes University

A thesis submitted in partial fulfilment of the requirements for the award of Doctor of Philosophy

January 2015

Abstract

The end-of-life vehicle (ELV) situation, international legislation and recycling issues for future multi-material vehicles all necessitate the development of new joining solutions which enable rapid disassembly for automotive vehicle maintenance or recycling scenarios. In this thesis, the innovations in adhesive disbonding technologies were comprehensively reviewed and divided into three categories of potential methods for disassembly of adhesive joints: general/conventional methods, tailored adhesive formulations, functional additives. It was found that the incorporation of functional additives into commercially available adhesive system generally received more attention and showed higher potential for automotive applications.

Thermally expandable microspheres (TEMs) were identified as the most promising approach and therefore selected for experimental study in this thesis. Four TEMs grades with different initiation temperature, surface chemistry and particle size distribution were provided by three TEMs manufacturers. A two component epoxy based structural adhesive 3M Scotch-Weld 9323 and EN AW-6082 T6 aluminium substrate were used in the experimental testing. The experimental test programme was established to investigate the disbonding performance and general properties of TEMs system. The results contributed to a better understanding of the TEMs concentration effect, TEMs' surface chemistry effect, environmental conditioning effect, disbonding mechanism, and TEMs/adhesive compatibility issue. Poor TEMs/adhesive adhesion, which led to interfacial disbonding under stress, was identified as the main reason for reduced in-service performance.

To address the issue of TEMs/adhesive compatibility, atom transfer radical polymerization (ATRP) with activators regenerated by electron transfer (ARGET) or ARGET ATRP technique was reviewed and employed to modify the TEMs surface. TEMs were grafted with poly(glycidyl methacrylate) (PGMA) chains which contain reactive epoxy groups to form strong covalent bonds with epoxy based adhesive system. TEMs were successfully modified at three temperatures (23 ^{o}C, 30 ^{o}C, and 37^{o}C) after 3 hours and 5 hours respectively. A clear trend of the temperature

effect on TEMs surface modification was observed. The mechanical properties and resistance to environmental conditioning of the TEMs/adhesives system were substantially improved. TEMs modified at 37^{o}C for 3 hours achieved the highest improvement whilst retaining the same disbonding characteristics.

Acknowledgement

First of all, I would like to express my sincere gratitude to my supervisors Dr James Broughton and Dr Pat Winfield for their excellent and infinite guidance, help, encouragement and patience throughout this PhD project.

I would also like to extend my thanks and appreciation to the following people for their contribution and support during this project:

- Professor Fernando Audebert for his invaluable time and help with scanning electron microscopy;
- Dr Nick Hooper, Dr Matthew Clark, Dr David Rodrigues, Mr Michael Hartman, Mr Kieron Tew for their advice and technical assistance;
- Dr Jonsson Magnus, Dr Jonas Vestin and Dr Anna Kron of AkzoNobel for the supply of thermally expandable microspheres and technical assistance;
- Dr Alison Crossley and Mr Chris Salter of Begbroke Science Park, Oxford Univerisity for their assistance with scanning electron microscopy and particle size distribution analysis.

I am indebted to Oxford Brookes University for funding this PhD project. Sekisui Chemical, Matsumoto Yushi-Seiyaku and AkzoNobel are gratefully acknowledged for their kindly support of TEMs samples.

Lastly, I would like to thank my parents, my family, Yanhan and my friends for their love and continuous support during my study.

Publications:

Article:

Lu, Y., Broughton, J. and Winfield, P. (2014) 'A review of innovations in disbonding techniques for repair and recycling of automotive vehicles', *International Journal of Adhesion and Adhesive,* 50, pp.119-127

Conference Paper:

Broughton, J., Winfield, P. and Lu, Y. (2013) 'Surface modification of thermally expandable microspheres for enhanced performance of disbondable adhesives', *Adhesion '13*, 04-06 September, 2013, University of York, UK

Abbreviations:

1K: One component

2K: Two components

4-META/MMA-TBB: 4-methacryloxyethyl trimellitate anhydride in methyl methacrylate initiated by tri-n-butyl borane

5P1HT: 5-phenyl-1H-tetrazole

ABS: Acrylonitrile butadiene styrene

ADC: Azodicarboxamide

ARGET ATRP: Activators regenerated by electron transfer atom transfer radical polymerisation

ASRs: Automotive shredder residues

ATFs: Authorised treatment facilities

ATR: Attenuated total reflection

BIBB: 2-Bromoisobutyryl bromide

BSH: Benzenesulfonyl hydrazide

CFAs: Chemical foaming agents

CNTs: Carbon nanotubes

CRP: Controlled radical polymerisation

$CuBr_2$: Copper(II)bromide

DMTA: Dynamic mechanical thermal analysis

ELVs: End-of-life vehicles

FEM: Front end module

FTIR: Fourier transform infrared spectroscopy

IUPAC: International Union of Pure and Applied Chemistry

GC: Gas chromatography

GMA: Glycidyl methacrylate

GPC: Gel permeation chromatography

IOMVM: International Organisation of Motor Vehicle Manufacturers

IPA: Isopropyl alcohol

JTRC: Joining technology research centre

k_{act}: Activation rate

k_{deact}: Deactivation rate

MEK: Methyl ethyl ketone

NMP: Nitroxide mediated polymerisation

NMR: Nuclear magnetic resonance

OEMs: Original equipment manufacturers

PDMS: polydimethylsiloxane

PDI: Polydispersity index

PEG: Polyehylene glyco

PET: Polyethylene terephthalate

PFA: Physical foaming agent

PGMA: Poly(glycidyl methacrylate)

PMDETA: N,N,N′,N′′,N′′-Pentamethyldiethylenetriamine

PMHs: Polymer metal hybrids

PMMA: Poly (methyl methacrylate)

PP: Polypropylene

PSD: Particle size distribution

pTSH: p-toluenesulfonyl hydrazide

PUR: Polyurethane

PVC: Polyvinyl chloride

RAFT: Reversible addition fragmentation chain transfer polymerisation

RDRP: Reversible-deactivation radical polymerisation

RNC: Reactive nanocomposite

SEM: Scanning electron microscopy

SLJs: Single lap joints

SIP: Surface initiated polymerisation

TEMs: Thermally expandable microspheres

TMA: Thermal mechanical analysis

Tg: Glass transition temperature

$T_{initiation}$: Initiation temperature

T_{max}: Maximum expansion temperature

UTS: Ultimate tensile strength

Contents

List of Figures

List of Tables

Chapter 1.Introduction

1.1. Background

Data issued by the International Organisation of Motor Vehicle Manufacturers showed that the global automotive industry has gradually recovered from the economic crisis in 2008; global vehicle production reached 84.1 million units in 2012 compared to 61.8 million units in 2009 (IOMVM, 2013). This can mainly be attributed to the significant increase in vehicle ownership seen in developing countries such as China and India. In 2009 for example, car production in China was the highest of all car producing countries, reaching 13.79 million (Zhao and Chen, 2011). From a sustainable development perspective, growing concerns have been raised about the environmental impacts of automotive vehicles and their increasing numbers, including energy consumption, greenhouse gas emissions, waste generation, vehicle maintenance and end-of-life vehicle (ELV) recycling.

1.2. Drivers for Change

To reduce the environmental impact, there are three main drivers for change. These are ELV situations, international legislation on ELV and the demand (including future security of supply) of materials.

1.2.1. End-of-life Vehicles (ELVs)

1.2.1.1. Processing of End-of-Life Vehicles

End-of-life vehicles are normally either scrapped for recycling or simply abandoned on the road. In terms of the latter choice, abandoned vehicles not only cause obstruction and safety problems in the public place but also increase disposal cost. The research conducted by Smith and co-workers showed that the devaluation of scrap metal, a poor vehicle registration system, weak legislation and the growth of cheap second-hand vehicles all contributed to an increase in the amount of abandoned vehicles. (Smith et al., 2004)

The recycling, recovery and reuse of ELVs have already raised worldwide concerns. Various nations have implemented different strategies to deal with the issues which vary considerably in severity (Zhao and Chen, 2011) (Santini et al., 2011) (Viganò et al., 2010) (Kim et al., 2004) (Zoppi and Lai, 2010). As product-take-back and legislation requirements on producer responsibility are implemented, the use of recycled materials is increasingly important (Go et al., 2011).

In the EU, to ensure end-of-life vehicles are disposed of properly, ELV legislations and Environmental Permitting Regulations require all vehicles to be taken to Authorised Treatment Facilities (ATFs) for depollution, dismantlement and deregistration. A Certificate of Destruction (CoD) will be issued for the last owner of the vehicle after deregistration. Updated information of all the registered ATFs in the UK can be found on Environment Agency's website (Department for Business, Innovation and Skills, 2012). Autogreen and Cartakeback are the two major free take-back service providers with ATFs throughout the UK. Within the ATF process, a network of companies cooperates in the recycling process. For example, in the UK, EMR focuses on the scrap metal recycling while sending the plastic rich fraction to their joint venture partners, MBA Polymers Inc., which specialises in separating and recycling different types of polymers.

Figure 1.1 reviews the general processing procedures of ELVs. Figure 1.2 illustrates the recycling and recovery rate (by weight) of ELVs in Europe in 2008. The recycling process of a range of separated materials at this stage was detailed in the studies conducted by Baeyens et al. (Baeyens et al., 2010a) (Baeyens et al., 2010b). The remaining parts pass through a shredder and separation process for ferrous and non-ferrous metals. The resulting residue is termed as Automotive Shredder Residue (ASR), also referred to as 'auto fluff' or 'auto shredder fluff' (Vermeulen et al., 2011).

Figure 1.1. Illustration of end-of-life vehicle treatment operations.

(Edwards et al., 2006)

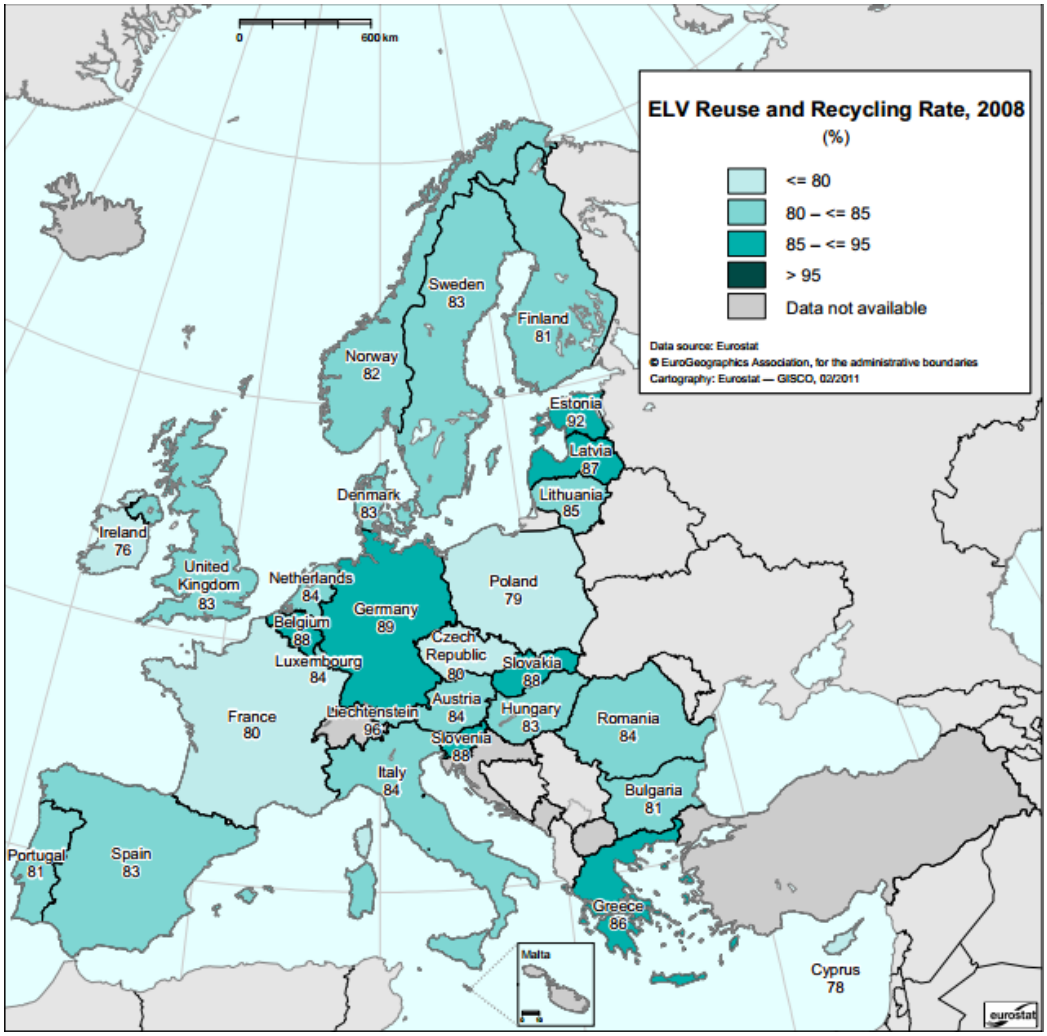

Figure 1.2. The recycling and recovery rate of ELVs at European Union in 2008. (European Commission, 2008)

1.2.1.2. Automotive Shredder Residue (ASR)

Vigano et al. (2010) estimated that EU countries produced approximately 1.9-2.3 million tons of ASR annually. This accounted for approximately 10% (by weight) of the total number of hazardous wastes produced and up to 60% of the total shredding wastes (Rossetti et al., 2006). ASR, constituting up to 25wt% of the vehicle, is composed of a variety of materials including metal, rubber, wood, dirt, textile, glass and up to 27 different types of plastics, although PP, PUR, PVC, ABS, PMMA and PET are generally identified as the major types (Kim et al., 2004) (Rossetti et al., 2006). The composition of ASR can differ significantly depending on the shredding and post-shredding methods applied.

Since the 1970s, landfill treatment and incineration have been the two major ASR processing methods. Landfill treatment still remains the most widely used method. In some parts of the world, certain measures are required, such as immobilising heavy metals before disposing in landfills. In addition to the environmental problems and ever increasingly stringent legislations, landfill treatment has now become cost-prohibitive and less appealing as an ASR processing method (Zorpas and Inglezakis, 2012).

To meet the European targets for the reuse, recycling and recovery of ELVs set by the EU Directive, research has focused on either more complete dismantling methods or ASR processing techniques. Vermeulen et al. (2011) believed that dismantling more materials before shredding is not economically viable in Western countries. This was attributed to the relatively high labour cost (compared to Asian countries) required in the dismantling process. From this point of view, a more efficient disassembly characteristic for future joining solution seems to be an obvious technology driver. Coates et al. (Coates and Edwards, 2006) conducted research focusing on both developing design methods to facilitate ELV recovery and current ELV processing economics. Their research highlighted the importance of a shift from manual vehicle dismantling to large volume automated post-fragmentation separation in achieving the 2015 target of 95% recycling set by the EU Directive.

1.2.2. Legislation

With the ever growing concerns for the recycling of end-of-life vehicles, legislation has developed in many parts of the world. The content below cited examples from Europe, Asia and America to compare and contrast legislations in different regions.

1.2.2.1. European Union

So far, the most influential legislation is the ELV Directive 2000/53/EC, which was enacted under the European Commission's priority waste streams program (Solid Waste and Emergency Response, 2008). According to this EU Directive (European

Commission, 2000), member states must ensure that ELVs are transferred to ATFs and properly recycled. Manufacturers are also encouraged to limit the use of hazardous substances and increase the use of recycled materials in new vehicles. Targets have also been set in different stages:

- From 1st of July, 2003: vehicles put on the market cannot contain lead, mercury, cadmium or hexavalent chromium (materials and components exempted are referred in the annex of the Directive);
- From 1st of January, 2006: reuse and recovery of a minimum of 85% per vehicle on average (recycling 80%) for vehicles produced after 1980; reuse and recovery of 75% per vehicle on average (recycling 70%) for vehicles produced before 1980;
- From 1st of January, 2015: increase the reuse and recovery rate to 95% while the reuse and recycling rate to 85%.

Other major legislations that can affect the disposal of shredder residues in EU include:

- Directive 2000/76/EC on the incineration of waste;
- Directive 1999/31/EC on the disposal of waste in landfills;
- Registration, Evaluation, Authorisation, and Restriction of Chemical Substances Directive (REACH);
- Environmental Permitting (England and Wales) Regulations SI 2010/675 on environmental permits and exemptions.

1.2.2.2. Asia

In Japan, the End-of-Life Vehicles recycling law, prompted by limited natural resource and land resource for landfill sites, was introduced in 2005 (Ministry of the Environment Government of Japan, 2003) (Jody et al., 2010). It is similar to the EU counterpart but extended to cover virtually all vehicles; the EU directive is restricted to passenger vehicles and light commercial vans only (Zhao and Chen, 2011). The law stipulated that it is the automakers' responsibility to provide

dismantling manuals whilst vehicle owners will be charged for the treatment of ELVs.

In South Korea, the Act for Resource Recycling of Electrical and Electronic Equipment and Vehicles offers the scheme for both the manufacturers and importers in terms of the restrictions on hazardous substances (from 1st July, 2008), recycling rates, design and methods recycling, etc. (Environment and labor committee of the national assembly of Korea, 2007) Unlike the EU directive, this Act does not address the recycling issues of tyres, batteries or air bags.

In China, Statute 307 regulates the disposal of ELVs in China. In 2001, the State Council of the People's Republic of China enacted the 'End-of-Life Vehicle Recycling Regulation', i.e. the Statute 307, which stipulates the responsibilities of local government and ELV recycling industry regarding registration capital and capacity of dismantling activities (Zhao and Chen, 2011).

The Automotive Products Recycling Technology Policy was enacted by the National Development and Reform Commission (NDRC) in 2006 aiming at establishing the ELV recycling system, including developing and promoting scrapped automotive products (Zhao and Chen, 2011). However, the enforcement was comparatively weak compared with Korea and Japan. This policy established a minimum of 85% reuse and recovery target by 2010. The use of hazardous chemicals such as lead, cadmium, hexavalent chromium and mercury is prohibited.

1.2.2.3. America

In the United States, no legislation has been developed on a federal level to address ELV recycling issues even though attempts have been made by some senators since 1991. The main argument appears to be that enacting legislations are not considered an effective method to improve recycling (Jody et al., 2010).

Instead, large manufacturers in the USA have shared this responsibility. In 1992, Ford, Chrysler and General Motors initiated a Vehicle Recycling Partnership to facilitate sustainable vehicle recycling both in North America and around the world

(Solid Waste and Emergency Response, 2008). Another term often referred to in the USA is 'Product Stewardship' which means every party involved in the lifespan of product share the responsibility for reducing its environmental impact.

1.2.3. Recycling Issues for Future Vehicles

Due to the depletion of natural resources and exacerbating environmental issues, fuel efficiency and CO_2 emission are two major concerns. One effective approach to these problems is to reduce vehicle weight due to the fact that approximately 75% of fuel consumption is caused by vehicle weight (Guillaume and Marechal, 2008). For example, a 100 kg reduction in weight could save 0.4 l/100 km fuel consumption.

Engines, running gears, and chassis frames, among other components, have been increasingly made of lightweight metals (Antrekowitsch et al., 2001). Low-weight, cost-effectiveness, production times, ease of installation are expected to be some of the key features for future automotive vehicle components. OEMs today have intensified their efforts in using lightweight materials such as polymers and composites, as substitutes of ferrous materials. Figure 1.3 shows the change of material use in automotive vehicles from 1977 to 2011. In more recent years, government initiatives, safety issues, increased demands of return on capital further facilitate the development of composite materials for future vehicles (Månson et al., 2012).

Waste management and environmental legislations now require higher rates of reuse, recycling and recovery. However, the use of polymer and composite materials complicates the recycling process. This is one of the main obstacles to the wide spread application and acceptance of lightweight materials in the automotive sector.

This difficulty can be explained from two aspects. Firstly, to separate composites and polymers from metals can be labour-intensive and expensive. Even though the industry has made significant progress on recycling technology (Jody et al., 2010),

the shift to lightweight material makes it more challenging. The main joining technique for polymers and composites is adhesive bonding as it generally outperforms traditional joining technologies when joining dissimilar materials and non-metal materials but it incurs more problems during the recycling process of end-of-life products.

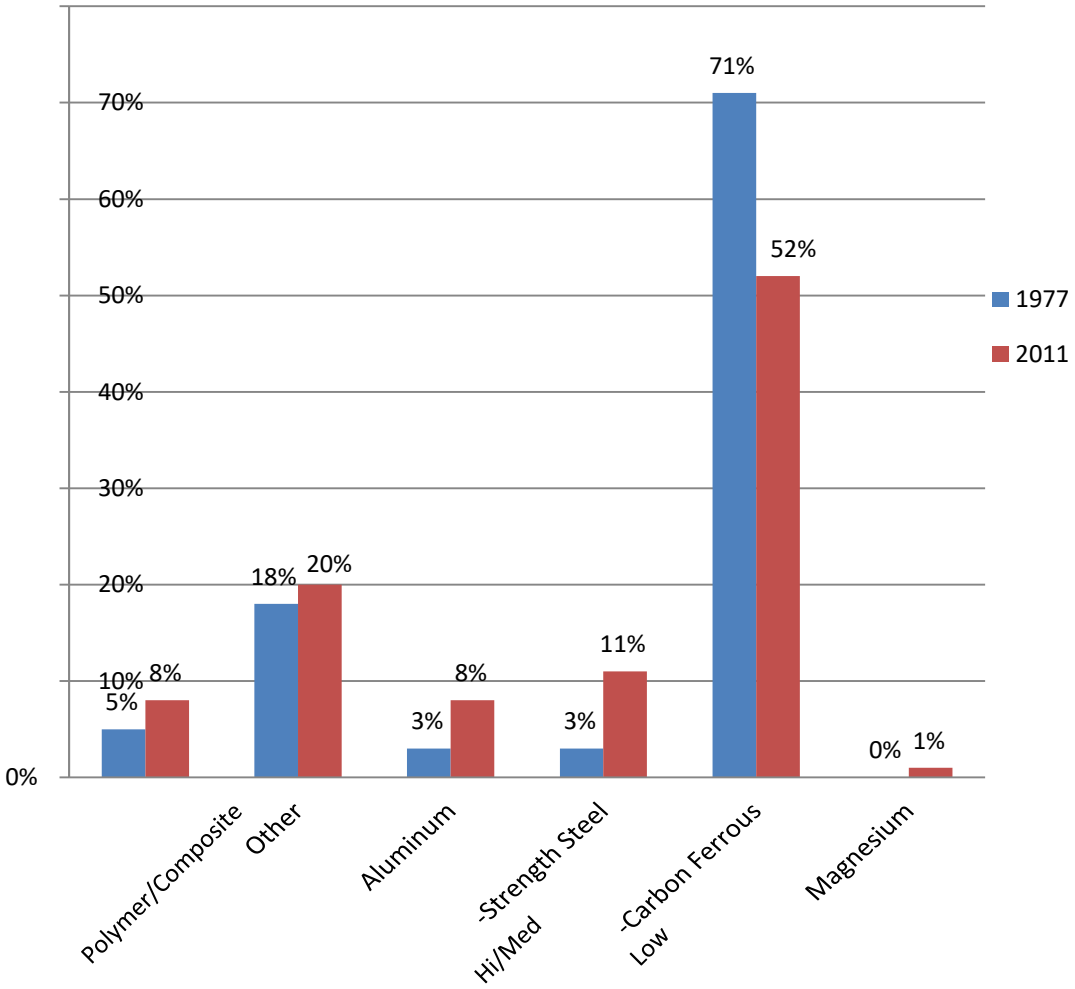

Figure 1.3. Material usage in automotive vehicles from 1977 to 2011. (Leibson, 2011)

Secondly, the recycling and recovering process of composite materials, due to their physical and chemical makeup, is difficult. The recycling of fibre constituents in some fibre reinforced composite has been a source of heated debate (Oliveuxa et al., 2012)(Correia et al., 2011). Facing the recycling challenges, many have

suggested that design for disassembly is now an essential requirement of the design process (Mangino et al., 2007). Specifically, a new joining technology which enables rapid disassembly is of great interest.

1.3. Summary of Findings

In summary, ever-growing numbers in the vehicle ownership has sparked increasing concerns on the environmental impacts of automotive vehicle life cycle. This chapter focused on the ELV recycling problems and reviewed drivers for change in three aspects: ELV situation, legislations as enforcement and recycling issues for future vehicles.

ELV recycling process was generally divided into three stages: depollution, dismantlement, deregistration. ASR was pointed out to contain complex composition which posed major environmental challenges. From a legislative perspective, ELV issues have gradually caught worldwide attention. The European Union has enacted more comprehensive and strict legislations whereas developing countries are catching up. Nevertheless, a positive trend for ELV recycling legislations has been clearly identified. Future vehicles recycling issues were mainly ascribed to the lightweight and multi-material trend which complicates the recycling process in two ways:

- It is labour-intensive and expensive to separate advanced materials such as various polymers and composites;
- Advanced materials are difficult to recycle due to their chemical or physical nature.

Along with the analysis of three key drivers for change, a new joining solution with the essential characteristics of rapid disassembly was identified as a key technology driver and proposed as one of the solutions for current problems.

1.4. Overall Aim of this Research

The overall aim of this PhD project is to evaluate and develop suitable bonding solutions which enable rapid disassembly of automotive vehicles for maintenance or end-of-life recycling purposes.

Chapter 2. A Review of Innovations in Adhesive Disbonding Technology of Automotive Vehicles

2.1. Scope of this Chapter

This chapter focuses on adhesive bonding due to its wide and increasing use in automotive vehicles. A general review of adhesive bonding applications in automotive industry is presented, using case studies to gain a deeper understanding. Innovations in adhesive disassembly technologies are then critically reviewed in order to select a suitable approach for further investigation.

2.2. Adhesive Bonding in Automotive Industry

One of the greatest challenges currently facing the automotive industry is the joining of dissimilar materials while maintaining mechanical properties and sufficient durability. Adhesive bonding is now considered as a replacement of conventional joining methods such as riveting, bolting and welding. The main advantages being:

- All solids can be joined including combinations of dissimilar materials, although pre-treatment may be necessary;
- More uniform distribution of stress and increased fatigue life;
- Weight savings;
- Corrosion between dissimilar materials can be prevented or reduced;
- Films and thin sheets can be bonded;

- Delicate parts such as electronic components can be joined;
- Relatively high impact resistance.

The application of adhesive bonding in car body joining can be subdivided into four main functions: sealants for body joints, spot-welding sealants and tapes, antiflutter bonding, and structural adhesive bonding and hem flange sealing (Brady et al., 1997). For structural applications, the combination of spot welding and adhesive bonding achieves a more efficient connection. For example, in comparison with the stiffness of a spot welded structure, adhesive bonding can offer 15 to 30% enhancement (Adams, 2005). Also, for a box-beam bonding application, research conducted by Henkel showed that the use of an impact resistant structural adhesive resulted in an approximately 30% increase of energy absorption compared to a spot-welded structure. (Hornung and Hajj, 2009)

Anti-flutter adhesives are applied in the form of soft elastic joints between the inner and outer panels on bonnets or sides to add the stiffness and dampen the effect of vibration and noise. A relatively low shrinkage and low modulus are always required for anti-flutter adhesives to compensate for tolerances after filling up gaps between components (Adams, 2005).

Body joint sealing adhesives behave as sealants and are normally applied after the assembly process in order to protect components from the influence of dust, water and other factors which could induce corrosion (Adams et al., 1997). Typical sealant types used in the body shop are acrylic esters, epoxies, polybutadienes, polyurethanes and PVC/epoxy blends. These adhesives have to go through a curing

process in an electro-coat oven. Consequently, this requires the handling strength of the body to be supplemented by joining techniques such as spot welding. Acrylic plastisols, reactive butyls, and non-setting rubber compounds are widely used in this area (Ebnesajjad, 2008).

Case Study 1: Adhesives in automotive interiors.

Adhesives are employed in automotive interior applications both for improved performance and for aesthetic design. Generally, reactive hot-melt adhesives are used with efficient robotic application because of their resistance to extreme temperatures (-40^{o}C to 125^{o}C) and the ability to achieve a green strength in a short period. For specific uses like lamp assembly and spare-tyre cover lamination, two-part epoxy adhesives and silicone adhesives are usually used (Sanchis et al., 2008)(Anderson, 2004). Since load bearing is not essential for the internal trims, ease of handling and assembly often determine the use of adhesives in this application. For instance, pressure sensitive adhesives in the form of two-side tapes are used to attach labels and decals (Anderson, 2004).

Case Study 2: Adhesive bonding for space frames.

An emerging application for adhesives in body assembly is the construction of the space frame. Over the past decades, adhesively bonded space frames including box-beam structure have been employed by a number of car manufacturers in concept cars and low volume models (e.g. Jaguar XJ220, Ford AIV, Lotus Elise and Aston Martin Vanquish) (Michalos et al., 2010) (Barnes and Pashby, 2000) (Vasilash, 1997). The relatively demanding mechanical property requirements for this major

structural component necessitate the application of high quality adhesive bonds. Hence, both a part pre-treatment process and high performance adhesives are typically used (Michalos et al., 2010)(Barnes and Pashby, 2000). For example, the production of the Lotus Elise space frame utilizes both an anodizing process for the extruded aluminum components and a high performance single part heat cured epoxy (with tensile strength of around 35MPa and Young's modulus of about 2700MPa) to achieve its desired properties(Vasilash, 1997).

The use of adhesives in space frame construction brings a number of benefits. One of the most significant ones is to fully extract the strength-to-weight benefits offered by the lightweight aluminum alloys which cannot be easily welded without losing properties (Barnes and Pashby, 2000)(Vasilash, 1997). The 68kg adhesively bonded space frame of the Lotus Elise achieved an astonishing 50% weight reduction compared with an equivalent steel construction bonded with spot welding (Vasilash, 1997). Compared with welding techniques, adhesive bonding also provides higher precision of the space frame structure due to the elimination of distortion that comes with the localised high temperature zone (Hornung and Hajj, 2009)(Vasilash, 1997). This is highly valued in high performance car structures because even tiny distortions (0.5mm) to the space frame can affect the handling of the vehicle (Adderley, 1988). Together with other typical advantages brought by adhesive bonding, the adhesively bonded automotive space frame has fully demonstrated its merits over the past decades.

However disadvantages also exist in an adhesively bonded automotive space frame. The limited production rate caused by the time consuming curing and joining

processes is one of the major concerns. Recent developments in robotic and curing facilities has achieved a production rate of about 3000 units per annum for a hybrid adhesively bonded space frame, however further developments are still needed for higher production volume (Barnes and Pashby, 2000)(Vasilash, 1997) (Mortimer, 2004). Also, the difficulties for maintenance and repairing should not be ignored. If an adhesively bonded space frame is damaged in an accident, it cannot be repaired using conventional techniques as with a steel chassis. Replacement of the whole space frame may occur under serious collision (Michalos et al., 2010)(Vasilash, 1997) (Crolla, 2009).

Case Study 3: Automotive Front End Module (FEM).

The front end module supports the cooling package, bonnet latch mechanism, headlights, bumper and many other components. The major requirements for the FEM include crashworthiness, thermal and chemical stability, and durability. Polymer metal hybrids (PMHs) technology has gained popularity in making automotive FEMs in recent years. The Lanxess group has been developing PMHs technologies for many automakers. BMW, in its 1, 3 and X3 series, the new Audi TT and Audi A8 employed the Lanxess' technology to produce front end modules (LANXESS, 2012). PMHs have been introduced as an approach to meet both structural and non-structural requirements while at the same time achieving a lightweight structure.

In addition to injection over-moulding and metal over-moulding technologies, adhesive bonding is another major approach to manufacture PMHs in the automotive industry (Marechal, 2006) (Grujicic et al., 2008).

Adhesively bonded PMHs technologies were first introduced and patented by Dow Automotive in 2003. Dow developed a low energy surface adhesive to bond glass-fibre reinforced polypropylene to a metal stamping (Naughton et al., 2002). Compared to traditional hybrid front end manufacturing such as rivet bonding and over-moulding, adhesive bonding improves the stiffness and minimises stress concentration by forming a continuous joint along the plastic to metal interface (Recktenwald, 2005). However, from an ELV recycling point of view, to separate polymers from metals in this adhesively bonded hybrid can be laborious and costly. Consequently, a method of rapid disassembly would be highly desirable.

2.3. Adhesive Disbonding Technologies and Recent Advances.

2.3.1. General methods for adhesive bonding disassembly

Previous research (McCurdy, 2011) conducted within the Joining Technology Research Centre (JTRC) at Oxford Brookes University summarised methods for disassembly of adhesive joints from various areas. The approaches for general adhesive bonding and novel methods were covered to a large extent.

The mechanical separation method of disbonding was identified as the most primitive approach. A range of patented works (Essig et al., 2004)(Brown and Kaufman, 2005) (Abrego, 2010) (Merz et al., 2000) have attempted to the assist disassembly process, yet there is a lack of clean separation of the substrates and the method is generally inefficient and laborious.

Thermally induced disassembly approaches can be achieved through both thermal softening (exceeding the adhesive's Tg) and thermal decomposition (exceeding the temperature of flammability-in-air or auto-ignition point). For the latter, the major concerns are the toxic and irritant emission gases that are produced as a result of chemical decomposition (Viganò et al., 2010).

Certain solvent or acid immersion techniques can also assist the adhesive disassembly process. Polar solvents such as isopropyl alcohol (IPA), methyl ethyl ketone (MEK) and acetone, can be very effective in cleaning and degreasing substrate surfaces and are mainly used in surface treatment processes (Elwell 1981)(Hodgin, 2009).

2.3.2. Tailored adhesive formulations for the ease of adhesive disassembly

To a large extent, the electronic chip industry started the research for disassembly of adhesive formulations to enable rapid removal of chips at end of life (Licari and Bakhit, 1991)(Wong and Wu, 2002)(Ardakani et al., 1996). Different approaches have been developed in different areas. Battelle Memorial Institute developed a thermally reversible isocyanate-based polymer formulation, the reversibility mechanism of which was based on the dissociation of the isocyanate-labile hydrogen based linkage to the isocyanate and labile-hydrogen starting groups (Markle et al., 1995). Upon dissociation, this polymer was found to become a free flowing melt, which was soluble in acids. Atochem and Yokohama used different chemistries in their research but achieved a similar system (Augustin et al., 1988)(Chino et al., 2004).

Sandia National Laboratories (Aubert, 2010) developed a thermally removable adhesive by incorporating thermally reversible furan-maleimide Diels-Alder adducts (which form below 60 ^{o}C and dissociate above 90 ^{o}C) to a low modulus epoxy adhesive formulation, Figure 2.1. However, experimental data in their research demonstrated only fairly weak lap shear strengths (between 3.36 and 4.65 MPa), which cannot be used for structural application. Also, the relatively low dissociation temperature rules out its use for many applications. This reversible Diels-Alder adduct has however drawn much attention and its properties were further investigated in recent research conducted by Claudio et al. (Toncelli et al., 2012).

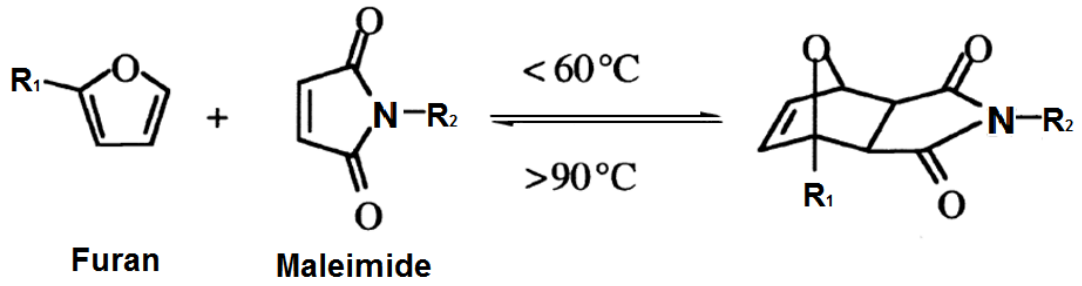

Figure 2.1. Reversible Diels-Alder reaction between furan and maleimide.

The DC Polymers (2011) adopted electrochemically active cross-linkers, which can be incorporated into the polymer structure. Electrochemical reduction can be triggered by applying an electric current. This leads to scission of the polymer backbone at cross-linker sites and thereby polymer degradation. Since crosslinking is quite common to all types of polymers, this technology can be theoretically applied to a wide range of polymeric materials. However, this technology is still restricted to preliminary studies and no mature product or experimental data has been published.

Developed by EIC Laboratories and as one of the most prominent and elaborate systems to date, ElectRelease is the trade name for a series of structural epoxy adhesives which can be dismantled fairly easily by applying an electric current at 10-50V, Figure 2.2. The disbonding mechanism is achieved through ion conduction along the resin-metal interface. Pseudo-micelles are formed by incorporating a nanoscaled backbone blocks of polydimethylsiloxane (PDMS) into a two-part amine-cured epoxy resin structure. The backbone structure is also attached to the arms of polyethylene glycol (PEG) which creates a comb-type polymer and pseudo-micelles structure in the uncured epoxy resin. Upon curing, the PEG micelle phase separates from the epoxy around the immiscible PDMS cores and forms a nano

scaled co-continuous network, Figure 2.2. High level ionic conductivity can be further achieved through post-treatment with suitable salts. (Shiote et al., 2009)

Copyrighted image removed from electronic version

Figure 2.2. Microscopic structure of ElectRelease. (Shiote et al., 2009)

The disbonding needs a metal as the positive substrate and another suitable material for the negative substrate. When two metal substrates are bonded using ElectRelease, disbonding at both interfaces can be achieved by reversing the polarity of the disbonding voltage. For non-conductive materials, an ElectRelease foil patch which is essentially two sheets of metal foil, is applied on the surface to enable electric conductivity. (Haydon, 2002)

The ionic conductivity determines the effectiveness of the disassembly process. However, epoxy resins normally have a relatively low ionic conductivity and high ionic conductivity polymers are typically in a rubbery or gel-like state. This is one of the reasons why EIC Laboratories adopted a nano-scaled block copolymer to modify the ionic conductivity while at the same time retaining the epoxy resin structure and therefore strength.

The development of ElectRelease technology has triggered intense interest in investigating electrically assisted disbonding adhesive formulations. Leijonmarck et al. (2012) investigated the ElectRelease technology and provided further understanding of the disbonding mechanisms. They observed a delamination process at the interface between the aluminium anode and the adhesive layer, detected the changes in polymer chemistry using Raman spectroscopy and also analysed the emission of volatile species using mass spectrometry. Four delamination mechanisms were proposed and discussed.

2.3.3. Functional additives for the ease of adhesive disassembly

There are numerous research papers and patents in the literature on incorporating certain additives or agents to trigger the disbonding process. One of the earliest examples was patented (Cook, 1976) by shoe manufacturers for separating shoe soles from uppers. The disbonding process was achieved by incorporating metallic inclusions into the adhesive to efficiently absorb and emit heat energy when subjected to alternating electro-magnetic field thereby activating the release of micro-encapsulated solvents, which would further degrade the polymeric structure. Probably influenced by this idea, Daimler-Chrysler and partners (Becher et al., 2004) patented similar work and specified examples of encapsulated solvents as organic amines or acids which can cleave an epoxide backbone. Microcapsules were recommended to be made of amino resin or metal halide. Obediat (2009) reviewed recent patented works of different microcapsule preparation methods used in the field of pharmaceutical. Work patented by the Nissan Motor Company (Yasuhiro and Kensho, 1976) mixed oxidising agents (ammonium perchlorate, potassium

permanganate, etc.) into the adhesive matrix which produced a self-burning reaction at elevated temperatures. The decomposition process generated abundant oxygen and caused failures in the bondline. However, the volatile nature of these oxidising agents is one of the major concerns for its application in automotive industry.

These approaches lay the foundation for many more recent and influential studies. Chemical foaming agents (CFAs) and thermally expandable additives have drawn most attention.

Henkel (Friese et al., 2001), IBM (Hanley and Kuczynski, 2006), US Army Research Laboratory (Minnicino and Sands, 2011) and Rescoll (Alcorta et al., 2006) (Foulc et al., 2012) investigated a series of CFAs including Azo compounds, and hydrazides. Different types of foaming agents were incorporated into adhesive systems to assist the disassembly process at elevated temperatures. Interestingly, Rescoll's research noted that CFAs would become mobilised at higher temperatures when the adhesive bondline softened and melted. Some CFA particles or microspheres would then migrate and finally decompose at the joint interface.

Research in the Joining Technology Research Centre (JTRC) at Oxford Brookes University (McCurdy, 2011) investigated the effect of the incorporation of functional additives on the dismantling characteristics of three vehicle OEM approved adhesives: two fracture toughened epoxies and one semi-structural polyurethane. The functional additives selected were four types of chemical foaming agents (CFA): p-toluenesulfonyl hydrazide (pTSH), benzenesulfonyl

hydrazide (BSH), azodicarboxamide (ADC) and 5-phenyl-1H-tetrazole (5P1HT). No discernible benefit was observed from the experimental data of CFA incorporated into the polyurethane based semi structural adhesive. However, the structural adhesive systems were found to be promising but still showed problems of additive/adhesive incompatibility, which therefore affected the long-term durability. More importantly, additive-matrix incompatibility issues were pointed out in this research.

In terms of thermally expandable additives, an early work patented by 3M (Tetsuo and Kohichiro, 2000) used inorganic materials such as dilated graphite, vermiculite, pearlite or mica as expanding additives. The expandable additive content was generally specified as 10 to 50wt%. Initiation temperature was reported to be 250^{o}C to 500^{o}C with expansion ratio normally 1.1. It is also claimed that these additives could enhance the heat resistance of an adhesive. However, neither experimental data nor any convincing proof was disclosed.

Expandable additives have also been used for adhesive disassembly in orthodontic application. The removal of orthodontic attachments has great risk of causing enamel damage if mechanical separation is undertaken improperly. The use of electrothermal, laser or ultrasonic methods may incur other problems such as expensive equipment cost, potential pulpal damage and mucosal burns (Naini and Gill, 2008) (Oztoprak et al., 2010). Tsuruoka et al. (2007) incorporated thermally expandable microspheres (TEMs) into 4-META/MMA-TBB (4-methacryloxyethyl trimellitate anhydride in methyl methacrylate initiated by tri-n-butyl borane) resin adhesive, which is widely used for bonding orthodontic brackets. The microspheres

used in this study were Matsumoto F-36D which starts to expand at 80 ^{o}C. They identified that an incorporation of 40wt% of these microspheres showed satisfactory bond strength before heating and a reduced bond strength by a third within 8s of heating. The Tokyo Institute of Technology (Nishiyama et al., 2003) (Ishikawa et al., 2005) also conducted research on adhesive disassembly using expanding microspheres manufactured by Matsumoto. These studies also looked at its application for construction materials. The weight fraction of microspheres used and the roughness of adherend surfaces were found to be two major factors in determining the dismantalability of the bonded joints.

Thermally expandable microspheres are generally constructed with a thermoplastic polymer shell and hydrocarbon core, which has a low boiling temperature. The density reduces from about 1100 kg/m^3 to 30 kg/m^3 at elevated temperature (Jonsson et al., 2009). TEMs were first developed by Dow Chemical Co. and currently are being manufactured by many companies such as Polychem Alloy, Sekisui Chemical, Matsumoto Yushi Seiyaku, Akzo Nobel and Sigma Aldrich. JTRC's research also investigated four different grades of physical foaming agents (TEMs) containing isobutene, isooctane or isopentane. These selected grades of additives provide a range of activation temperatures and decomposition/expansion efficiencies. Their research showed that polyurethane based adhesive matrix were more likely to absorb the energy as a result of TEMs expansion whereas brittle epoxy based adhesive showed higher disbonding efficiency.

The Army Research Laboratory (Minnicino and Sands, 2011) investigated a reactive nanocomposite (RNC) approach to solve a rapid disassembly problem. The

disassembly is thermally triggered and a physical change occurs as an additional interface is required for the RNC to be inserted into the bondline. However, no further information was disclosed.

Reviewing most of these current studies on functional additives, it is noted that none of the approaches mentioned create a system sufficiently effective for the disassembly of an adhesive application in the automotive industry. Disassembly efficiency and additive-matrix compatibility were identified to be two major concerns, which were either vaguely mentioned or completely neglected in most patented works. Some studies have identified these problems to be main obstacles but failed to provide a feasible solution. JTRC's research had identified additive-matrix incompatibility and noted that the incorporation of additives affect mechanical properties and durability by acting as weak links in the matrix, or in some cases, reacting with the matrix. Jonsson et al. (2009) successfully modified TEMs by grafting glycidyl methacrylate (GMA) on the surface. Atom transfer radical polymerization using activators regenerated by electron transfer (ARGET ATRP) was employed. Special treatment was also used to retain the expansion ratio of the TEMs.

De-Bonding Ltd and Evonik have focused on developing a system with efficient disassembly processes. The research of De-Bonding Ltd has looked at the dismantling of automotive glazing on ELV by incorporating TEMs in the adhesive bondline (Manfrè, 2005a)(Manfrè, 2005b)(Carter, 2008). In cooperation with the Armes group at Sheffield University, their research (Schmid et al., 2009) has successfully synthesised polypyrrole-coated TEMs which are only microns in size.

The research investigated the effect of the TEMs on the delamination of the adhesive joints. An infra-red lamp was adopted as the heating source. Polypyrrole has a broad absorption peak (900-1500 nm) in the infra-red. This provides the polypyrrole-coated TEMs with a very efficient thermal energy absorbance. Experimental results showed great potential for the application of reversible adhesion of car glazing and panels for both maintenance and recycling purposes.

Evonik developed a type of adhesive tape called Magsilica. Magsilica is used as a nano susceptor which is basically a powder of iron oxide particles embedded in silicon dioxide nanoparticles. These particles behave as nano magnets when subjected to external magnetic field, which can heat up for the purpose of curing and disassembly (Evonik, no date). This has achieved two major advantages: shortened cure times and reversible bonding. Evonik has patented their work and showed several examples for its use (Kolbe et al., 2004). A major concern is that conductive or magnetic components can cause electromagnetic shielding, which deactivates the heating mechanism. McCurdy in JTRC (McCurdy, 2011) attempted to replicate the dismantling characteristics on a toughened epoxy adhesive incorporated with MagSilica powder. Half size single lap joints (ISO 4587) were made from 2 mm thick steel substrate with a 0.2 mm adhesive bondline thickness. An induction heating method was adopted and a temperature of 120°C (above epoxy resin Tg) was used to lead to disbonding within 30s. However, no satisfactory material separation was recorded. Reasons were attributed to the ineffectiveness of direct induction heating which led to large residue strength of structural adhesive.

2.3.4. Other relevant advances

The addition of functional additives into adhesives can potentially influence certain adhesive properties. The University of Pennsylvania and Loughborough University have both conducted research on the addition of carbon nanotubes (CNTs) into conventional epoxy (Bogue, 2011). Thermal conductivity, mechanical properties, heat resistance and long term durability were all seen to increase significantly with even a small concentration of CNTs. Graphene technology, with lower production cost compared with CNTs was also seen to have similar effect (Kuilla et al., 2010). It is the author's opinion that by incorporating CNTs or grapheme into the adhesive, the improvement in thermal conductivity could enhance the disassembly efficiency as heat could be transferred to functional additives much faster. Also, the mechanical properties and durability could be compensated to a large extent. Lumia Adhesives developed Adhelight (Tunius, 2011), which maintains strong adhesion but loses most strength within 15 seconds when exposed to light. 0.05% to 10% of photoinitiator was normally incorporated into the adhesive matrix. This technology was developed for medical skin applications. Sethi et al. (2008) synthesised micro-patterned carbon nanotube-based tapes which was inspired by the hierarchical hairy structure of a gecko foot. This technology has formed the basis of a new class of adhesive which adapts to a continuous bonding and disbonding process.

A comparison and overall rating of all disbonding techniques discussed in this chapter can be found in Table 2.1. The incorporation of thermally expandable microspheres or chemical foaming agents into current commercial adhesive system

both achieve the highest rating (four stars) in the Table 2.1. Currently their automotive applicability is limited mainly by their compatibility with adhesive matrix. The chemical foaming agents react with the adhesive matrix and change its chemical structure. Thermally expandable microspheres can act as weak physical link. The authors believe that the thermally expandable microspheres approach has more potential for automotive applications.

Table 2.1. Comparison and Rating of Disbonding Techniques.

Techniques	Disbonding Condition	Automotive Applicability	Complexity	Capital Cost	Disbonding Efficiency	Rating *
Mechanical separation	N/A	Low	Low	Low	Low	*
Thermally reversible structure	Temp. (100 -250^{o}C)	Low	High	Med	Med	**
Thermally removable adhesive	Temp. (90 ^{o}C)	Low	High	Med	Med	**
Electro-chemically reversible structure	Electric Current (not specified)	N/A	High	High	N/A	**
Ionically conducting epoxy adhesive	Electric Current (10-50V)	Med	High	High	High	***
Oxidising agents	Temp. (300 ^{o}C)	Low	Med	Med	Med	**
Microcapsules	Temp. (175 ^{o}C)	Low	High	Med	Med	**
Thermally expandable additives	Temp. (250 -500^{o}C)	Low	Med	Med	Med	**
Chemical foaming agents	Temp. (130 -250^{o}C)	Med	Med	Med	High	****
Thermally expandable microspheres	Temp. (120 -200^{o}C)	Med	Med	Med	High	****
Light sensitive switchable adhesive	Exposure to light (20 seconds)	Low	High	High	High	**
Gecko inspired adhesive	N/A	Low	High	High	High	**

Note: *Rating: 1* to 5* from low to high rates. Med: Medium; Temp: Temperature.

2.4. Summary of Findings

Below is a summary of the key findings:

- Adhesive bonding outperforms conventional joining solutions, particularly where multi material assemblies are concerned. However, one of their main limitations is their poor disassembly efficiency;
- Innovations in adhesive disassembly technology have been thoroughly reviewed for their applications in many different industry sectors; Tailored adhesive formulation and functional additives were identified to be the two major routes forward;
- The functional additives approach (such as chemical foaming agents, oxidising agents, thermally expandable microspheres) has received more attention because they can be introduced into existing adhesive products;
- Functional additive/adhesive compatibility and disbonding efficiency have been identified as the two major problems concerning the functional additives approach;
- CFAs are likely to cause side reactions while TEMs act as weak links reducing the mechanical properties and long term durability of adhesive system;
- For TEMs approach, tough matrix (polyurethane adhesive) compared with brittle matrix (epoxy adhesive) showed reduced benefit since more energy (as a result of TEMs expansion) can be easily absorbed by the matrix;
- The incorporation of thermally expandable microspheres (TEMs) in current adhesive system to assist disassembly process was identified as one of the most promising approaches.

2.5. Work to be Undertaken

2.5.1. Aim of Research

The overall aim of this PhD project, as stated in Chapter 1, is to evaluate suitable joining solutions which enable rapid disassembly for automotive applications. This chapter has focused on adhesive joining solutions and presented a comprehensive literature review on adhesive disbonding technologies. A clear trend of adhesive disbonding technology using functional additives has been identified as one of the most promising approach. The work to be undertaken will therefore be focused on functional additives approach, specifically, thermally expandable microspheres (TEMs).

2.5.2. Objectives

The overall objectives of this project are:

- Investigate the disbonding characteristics of adhesive system using a range of TEMs (high initiation temperature, different surface chemistry and particle size distribution) currently available from major manufacturers;
- Investigate and understand the disbonding mechanism and compatibility issues of TEMs/adhesive system;
- Develop a surface modification technique to address the TEMs/adhesive compatibility issue.

2.5.3. Project Structure

The structure of this project can be divided into four phases as shown in Figure 2.3. The first two phases of work covering background information and literature review have been completed in Chapter1 and Chapter 2.

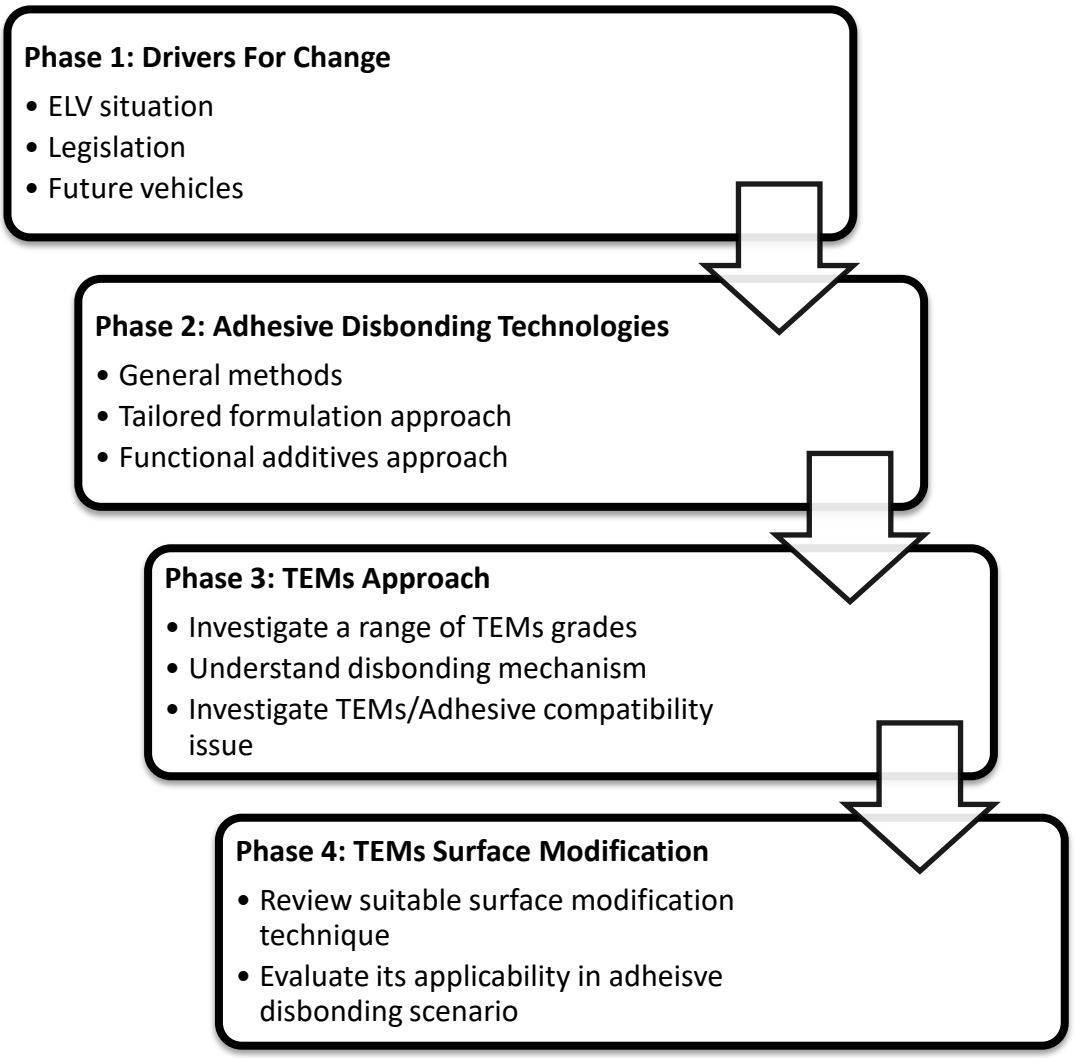

Figure 2.3. Illustration of organisational structure of the project.

2.5.4. Expected Project Outcomes

In line with the overall aim and objectives of this project, the expected outcomes would contain the demonstration and validation of an adhesive system that can be disbonded with the incorporation of TEMs and a suitable TEMs surface modification method to improve TEMs/adhesive compatibility.

Chapter 3. Experimental Materials and Surface Modification Technique Selection

3.1. Adhesive

Adhesive selection was mainly based on the research in the literature. Previous research by Joining Technology Research Centre (JTRC) at Oxford Brookes University has investigated one component (1K) and two components (2K) adhesives for both structural and semi-structural applications (McCurdy, 2011). Semi-structural adhesives were discarded due to the reduced benefits of using functional additives to enable adhesive disbonding. 1K adhesives generally require a higher curing temperature which is likely to induce the activation of functional additives. Therefore, for the current research, a 2K structural epoxy adhesive 3M Scotch-Weld 9323 was used. It is an amine cured epoxy adhesive with excellent adhesion to a range of substrates and good resistance to harsh environments, see Appendix for datasheet.

In order to maintain consistency in the research and provide comparable experimental data, the curing regime used JTRC's internal standard: cured at 90 °C for 90 minutes and followed by room temperature post cure of 7 days.

3.2. Substrate

Aluminium was chosen as the substrate material due to its wide applicability and ever-growing usage in automotive vehicles. For automotive structural components, 6000 series aluminium alloys are more commonly used, Table 3.1.

To accommodate experimental tests, mainly single lap shear test, the substrate material has to withstand a minimum tensile stress which can be estimated from the tensile lap shear strength of the selected structural adhesive. For the Scotch-Weld 9323 epoxy adhesive, this value is approximately 35MPa (upper limit value) at room temperature. For single lap joints with overlap area of 25mm*15mm, this means a minimum tensile stress of 262.5 MPa for substrate with cross section area

of 25mm*2mm. (All dimensions cited in the above estimation were used in this research)

Table 3.1. Typical grades of aluminium alloys for structural applications.

(McCurdy, 2011) (Rowe, 2012)

Alloy*	Proof Stress (MPa)	Ultimate Tensile Strength (MPa)	Elongation (%)
6181 -T4	105	215	24
6501 - T4	70	135	26
NG5754	110	240	24
6014 - T4	110	210	24
6014 - T5	225	285	17
6014 -T6	260	300	15
6111 -T4	150	280	26
6082 -T6	290	340	6

***Designations according to AA or EN AW**

To ensure research consistency with previous studies within JTRC, EN AW-6082 T6 in a nominal sheet thickness of 2 mm manufactured by Arenastock Ltd was selected. 6082 grade aluminium is a medium strength alloy (highest strength in all the 6000 series) with satisfactory mechanical properties, corrosion resistance and machinability.

3.3. Thermally Expandable Microspheres (TEMs)

Thermally expandable microspheres (TEMs) are micron scaled spherical particles comprised of a thermoplastic shell material (2-15um thickness) and encapsulated hydrocarbon core which has a low boiling temperature. At elevated temperature, shell softening and hydrocarbon gasification allows TEMs to expand 30 to 80 times in volume, Figure 3.1.

TEMs have been widely used as physical foaming agents and lightweight fillers in various industrial applications including anti-slip coatings, automotive underbody coatings, three dimensional design, structural foams, sound damping coatings etc. (Jonsson et al., 2009). Unexpanded TEMs have good processability and can generally withstand the pressure and shear force during extrusion moulding, injection moulding, etc. (e.g. Matsumoto Microsphere grade TEMs can withstand 30MPa pressure). Since its first invention in the 1970's, different proprietary methods have been developed by TEMs manufacturers such as Akzo Nobel, Sekisui, Henkel, Matsuomoto Yushi-Seiyaku, etc. To fill the knowledge gap of TEMs properties and synthesis methods in academia, Jonsson and co-workers (Jonsson, 2010) (Jonsson et al., 2009) conducted a series of research to investigate general TEMs synthesis method using suspension polymerisation, TEMs expansion properties and TEMs surface modification. Readers are referred to their studies for a more comprehensive understanding of TEMs synthesis and properties.

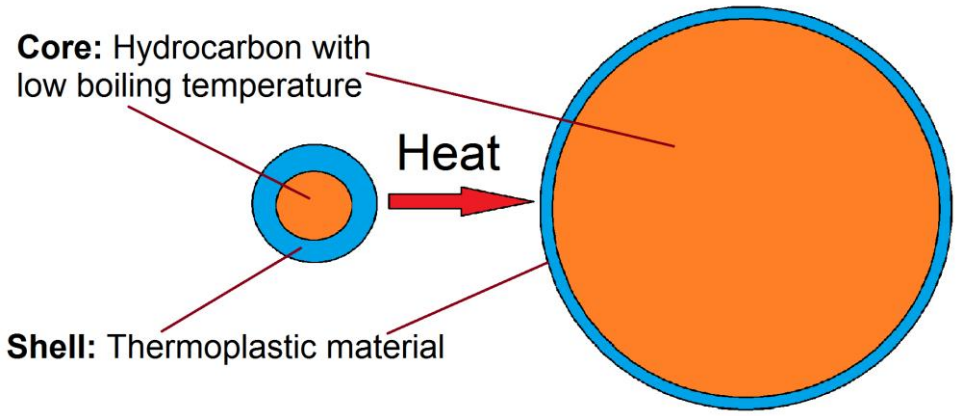

Figure 3.1. Schematic illustration of TEMs structure.

To achieve good expansion property, it is critical that the outer shell material of the TEMs should have:

- Good barrier property to retain hydrocarbon inside;
- Thermal stability;
- Good deformability at elevated temperature to allow expansion.

In terms of shell material chemical composition, acrylonitrile or vinylidene chloride are commonly used as the main component but methyl methacrylate, methyl acrylate and other monomers might be used to form copolymers for a better microsphere performance (Jonsson, 2010).

For the scope of this project and the expectation to develop a disbondable adhesive system, it is essential to understand the expansion process of these microspheres. Manufacturers normally provide two critical temperatures in their datasheets:

- Initiation temperature ($T_{initiation}$) : this is the temperature when microspheres start expansion;
- Maximum expansion temperature (T_{max}) : this is the temperature when microspheres reach maximum expansion ratio.

As illustrated in Figure 3.2, TEMs will undergo a temperature induced volumetric change from an unexpanded state, through expansion initiation, to maximum expansion, and final shrinking stage.

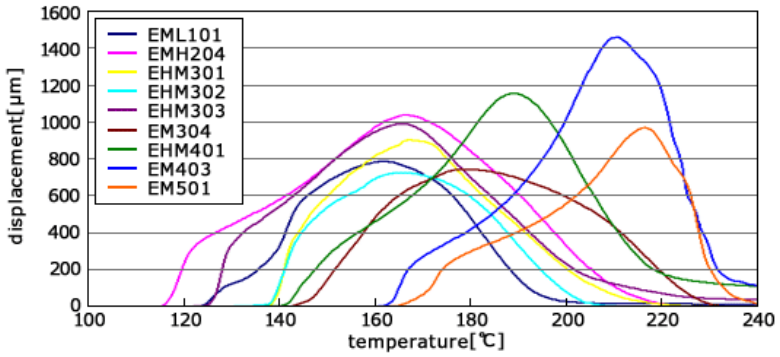

Figure 3.2. Thermal mechanical analysis of different grades of TEMs from Advancell. (Matsumoto Yushi-Seiyaku, no date)

Previous research conducted by JTRC (McCurdy, 2011) has pointed out that the premature expansion of TEMs during curing and the paint baking process in an oven could damage the integrity of adhesive system. To avoid this potential problem, the current research employed high temperature initiated TEMs grades. Table 3.2 showed basic information of the four TEMs grades selected for this research.

Table 3.2. Basic information of selected TEMs grades. (see Appendix)

Tradename	Grade	T initiation (C^o)	T max (C^o)	Particle size(um)
Matsumoto	F230D	180 - 190	220 - 240	20-35
Advancell	EM501	165	217	24.7
Expancel	920DU120	123 - 133	194 – 206	29 - 38
Expancel	920DU120HEMA	123 - 133	194 – 206	29 - 38

These four grades of TEMs were kindly provided by two Japanese manufacturers (Matsumoto Microsphere F230D and Advancell EM501) and one Swedish manufacturer (Expancel 920DU120 and Expancel 920DU120HEMA). In addition to the differences in critical temperatures and particle size distribution, it should also be noted that:

- EM501 grade is reported to have a sharp particle size distribution (PSD), which could potentially offer a better expansion efficiency;
- The thermoplastic shell of Expancel 930DU120 grade TEMs is composed of a copolymer of acrylonitrile, methacrylonitrile and methyl methacrylate, see Appendix;
- 920DU120HEMA grade is an experimental grade: this is the 920DU120 grade to which 15wt% 2-hydroxyethyl methacrylate (HEMA) has been added on the thermoplastic shell (hydroxyl groups brought by HEMA could potentially enhance adhesion and wetting with epoxy adhesive matrix);
- The thermoplastic shell of EM501 grade TEMs is composed of copolymers of acrylonitrile and methacrylonitrile, see Appendix.

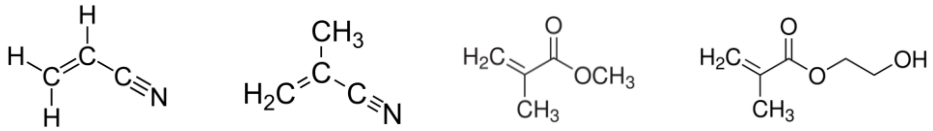

(a) (b) (c) (d)

Figure 3.3. Chemical structures of key monomers in shell composition. (a) Acrylonitrile; (b) Methacrylonitrile; (c) Methyl Methacrylate; (d) 2-Hydroxyethyl methacrylate;

3.4. TEMs Surface Modification Technique

As has been identified in the literature research, disbonding efficiency and additive/matrix compatibility are major concerns for automotive disbonding techniques. For the TEMs approach adopted in this project, a suitable surface modification technique needs to be selected to especially improve TEMs/adhesive compatibility while retaining satisfactory in-service disbonding effectiveness.

For the scope of this project, the most related research regarding TEMs surface modification was jointly conducted by Debonding Ltd and the Armes group at Sheffield University (Carter, 2008) (Schmid et al., 2009). TEMs were successfully coated with polypyrrole, which has a broad absorption peak (900-1500nm) in the infrared, by in-situ deposition. The initiation time of polypyrrole coated TEMs was significantly shortened (162 ± 2 seconds to 11 ± 1 seconds) using a near-infrared lamp to induce localised heating. However, this research did not evaluate the performance of polypyrrole coated TEMs incorporated into composite materials. Changes to mechanical properties or long-term durability remain unknown. Additionally, no convincing analysis was given to assess the reliability of the polypyrrole coating, e.g. exfoliation and degradation problems. Chemical treatments or adhesion promoters can also be used to increase additive dispersibility and therefore additive/matrix interaction.

However, these methods can only improve the intramolecular van der Waals force or hydrogen bonding between TEMs and adhesive matrix. To this extent, a method to create strong covalent bond between TEMs and adhesive matrix is preferred.

Surface grafting technology is one successful means of producing strong covalent bonds. 'Grafting to' and 'grafting from' are two common approaches (Zheng and Stover, 2003). In the 'grafting to' approach, end-functionalised groups (e.g. hydroxyls, epoxides and thiols) react with a suitable surface to form covalent bond. However, limitations such as low grafting density or difficulties in the synthesis of suitable functionalised polymers restrict its wider application. The 'grafting from' approach, in which polymer chains grow from the surface (Surface Initiated Polymerisation 'SIP'), shows wider applicability. Jonsson and co-workers demonstrated the feasibility of growing poly(glycidyl methacrylate) chains from thermally expandable microspheres via ARGET ATRP whilst retaining their expansion properties (Jonsson et al., 2009).

Among all SIP techniques, controlled radical polymerisation is preferred due to the better control over molecular architecture design, which leads to tailored material properties. Controlled radical polymerisation (CRP), or reversible-deactivation radical polymerization (RDRP) as International Union of Pure and Applied Chemistry (IUPAC) recommended, have been extensively studied, including nitroxide mediated polymerisation (NMP), atom transfer radical polymerisation (ATRP) and reversible addition fragmentation chain transfer polymerisation (RAFT).

First discovered in 1995(Wang and Matyjaszewski, 1995)(Kato et al., 1995), ATRP provides a simple and controlled polymerisation solution, which can be conducted in industrial equipments, with good control of molecular weight, structures and high degree of chain end functionality. The ATRP technique has been applied to various areas including cell adhesion (Barbey et al., 2009) (Bencherif et al., 2009), drug release (Vasani et al., 2011), anti-biocorrosion coatings (Yuan et al., 2009), silicon wafers (Zhu and Edmondson, 2011), etc. Figure 3.4 shows ATRP publication in recent years.

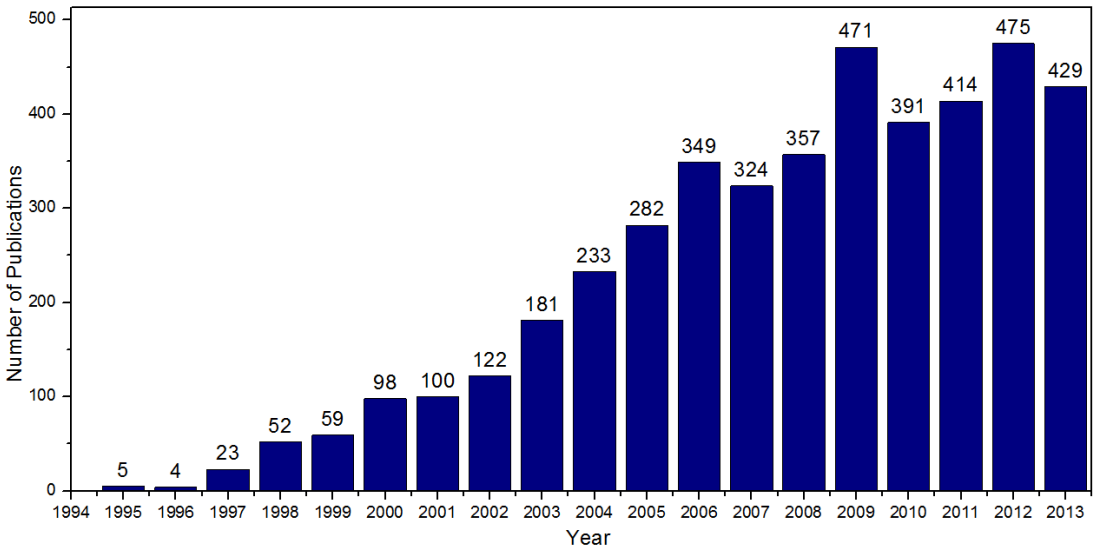

Figure 3.4. ATRP publications on ACS Publications. Source: http://pubs.acs.org/; Search settings: ATRP, accessed August, 2014.

The following section provides a brief literature review of ATRP technique with its mechanisms and kinetics. Recent relevant advances of using surface-initiated ATRP in the particle surface modification process are summarised.

3.4.1. Atom Transfer Radical Polymerisation (ATRP)

3.4.1.1. Mechanism and Kinetics

The ATRP process depends on the dynamic equilibrium illustrated in Figure 3.5. Due to its wide application, the following discussions will be based on using a copper complex as an example. The dormant R-X bonds, which represents alkyl halides/macromolecular species, reacts with Cu^{1+}/L (or other transition metal complexes with ligands) which causes the homolytic cleavage of the alkyl halogen bond. This leads to the formation of R^* (propagating radicals) and X-Cu^{2+}/L (or halide ligands with a transition metal complex in higher oxidation state) (Matyjaszewski, 2012) (Bergenudd, 2011) (Braunecker and Matyjaszewski, 2007). The concentration of propagating radicals [R^*] is balanced by the rates of activation (k_{act}) and deactivation (k_{deact}). In theory, the macromolecular chains should all remain end-capped with the reversible halogens and could be further used as macroinitiators, i.e. the termination is reversible (Bergenudd, 2011).

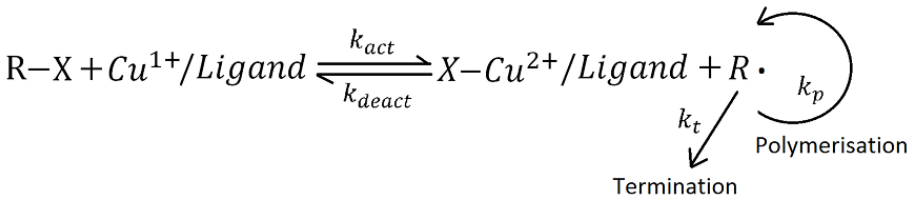

Figure 3.5. ATRP mechanism (R-X is dormant halides/macromolecular species, X is halogen, R• is growing chain radical).

Assuming a steady state reaction, the rate of polymerisation is determined by the monomer concentration [M], radical concentration $[P_n^*]$ and propagation rate constant k_p, shown in Equation below.

$$R_P = k_P[\mathrm{M}][\mathrm{P_n^*}] = k_P\ \mathrm{K_{ATRP}}\frac{[\mathrm{P_n^*X}][\mathrm{Cu^I/L}][\mathrm{M}]}{[\mathrm{X-Cu^{II}/L}]} \quad \text{……Equation 3.1}$$

The value of K_{ATRP}, defined as the ratio of K_{act} and K_{deact}, can be obtained from experimental analysis of polymerisation mixture using common techniques such as nuclear magnetic resonance (NMR) spectroscopy, gas chromatography (GC), gel permeation chromatography (GPC), etc. These reaction constants are highly temperature dependent. Both Arrhenius empirical equation and Eyring equation are commonly used to describe this temperature dependence. Research has shown that ATRP initiators with less activity such as alkyl halides can be accelerated at a higher rate than active initiators by increasing reaction temperature (Seeliger and Matyjaszewski, 2009).

3.4.1.2. ATRP components

To gain a precise control of polymer properties such as molecular weight, polydispersity and polymer architecture, it is crucially important to choose the key components of the ATRP systems, including monomer, solvent, initiator and catalyst/ligand system.

ATRP monomer is normally an unsaturated chemical that can be used to stabilise a propagating radical, such as methacrylates, acrylonitrile and styrenes. ATRP initiator

begins polymerisation by generating propagating chains. To achieve a low PDI, initiation rate must be higher than the propagating rate to ensure all the chains growing at the same time. Also, a low PDI can be achieved if the R-groups in alkyl halides have similar structure in both initiator and monomer (Carlmark, 2002). Initiator activity depends on lots of factors such as initiator substitution (primary < secondary < tertiary), radical stabilising α-substituent (e.g. *−C(O)NEt2<−Ph<−C(O)OMe<–CN*), and leaving atom/group (e.g. methyl 2-halopropionates: *Cl* < *Br* < *I*) (Tang and Matyjaszewski, 2007).

A suitable solvent is necessary not only as a media for the dissolution of other ATRP components but also for the control of polymerisation rate (He et al., 2013). Horn and Matyjaszewski (2013) conducted research using 14 different solvents to investigate their effects on the ATRP activation rate (k_{act}) and identified up to 30 times difference. The main reason was attributed to the fact that the solvent with the highest dipolarity/polarizability was more prone to stabilise the catalyst/ligand complex to a higher degree. Bergenudd (2011) investigated the solvent effects on ATRP of oligo(ethylene glycol) methacrylate) using five Cu complexes with six monomer-solvent mixtures. The research showed that solvent choice had significant influences on the apparent rate constant and reduction potentials of the copper complexes, which affected the degree of control over polymerisation process. It was also pointed out that catalyst choice played a more important role. In terms of ATRP catalysts (e.g. Cu, Fe, Ti, Mo, Re, Ni, etc), Cu complexes show the best efficiency and suitability (Carlmark, 2002). Fe complexes are more preferred for their biocompatibility in relevant applications (He, et al., 2013).

3.4.2. Activators Regenerated by Electron Transfer (ARGET) Initiation System

Despite its success, the application of conventional ATRP technique in large scale industrial productions has been hindered by some key drawbacks. In recent years, different initiation systems have been developed. ARGET ATRP has been one of the most successful ATRP initiation systems with the following advantages:

- Only 50 ppm catalyst are required which makes purification/disposal process of toxic components cheaper or sometimes unnecessary especially for industry application (Shen et al., 2004);
- ARGET ATRP system has higher tolerance to oxygen and a catalyst can be added in oxidatively stable state (Braunecker and Matyjaszewski, 2007).

In the ARGET ATRP system, an excessive amount of reducing agent is added to continuously regenerate Cu^{I} throughout the reaction. Side reactions such as outer sphere electron transfer can also be inhibited significantly with the decrease of catalyst concentration (Braunecker and Matyjaszewski, 2007). Readers are referred to Matyjaszewski et al. (2006) for an investigation of catalyst concentration, ligand selection, ligand concentration and reducing agents used in the ARGET ATRP process.

3.4.3. Surface Initiated ATRP (SI-ATRP)

With the recent development of ATRP techniques, SI-ATRP has been extensively studied as a means of surface modification both for flat and spherical surfaces. The architecture and chemistry of tethered polymer chains grown from substrate surface can significantly alter material properties. Recent studies (Marutani et al., 2004) (Bansal et al., 2006) (Harton and Kumar, 2007) (Akcora et al., 2009) have proposed theories and also experimentally demonstrated that nanoparticles with long and densely grafted chains may contribute to an improved wettability and dispersion in matrices. Therefore, it is critically important to accurately understand SI-ATRP system.

SI-ATRP generally follows the same mechanism as conventional ATRP techniques. However, the existence of a functionalised surface leads to some differences, of which initiator immobilisation and chain conformation are identified and mainly discussed below.

3.4.3.1. Initiator Immobilisation

Initiators have to be immobilised onto the functionalised surface before polymerisation. Different surface conditions require different initiator immobilisation techniques. Common immobilisation techniques have been categorised into three approaches and summarised in Table 3.3 (Zhu, 2012):

- Direct reaction with electrophilic initiator; (Carlmark, 2002) (Lindqvist et al., 2008) (Xu et al., 2007) (Yao et al., 2008)
- Monolayers approach; (Kim et al., 2000)(Shah et al., 2000(Matyjaszewski et al., 1999) (Jeyaprakash et al., 2002)
- Macroinitiator approach. (Mizutani et al., 2008) (Liu et al., 2004) (Edmondson et al., 2008) (Edmondson et al., 2009)

Table 3.3. Summary of initiator immobilisation approaches.

Approach	Brief Description	Sub-categories	Limitations
Direct reaction	Involves reaction of electrophilic initiator with OH or NH_2 groups on the substrate surface	-OH groups	Substrate surface needs to contain or be pre-functionalised with -OH or -NH_2 groups.
		-NH_2 groups	
Monolayers	Initiating groups are immobilised onto a monolayer pre-formed on substrate surface	Thiol-noble metal (gold) bonding	Susceptible to oxidation which incurs desorption issues; too expensive for industrial applications.
		Silane-silanol bonding	Use of expensive and toxic reagents, e.g. H_2PtCl_6 and $HSiCl_3$.
Macroinitiator	Macroinitiators (containing numerous initiating groups) are immobilised onto substrate surface	Polyelectrolyte	Generally more attractive and has broader application but requires certain surface chemistry.
		Non-polyelectrolyte	For immobilisation via solution deposition, further grafting may introduce a lack of reliability and susceptibility to desorption; For immobilisation via in situ synthesis, complex surface treatments may be required.

3.4.3.2. Chain Conformation

The conformation of tethered polymer chains, as they grow during polymerisation, is vitally important to the ATRP process as well as the properties of modified surface. Chain conformation is mainly affected by *grafting density*, *surface curvature* and *chain length*. Daoud and Cotton (Daoud and Cotton, 1982) have presented theoretical studies on the conformation of a star shaped polymer and proposed a model which has been further applied to polymer brush systems. Depending on the grafting density, three types of conformational behaviours were categorised as:

- 'Mushroom-like' regime (when the diameter of chain gyration is larger than the distance between grafting points);
- Semidilute polymer brush (SDPB) regime;
- Concentrated particle brush (CPB) regime. (Dukes et al., 2010)

With the increase in grafting density, the conformation of tethered polymer chains will change from a 'mushroom-like' regime to SDPB and to CPB. The reader is referred to (Hui et al., 2014) (Dukes et al., 2010) (Wu et al., 2003) (Barbey et al., 2009) (Bombalski, 2007) for more in-depth studies of the theories and models of polymer brush system.

In terms of surface curvature, SI-ATRP can be conducted on both spherical (concave or convex) and flat surfaces. Numerous studies have presented theories of curvature effect on the conformation of polymer brushes (Wijmans and Zhulina, 1993) (Zhulina and Borisov, 1996) (Tagliazucchia and Szleifer, 2012). It is generally believed that higher surface curvature endows more freedom to growing chains by separating active chain ends from interchain termination reactions. This effect has been experimentally tested in a recent research conducted by Benjamin and co-workers (Cheesman et al., 2013). Using ARGET ATRP technique to grow poly [2-(diethylamino)ethyl methacrylate] on silica particles with different diameters (120nm, 200nm, 450nm, 840nm), their research showed a positive correlation of curvature and dry brush thickness after 30 minutes of growth.

3.4.4. TEMs Surface Modification via ARGET ATRP

The TEMs surface modification work in this research was inspired by the pioneering study conducted by Jonsson and co-workers (Jonsson et al., 2009). Poly(glycidyl methacrylate) (PGMA) chains were grown from TEMs' surfaces using activators regenerated by electron transfer atom transfer radical polymerization (ARGET ATRP) technique.

Since each glycidyl methacrylate molecule contains one epoxide group, poly(glycidyl methacrylate) chains contain an amount of n epoxide groups (n denotes the degree of polymerisation). Modified TEMs with epoxide groups can react with the hardeners during curing process of epoxy based adhesive forming covalent bonds thereby strengthening the TEMs/adhesive composite, see Figure 3.6.

As has been reviewed in this chapter, a range of factors (temperature, solvent, catalyst, concentration, etc) will affect the polymerisation process in ARGET ATRP. For the scope of this project, the effect of temperature on TEMs surface modification was further studied based on the pioneering research by Jonsson. Experimental procedures and chemical usage are detailed in Chapter 4. The objectives of TEMs surface modification work are to:

- Grow PGMA chains from TEMs to improve TEMs/adhesive compatibility;
- Retain TEMs' expansion property which affects the disbonding performance of TEMs/adhesive system.

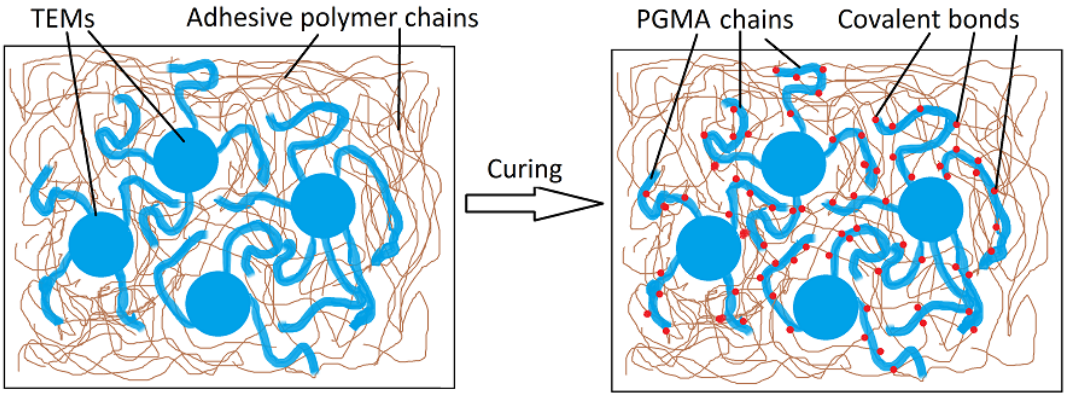

Figure 3.6. Schematic illustration of covalent bonds formed between modified TEMs (PGMA chains grafted) and adhesive.

3.5. Summary

This chapter reviewed surface modification techniques and focused on introducing one of the most successful 'grafting from' techniques: surface initiated atom transfer radical polymerisation. The general ATRP mechanism and key components were reviewed. It was noted that the architecture and chemistry of polymer chains, tethered to the substrate surface, would significantly affect the modified surface properties. Initiator immobilisation and chain conformation, which are affected by surface curvature, chain length and grafting density, were investigated for a better understanding of SI-ATRP system. The ARGET ATRP technique was finally selected to be employed in this research for TEMs surface modification.

In summary, selected materials for testing are listed below:

- Adhesive: 3M Scotch-Weld 9323 2K epoxy adhesive;
- Substrate: EN AW-6082 T6, 2mm thickness;
- Thermally expandable microspheres: Matsumoto Microsphere F230D, Advancell EM501, Expancel 920DU120 and Expancel 920DU120HEMA.

Chapter 4. Experimental Methodology

4.1. Experimental Test Programme

To fulfil the overall objectives of this project, the experimental test programme was designed and divided into four stages. This section provides a general description of each stage's work. Test methods and procedures involved at different stages are detailed in section 4.2.

4.1.1. Stage 1: Characterisation of Test Materials

It is essential to understand and verify the relevant properties of all test materials before investigating the disbonding performance and general properties of TEMs/adhesive Composite. Bulk tensile properties were measured for aluminium substrate and adhesive matrix. Viscoelastic behaviour of the adhesive was determined using dynamic mechanical thermal analysis (DMTA).

For TEMs, since different manufacturers adopted different methods, consistent measurements of all key properties are undoubtedly essential. Key properties which may affect TEMs performance in adhesive disbonding scenario included particle size distribution analysis, surface chemistry (Fourier transform infrared) and microstructure characteristics (scanning electron microscope).

4.1.2. Stage 2: Disbonding Performance of TEMs/Adhesive System

The second stage of work was to investigate the disbonding performance of all selected grades of TEMs and determine the optimum formulations for the next stage of work. To establish a consistent disbonding effectiveness test for this project, literature research and experimental work were conducted.

Due to its simple configuration and wide use in standard testing (e.g. BS EN 15336:2007, BS EN 1465:2009), the single lap joint (SLJ) was chosen as the joint type in the disbonding effectiveness test. In terms of the best disbonding temperature, as was mentioned in Chapter 3, manufacturers normally provide two

critical temperatures: expansion initiation temperature ($T_{initiation}$) and maximum expansion temperature (T_{max}). However, it is noted that there is a third temperature referring to the end point of the temperature-expansion curve obtained from thermal mechanical analysis (TMA) test, see Figure 3.2. This third temperature marks the end of TEMs shrinking as a result of hydrocarbon gas leakage at temperatures higher than T_{max}. In this thesis, this third temperature is referred to as T_3. An illustration of these three critical temperatures is shown in Figure 4.1. All T_3 of selected TEMs grades are listed in Table 4.1. Figure 4.2 gives a direct observation of the volume change of 0.5 grams of EM501 grade TEMs at different critical temperatures.

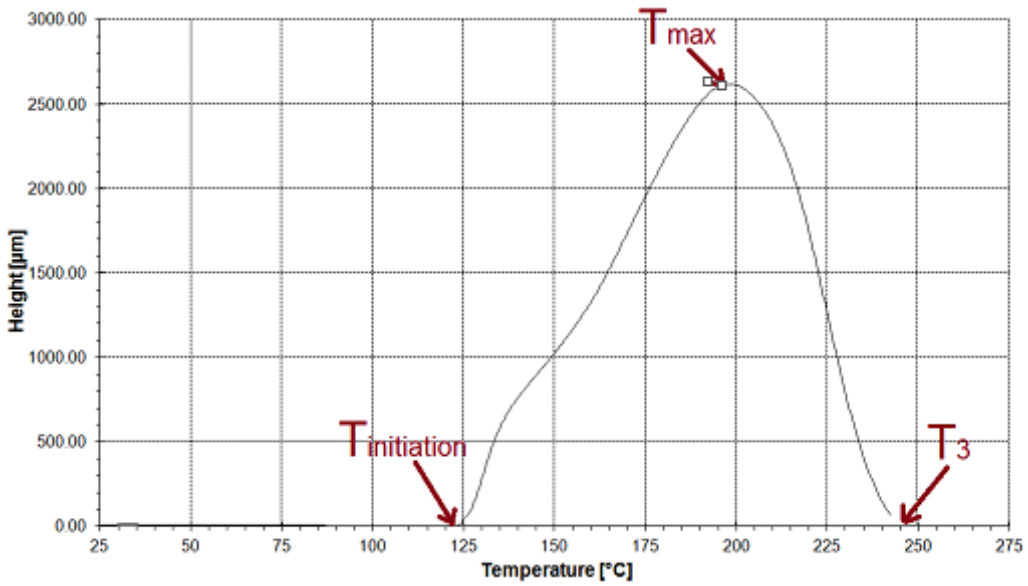

Figure 4.1. Thermal mechanical analysis of 930DU120 grade TEMs with critical temperatures marked.

Table 4.1. Critical temperatures of selected grades of TEMs.

Tradename	TEMs Grade	$T_{initiation}$ (°C)	T_{max} (°C)	T_3(°C)
Matsumoto	F230D	180 - 190	220 - 240	265
Advancell	EM501	165	217	240
Expancel	930DU120	123 - 133	194 – 206	245
Expancel	930DU120HEMA	123 - 133	194 – 206	245

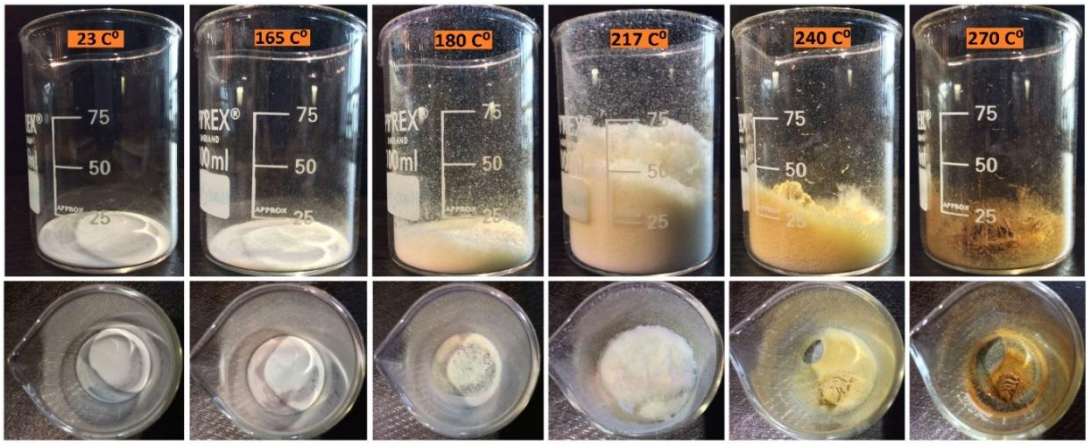

Figure 4.2. 0.5 grams of EM501 grade TEMs under different temperatures.

To achieve the best disbonding performance for TEMs/adhesive system, the author believes that adhesive joint should be heated to T_3. This was supported by preliminary experimental results shown in Table 4.2, which compared residual tensile lap shear strength of 20wt% EM501 (T_3=240 °C) incorporated 9323 epoxy adhesive both before and after oven heat activation (60s hold time). Tensile lap shear strength was measured according to the procedures detailed in 4.2. All tests were performed at ambient temperature. It can be seen from the results that the residual strength showed only 8.6% decrease at 165 °C ($T_{initiation}$) and 45.4% decrease at 217 °C (T_{max}). Residual strength of adhesive joints reduced to 5.2 MPa (70.1% decrease) at 240 °C (T_3) and showed no significant change at higher temperature, e.g. 270 °C. Photographs of fracture surfaces showed 100% cohesive failure at 165°C and mixed mode failure at 217°C, 240°C and 270 °C.

Table 4.2. Residual strength at different heat activation temperatures for 20wt% incorporation of EM501.

	23 °C	165 °C	217 °C	240 °C	270 °C
Average(MPa)	17.4	15.9	9.5	5.2	4.9
Standard Deviation	0.91	0.49	0.98	0.78	0.24

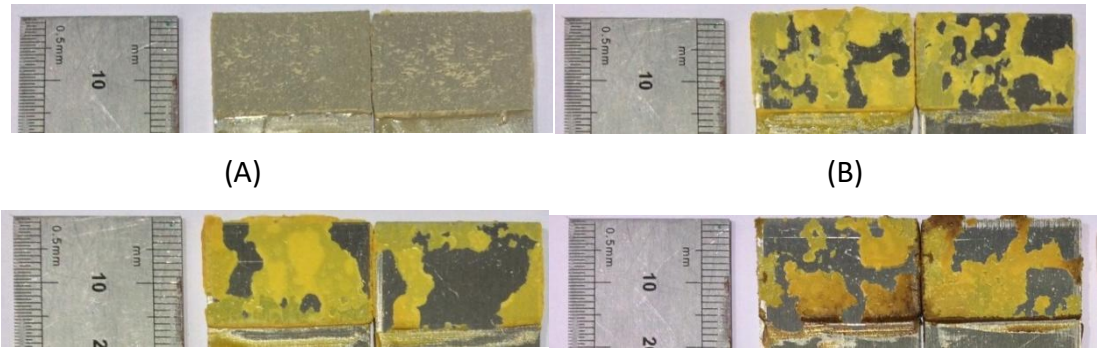

(A) (B)

(C) (D)

Figure 4.3. Photographs of fracture surface of adhesive incorporated with 20wt%EM501 at different heat activation temperatures. (A) 165 °C; (B) 217 °C; (C) 240 °C; (D) 270 °C.

It was noted from the literature research that there was no current method to establish disbonding effectiveness for an adhesive joint. Previous research within JTRC (McCurdy, 2011), reported a method which used a hot air gun for heat activation and measured the elapsed time taken to induce adhesive failure (chemical foaming agents or TEMs incorporated) as one of the references for disbonding effectivenss evaluation.

The author has made similar attempts using this method in the preliminary experimental work. However, possibly due to the differences in material selection, adhesive failure was not identified in most cases and residual strength had to be measured subsequently. Large deviation of the elapsed time recording also poses a potential problem. The author believes that this previous method may well be a better reflection of a practical disbonding scenario where the joint is separated at a temperature higher than the glass transition temperature of adhesive matrix (Tg is around 90°C for Scotch-Weld 9323), but cannot preclude the temperature effect and provide an accurate evaluation of TEMs' performance.

Considering all these inherent problems, a simplified and well controlled disbonding effectiveness test method was therefore proposed to better investigate the behaviour of TEMs and disbonding mechanism of TEMs/adhesive system. Tensile lap shear strength before and after oven heat activation were measured with the reduction rate calculated for disbonding effectiveness analysis. Samples after heat

activation were allowed to cool down to room temperature before residual strength measurement.

For the sake of material saving and reducing the amount of experimental work, the effect of TEMs concentration on disbonding performance was only investigated on one grade of TEMs, EM501. The optimum TEMs concentration was then chosen to evaluate the disbonding effectiveness and environmental conditioning test of the other three grades of TEMs. SEM imaging was used throughout this stage to characterise microstructural changes. The experimental strategy at stage 2 was summarised in Figure 4.4.

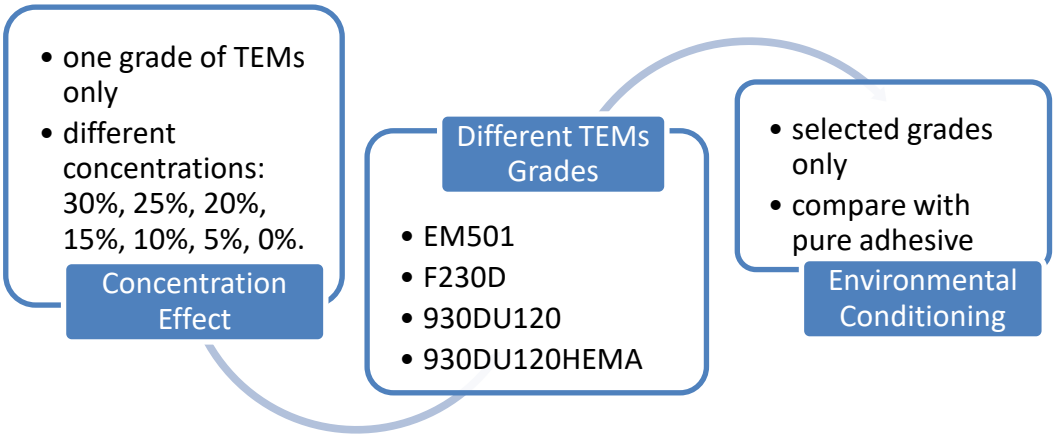

Figure 4.4. Illustration of experimental strategy at Stage 2.

4.1.3. Stage 3: TEMs/Adhesive Composite Bulk Property

The third stage investigated the bulk properties of TEMs/adhesive composite. Bulk tensile test and dynamic mechanical thermal analysis were all employed to investigate a series of material properties and generate more information on the TEMs/adhesive compatibility issue. Test specimens were divided into two categories: a) unconditioned specimens; b) environmentally conditioned specimens. Only selected grades of TEMs with optimum concentration based on the results from Stage 2, were studied at this stage.

Before environmental conditioning test could be undertaken, water immersion test was conducted to measure the time taken to achieve complete water saturation ($t_{saturation}$) in the pure adhesive and TEMs/adhesive composite. For this purpose, the test procedures, detailed in 4.2.7., were simplified to obtain the $t_{saturation}$ point. The diffusion of water in structural adhesives complies with the Arrhenius equation which showed a positive correlation between diffusion rate and temperature (Adams et al., 1997). On this basis, a temperature of 40 ^{o}C was used to accelerate the hygrothermal ageing process. Test specimen dimensions matched the gauge length region of bulk tensile specimens to give a best prediction of $t_{saturation}$ for tensile test specimens as well.

4.1.4. Stage 4: TEMs Surface Modification via ARGET ATRP

At this final stage, the surface modification of TEMs was carried out to address the compatibility issues both identified from literature and investigated in the experimental work conducted at earlier stages of this research. The surface modification work was relied upon reacting with hydroxyl groups present on the surface of TEMs. This means only 930DU120HEMA grade was used at this stage.

4.1.4.1. General TEMs Surface Modification Procedures

This general TEMs surface modification process was an adaptation of the recent research conducted by Jonsson and colleagues (Jonsson et al., 2009). The whole process was mainly divided into two steps, as illustrated in Figure 4.5.

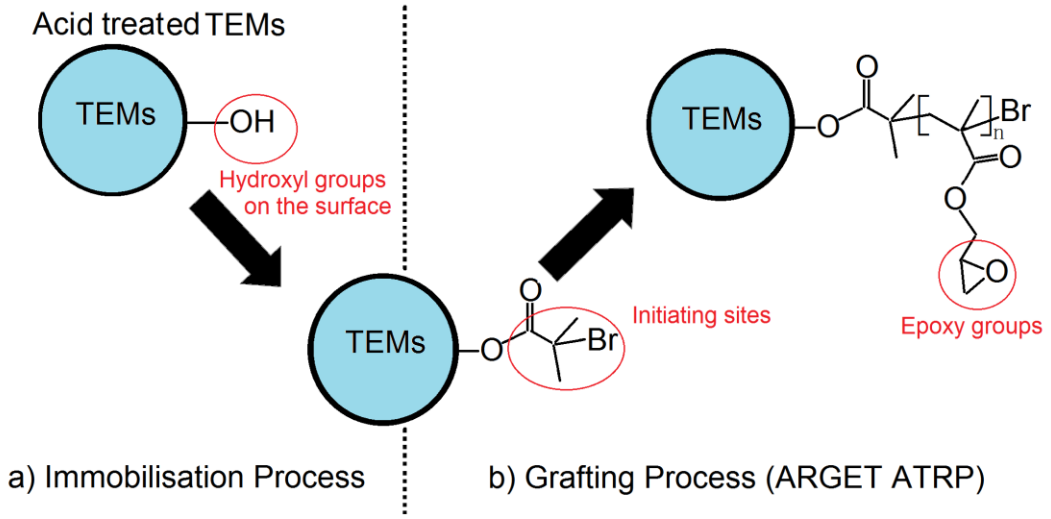

Figure 4.5. Schematic illustration of TEMs surface modification process.

a) Immobilisation Process

This first step was to covert hydroxyl groups on TEMs to α-bromo ester. Prior to immobilisation, TEMs were treated with 10wt% sulphuric acid solution to remove Magnesium hydroxide contained in the TEMs powder, see Appendix. Deionised water was used in the subsequent filtering and rinsing process. Sulphuric acid, which would cause unwanted chemical reactions in the immobilisation process, must be thoroughly cleansed. The TEMs were then dried at 60 ^{o}C in the oven for 8 hours after acid treatment.

The chemical reaction involved in immobilisation process is highly exothermic and requires extra precautions. 2-Bromoisobutyryl bromide (BIBB) was therefore first diluted with a certain amount of dichloromethane and then added drop wise to the TEMs solution which contains dichloromethane as solvent, triethylamine as a reducing agent and 4-(Dimethylamino)pyridine as a catalyst. The triethylamine was dried with molecular sieves (4 Angstroms and 8-12 Mesh) prior to use. It was shown

in the literature that the hydrocarbon content, which controls the expansion property of TEMs, decreases after 2 hours immersion in dichloromethane (Jonsson et al., 2009). The solution was stirred gently at room temperature for 2 hours using a magnetic stirrer. After immobilisation, TEMs were washed with dichloromethane and dried at 50 ^{o}C for 1 hour. The chemical quantities used in the immobilisation process are listed in Table 4.3. All chemical were used as received unless otherwise specified. The experimental setup is shown in Figure 4.6(Left).

Table 4.3. Chemical usage during immobilisation process.

Chemical Name	Function	Dosage	Chemical Structure	Supplier/ Grade
Sulphuric acid treated TEMs	N/A	5 g	N/A	N/A
Triethylamine	Reducing Agent	5 g	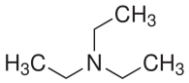	Sigma-Aldrich (≥99%)
4-(Dimethylamino) pyridine	Catalyst	12.6 mg	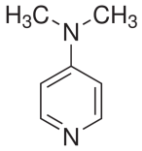	Sigma-Aldrich (≥99%)
2-Bromoisobutyryl bromide	ATRP Initiator	11 g	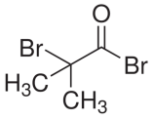	Sigma-Aldrich (98%)
Dichloromethane	Solvent	50 ml		Fisher Scientific (≥99%)

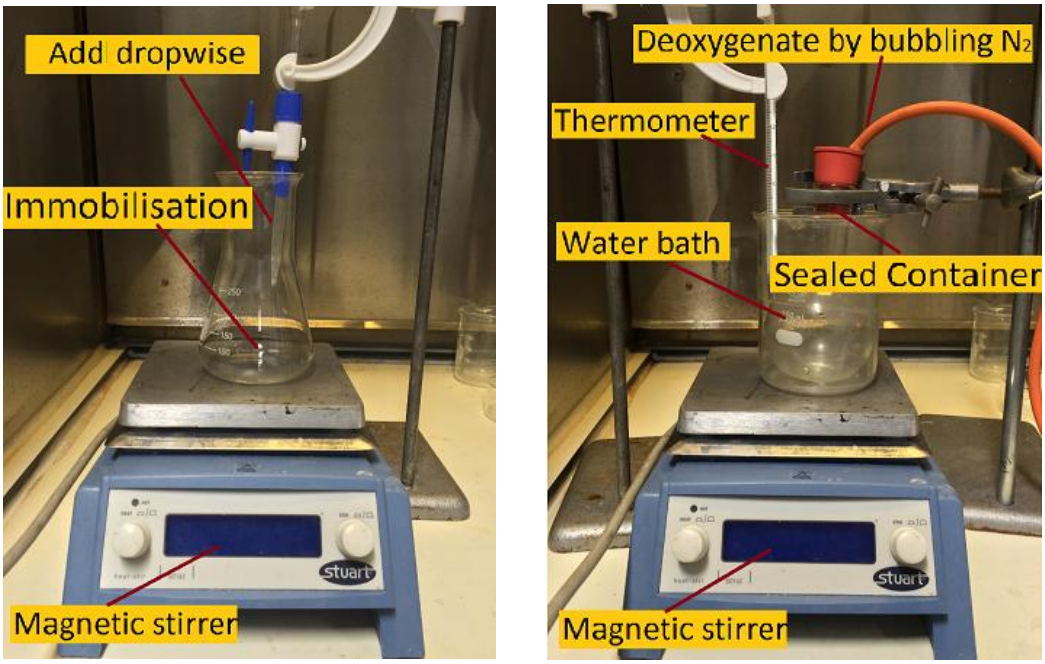

Figure 4.6. Experimental setup of TEMs surface modification.
(Left) Immobilisation process; (Right) ARGET ATRP process.

b) ARGET ATRP with TEMs

The second step was to grow PGMA chain from TEMs surface using α-bromo ester as initiating sites. Glycidyl methacrylate (GMA) was first passed through a column of inhibitor remover to remove monomethyl ether hydroquinone (100ppm as inhibitor) prior to use. N,N,N′,N′′,N′′-Pentamethyldiethylenetriamine (PMDETA), GMA and Copper(II) bromide was added to toluene solution in a rubber septa sealed container. The mixture was ultrasonically treated for 10 minutes for full Copper(II) bromide dissolution. The container was then deoxygenated by bubbling nitrogen gas for 5 minutes. Polymerisation was initiated by adding TEMs and L-ascorbic acid and heated up to certain temperatures specified in the latter section. After polymerisation, the TEMs were washed with toluene and dichloromethane and dried at 50 ^{o}C in an oven for 5 hours. See Table 4.4 for chemical quantities used in this step. The experimental setup of ARGET ATRP is shown in Figure 4.6(Right).

Table 4.4. Chemical quantities during ARGET ATRP process.

Chemical Name	Function	Dosage	Chemical Structure	Supplier Grade
Immobilised TEMs	Macroinitiator	3g	N/A	N/A
Toluene	Solvent	30ml	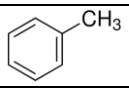	Sigma-Aldrich (98%)
Copper(II) bromide	Catalyst	2.52mg	$CuBr_2$	Sigma-Aldrich (99%)
Glycidyl Methacrylate	Grafting monomer	32.4g	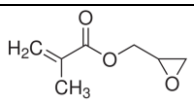	Sigma-Aldrich (97%)
PMDETA	ATRP Ligand	47.1mg	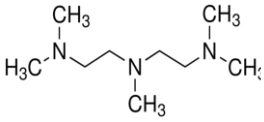	Sigma-Aldrich (99%)
L-Ascorbic Acid	Reducing agent	50 mg	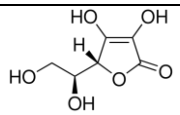	Sigma-Aldrich (≥99%)

4.1.4.2. Investigation of the Effect of Temperature on TEMs Surface Modification via ARGET ATRP

To grow PGMA chains from the TEMs' surface while retaining their expansion properties, key parameters need to be carefully controlled. The effect of temperature was investigated to optimise the ARGET ATRP system for better TEMs surface modification. TEMs surface modification was conducted at three different temperatures: 23 ^{o}C, 30 ^{o}C, 37 ^{o}C.

Regardless of chain terminations, modification for longer periods will ideally achieve longer polymer chains. However, solvent can have an adverse effect on TEM properties as a function of time. As was introduced in Chapter 3, the expansion property of TEMs is mainly determined by the hydrocarbon content confined within the outer shell material. Although the shell material generally has good chemical resistance (see Appendix), it was shown in the literature (Jonsson et al., 2009) that long time immersion in certain solvents could plasticise or even degrade the shell material which would result in the leakage of hydrocarbon. This is especially notable when TEMs are exposed to high shear forces during solvent immersion. Therefore, for each temperature set, TEMs were modified for 3 hours

and 5 hours and characterised for changes. All other parameters remain unchanged as stated in the general procedure. In total, six variations of modified TEMs (two time sets and three temperature sets) were produced.

Attenuated total reflection (ATR) FTIR spectroscopy and SEM imaging were employed for the TEMs characterisation at this stage. Both of these techniques have been widely used to identify material's chemical functionality and microstructure. ATR FTIR allows non-destructive characterisation of solid and liquid samples without complex preparation process.

4.1.4.3. The Effect of TEMs Surface Modification on TEMs/Adhesive composite properties

Adhesive SLJs with modified TEMs incorporation were examined for changes in tensile lap shear strength and disbonding effectiveness. The best acting modified TEM variation was then incorporated into the adhesive and investigated for bulk properties (tensile test and DMTA test) in both unconditioned and environmentally conditioned scenarios.

4.2. Experimental Test Methods and Procedures

In this section, detailed procedures and experimental settings are given for each test technique used in this research.

4.2.1. Particle Size Distribution Analysis

The mean particle size and size distribution of thermally expandable microspheres (original TEMs and modified TEMs) were measured using laser diffraction particle size analyser Mastersizer 2000 equipped with a Hydro 2000MU dispersion unit. Particle refractive index and particle absorption index were set as 1.4 and 0, respectively. Deionised water was used as the dispersant.

Apart from the detailed particle size distribution data, D(0.1), D(0.5) and D(0.9), defined as the size value at which 10%, 50% and 90% particles are composed of smaller particles, were also cited in the results. The default output data of span (width of the distribution) and D[4,3] (volume weighted mean), defined in the following equations, were noted in the results.

Span=————————……..Equation 4.1.

D[4,3]=————……..Equation 4.2.

Where Di and Vi represents the geometric mean of each channel and volume fraction respectively.

4.2.2. Fourier Transform Infrared Spectroscopy

Fourier Transform InfraRed (FTIR) is extensively used as an analytical technique for the identification of a wider range of materials, both qualitatively and quantitatively (Smith, 2011). FTIR works by passing IR radiation through a sample and measuring the absorbed (or transmitted) radiation as a result of the dipole moment and excitation of molecular bond vibrations (stretching or bending). An interferometer

is employed to measure IR radiation of all frequencies simultaneously. The resulting interferogram is then converted into an FTIR spectrum (%transmittance or %absorption versus frequency) via the Fourier transformation mathematical technique. FTIR characterisation is normally conducted in the region of 4000 - 400 cm^{-1} which contains the information of most materials except for homonuclear diatomic molecules (IR inactive due to no dipole moment change) such as N_2, O_2, etc. Sample preparation is a very complex process for conventional FTIR test to obtain good quality data. Attenuated total reflection (ATR) FTIR is nowadays used to overcome sample preparation difficulties. As an infrared beam enters the ATR crystal (high index crystal), the internal reflectance generates an evanescent wave when it extends to the sample in contact with crystal, see Figure 4.7. The evanescent wave is then attenuated and collected from the IR detector. ATR FTIR requires sound contact between sample and ATR crystal since the penetration depth is only a few microns.

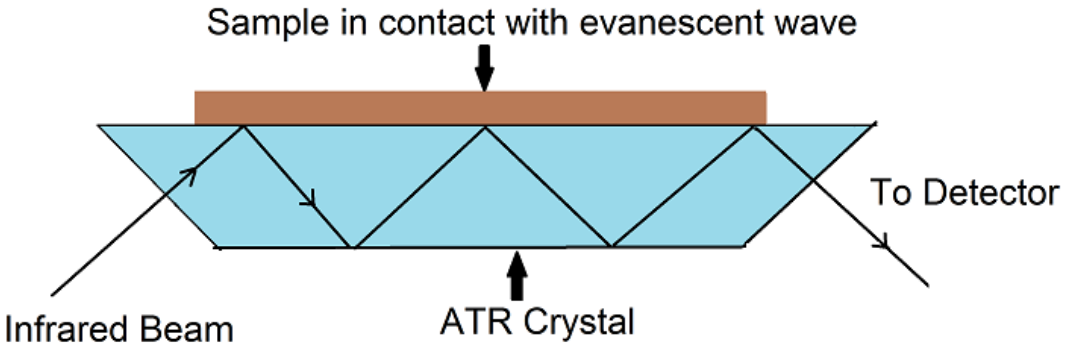

Figure 4.7. Schematic illustration of ATR system.

Thermally expandable microspheres (different grades and modified microspheres) were characterized using PerkinElmer Spectrum FTIR Spectrum 65 equipped with ATR accessory. The wavelength range was from 600 cm^{-1} to 4000 cm^{-1}. For each sample, 32 scans were obtained with a resolution of 4 cm^{-1}. The ATR crystal surface was cleaned with cellulose tissue and isopropanol prior to test. Background scan was performed before test. TEMs powder were carefully spread over ATR crystal with a spatula and firmly clamped to ensure good contact.

4.2.3. Tensile Lap Shear Test

SLJ was used to investigate the disbonding effectiveness. The following section describes the preparation and test procedures.

4.2.3.1. Single-Lap-Joint Specimens Preparation

Single-lap-joint specimens were prepared using pre-cut EN AW-6082 T6 aluminium substrates. Dimensions are shown in Figure 4.8, which was mainly based on BS EN ISO 1465:2009. Acetone was used to degrease the surface prior to bonding. A Speed Mixer DAC 150-FVR-K was used to mix adhesive with TEMs. Prior to the incorporation of TEMs in Scotch-Weld 9323 adhesive joints, epoxy resin (part B) and amine hardener (part A) were mixed first for 30 s at 3000 rev/min to achieve a low viscosity adhesive mixture. TEMs were then added and mixed for another 60 s at 3000 rev/min to ensure good dispersion. Bondline thickness was controlled to be around 0.2 mm using 5wt% solid glass spheres (diameter = 212nm -242 nm), which was added when mixing epoxy resin and amine hardener. Two foldback clips per joint were used to exert pressure during the curing process. Care was taken to remove adhesive fillets using a spatula. The specimens were cured at 90°C for 90 minutes.

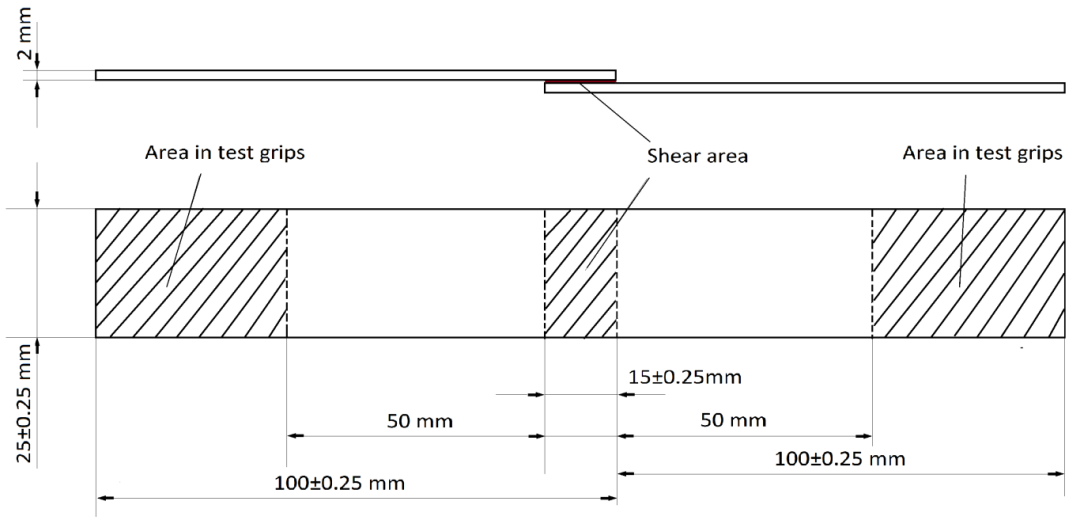

Figure 4.8. Dimensions of single-lap-joint specimen.

4.2.3.2. Tensile Lap Shear Test Procedures

Tensile lap shear tests were performed using an Instron 5582 tensile testing machine with 100kN load cell and a displacement rate of 1 mm/min. Tests were conducted at (23 ± 4) °C and (30 ± 5) % relative humidity. Specimen protect feature was enabled with a 10 N limit. Overlap area dimensions of joint specimens were measured by digital Vernier calliper. To save materials and reduce the amount of experimental work, three specimens were used for each test. More specimens were tested when large deviation occurred. Instron PC software Bluehill was adopted to record tensile force and crosshead displacement. Maximum shear stress τ_{SLJ} was calculated by following equation,

$\tau_{SLJ} =$—— **……Equation 4.3.**

where τ_{SLJ}= Tensile lap shear strength (MPa)

F_T = Tensile Load at fracture (N)

l = Length of overlap area (mm)

w = Width of overlap area (mm)

4.2.3.3. Determination of Failure Patterns

The determination of failure patterns was in accordance with BS EN ISO 10365:1995. The main adhesive failure patterns were shown in Figure 4.9.

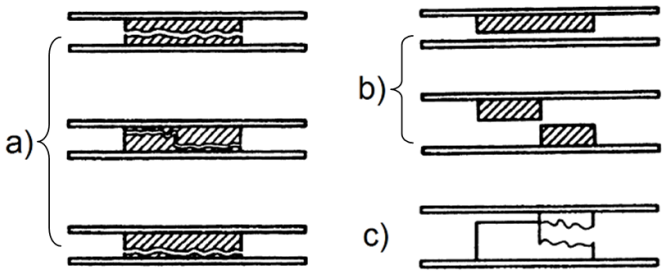

Figure 4.9. Illustration of main adhesive failure patterns.
(a) cohesive; (b) adhesive; (c) mixed mode. (BS EN ISO 10365)

4.2.4. Disbonding Effectiveness Test

As was discussed in the Experimental Test Programme section 4.1, the specimens were heated to T_3 to give the best disbonding performance in the adhesive bond line. Oven heat activation was argued as a better controlled method. To keep the consistency of test method, a maximum temperature of 270 ^{o}C was selected which covered the T_3 of all grades of TEMs. Following procedures were implemented:

- Single-lap-joint specimens were prepared as detailed in 4.2.3 (general preparation procedures) and 4.2.8 (environmental conditioning procedures).
- Test specimens were placed in the oven, heated up from room temperature to 270 ^{o}C and held for 1 minute to ensure the same temperature was achieved in the bondline.
- After heat activation, test specimens were allowed to cool down to ambient temperature prior to testing.
- The residue tensile lap shear strength was measured in accordance with the same procedures as stated in 4.1.3.
- The reduction in strength in percentage was calculated for each formulation as a reference for the assessment of disbonding effectiveness.

Disbonding Effectiveness = ———— **…….Equation 4.4.**

Where τ_{SLJ} represents the tensile lap shear strength for SLJs before heat activation represents the residual tensile lap shear strength for SLJs after heat activation.

4.2.5. Bulk Tensile Test

This bulk tensile test was performed to investigate the bulk properties of aluminium substrate and TEMs/adhesive composite. The preparation and test procedures are detailed in the following sections.

4.2.5.1. Aluminium Tensile Specimens Preparation

Aluminium tensile specimens were machined from EN AW-6082T6 aluminium plates in accordance with BS EN ISO 6892-1:2009. Schematic illustration and dimensions of specimen are shown in Figure 4.10 and Table 4.5.

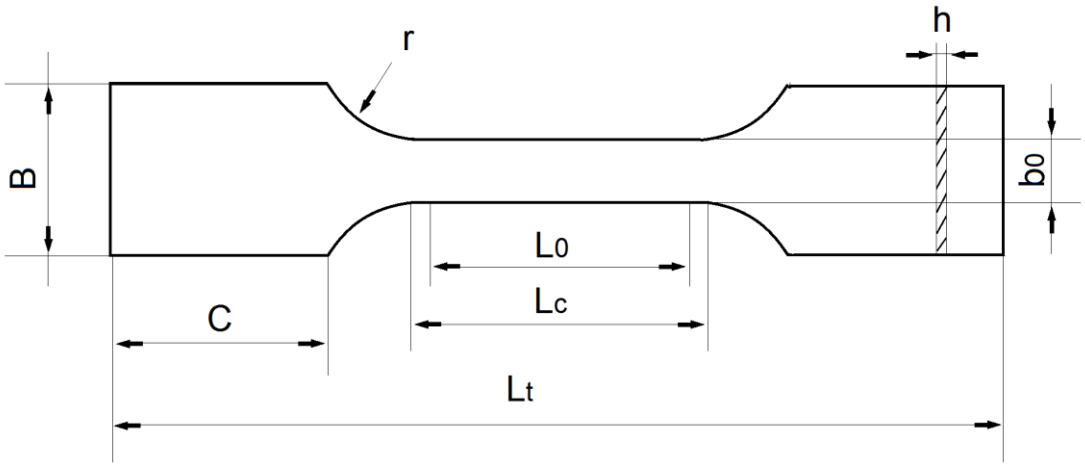

Figure 4.10. Schematic illustration of aluminium tensile specimen.

Table 4.5. Dimensions of aluminium bulk tensile specimen.

	Specimen type	Dimension (mm)
L_t	Overall length	190
L_c	Length of narrow parallel-sided portion	65
r	Radius	20
B	Width at ends	25
b_0	Width at narrow portion	12
h	Thickness	2
L_0	Original Gauge length	50
C	Length of the gripped ends	50

4.2.5.2. Adhesive Tensile Specimens Preparation

Adhesive tensile specimens were prepared by moulding to dimensions in accordance with BS EN ISO 527-2:2012. Due to the limited availability of TEMs, the small specimen configuration was selected for material saving purpose. Schematic illustration and dimensions of specimen are shown in Figure 4.11 and Table 4.6. The mould of tensile bars was cut from polytetrafluoroethylene sheet, which was selected for the ease of demoulding process, Figure 4.12.

A Speed Mixer DAC 150-FVR-K was used to mix adhesive with the TEMs. To achieve a good dispersion, epoxy resin and amine hardener were mixed for 30 s and then TEMs were added and mixed for another 60 s. Mixing speed was controlled at 3000 rev/min. Adhesive and TEMs mixture were then filled in the mould using a spatula. Each tensile bar cavity was overfilled slightly to reduce the possibility of trapped air bubbles. Mould was closed and cured for 90 minutes at 90 °C.

After curing, tensile bars were demoulded gently and cleaned off burrs. Tensile bars with observable voids (with the help of backlight) in the reduced section were discarded.

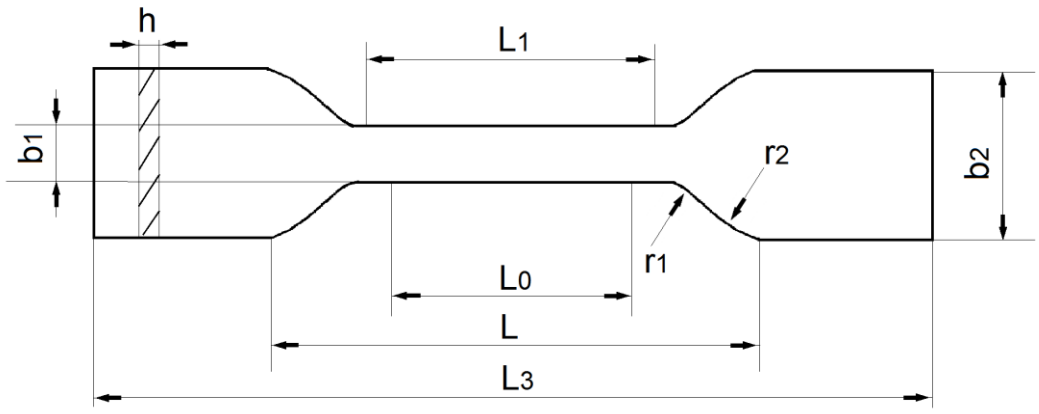

Figure 4.11. Illustration of adhesive tensile bar specimen.

Table 4.6. Dimensions of adhesive tensile bar specimen.

	Specimen type	Dimension (mm)
L_3	Overall length	≥75
b_2	Width at ends	12.5 ± 1
L_1	Length of narrow parallel-sided portion	25 ± 1
b_1	Width at narrow portion	4 ± 0.1
r_1	Small radius	8 ± 0.5
r_2	Large radius	12.5 ± 1
L	Initial distance between grips	50 ± 2
L_0	Gauge length	20 ± 0.5
h	Thickness	2 ± 0.2

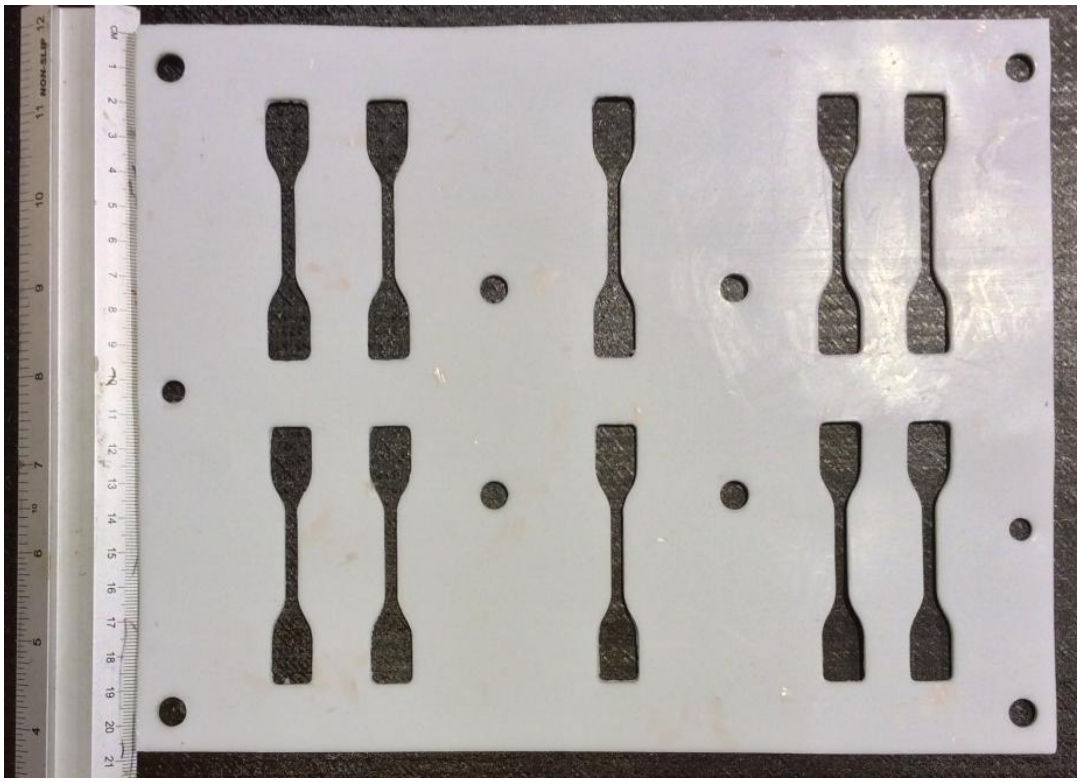

Figure 4.12. Photograph of adhesive tensile specimens mould.

4.2.5.3. Test Procedures

Following test procedures were implemented for the bulk specimens

- Tensile test was conducted at (23 ± 2) °C and (30 ± 10) % relative humidity on Instron 5582 with a displacement rate of 1 mm/min.;
- 5kN load cell was used for adhesive tensile test and 100kN load cell was used for aluminium tensile test;
- Instron PC software Bluehill was used for data recording and data were automatically converted into stress and strain by following equations;
- Care was taken to align tensile bars with test machine;
- Grips were tightened evenly and carefully to avoid slippage or any movement during the test;
- Instron extensometer 2630-106 with 12.5 mm travel (axial) was sprung clipped over the specimen gauge length;
- Width and thickness measurement were taken at three points along the gauge length with the arithmetic average value calculated;
- For adhesive tensile tests, Young's modulus was determined between 0.05% to 0.25% strain range using the equations below.

σ —…….**Equation 4.5.**

Where σ= Tensile stress (MPa); F = Tensile Load (N); A = Mean average cross sectional area of gauge length (mm^2)

Ɛ = ——…….**Equation 4.6.**

Where Ɛ = Tensile strain (%); L_0 = original gauge length; ΔL_0 = change in length.

$$E_T = \frac{\sigma \quad \sigma}{\quad\quad}$$ …….**Equation 4.7.**

Where Ɛ = Tensile strain (%); E_T represents the Young's Modulus.

4.2.6. Dynamic Mechanical Thermal Analysis

DMTA is a non-destructive and effective method which bridges mechanical properties and the microstructural influence of materials. It works by applying a sinusoidal stress to test a specimen with resulting strain recorded. Stiffness and damping (energy dissipation) are measured and reported as modulus and phase angle tan δ (defined as the ratio of loss modulus E'' to the storage modulus E') as a function of time, temperature and frequency. A typical DMTA curve was shown in Figure 4.13.

DMTA test was carried out with Tritec 2300 DMA and analysed using the Triton Technology software Universal Analysis 2000.

- DMTA specimens were made from the bespoke mould shown in Figure 4.14;
- Preparation procedures including microspheres/adhesive mixing, mould filling, curing and demoulding followed the same procedures as detailed in tensile bar preparation procedures (4.2.5.);
- Rectangular prisms, (dimensions 2mm*20mm*4mm) were cut and measured at three discrete points prior to testing;
- DMTA test machine was calibrated and setup for dual cantilever testing;
- The temperature was ramped from 23^{o}C to 105^{o}C at a rate of 3 ^{o}C/min;
- Care was taken when clamping specimens to avoid twisting or distortion;
- Frequency was defined as 1Hz;
- Glass transition temperature Tg was determined at the peak tanδ point.

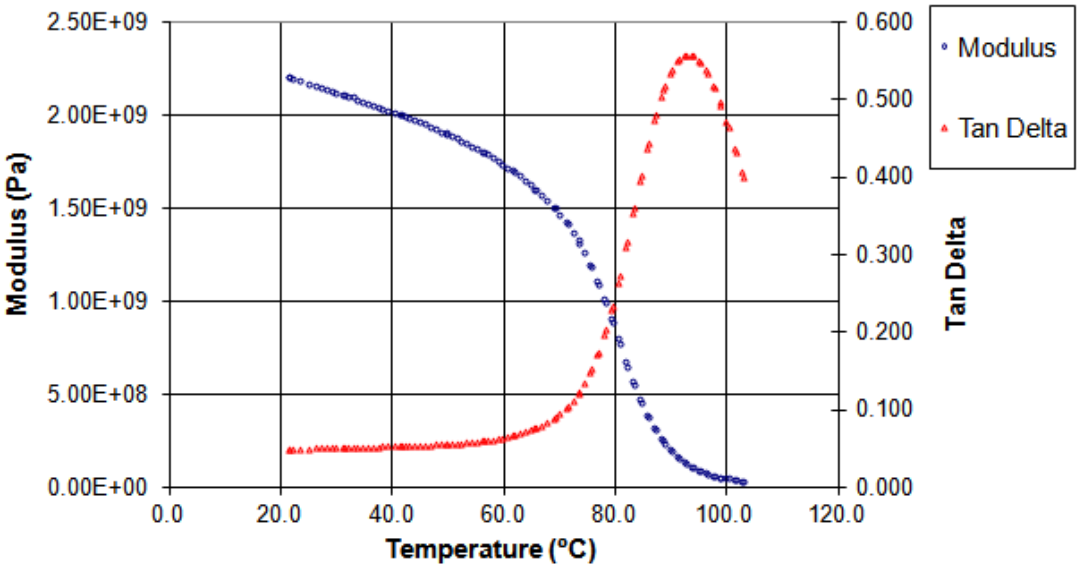

Figure 4.13. Typical DMTA curve for epoxy adhesive.

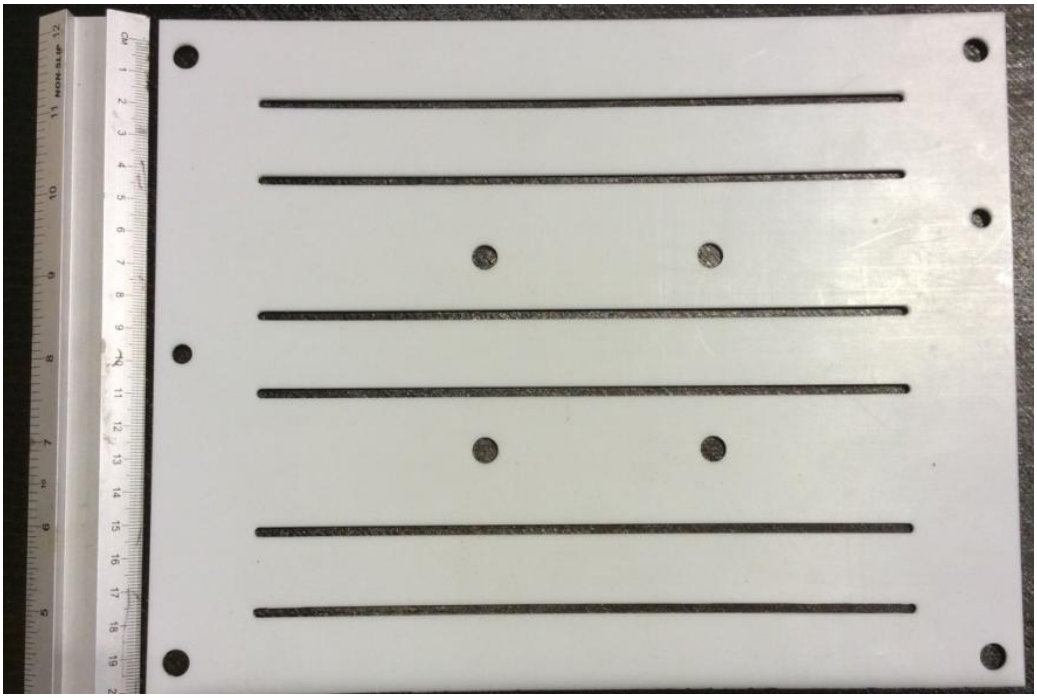

Figure 4.14. Photograph of DMTA specimen mould.

4.2.7. Water Immersion Test

Water immersion tests were prepared using untested DMTA specimens. All specimens were examined to ensure they were free of entrapped air voids to avoid erroneous measurement. The following procedures were implemented:

- Rectangular prisms (same geometrical dimensions with gauge length region of tensile bars: 2mm*4mm*20mm) were cut into 0.3000 ± 0.0005 g samples;
- All specimens were immersed in deionised water maintained at (40 ± 2) ^{o}C in the oven;
- For each formulation evaluated, 5 specimens were conditioned and measured at following time points: 2 hours, 4 hours, 8 hours, 16 hours , 24 hours, and every 24 hours until a consistent reading was observed in 5 consecutive days;
- Special care was taken to remove water on the specimen surface before each weighing operation;
- Precision for all weighing operations was controlled at 0.0001g;
- Specimen weight and corresponding time was recorded for analysis.

After $t_{saturation}$ was observed, all specimens were dried in the oven at 80^{o}C until the original weights of specimens have been achieved. This drying time was also referred to in the environmental conditioning test.

4.2.8. Environmental Conditioning Test

Environmental conditioning test was designed to evaluate the adhesive performance subject to hygrothermal ageing conditions over a 29-day cycle. To understand both the performance of adhesive joints and adhesive bulk property, two types of specimens are involved in this test: Single-lap-joint specimens and bulk tensile specimens. Environmental conditioning plans for both types of specimens are summarised in Table 4.7.

Table 4.7. Environmental conditioning plan.

	Immersion at 40°C in deionised water	Oven heating at 80°C	Ambient conditioning (23°C; 30-40% humidity)
Single Lap Joints	21 Days	7 Days	1 Day
Tensile Bars	$t_{saturation}^{*}$	t_{drying}^{*}	1 Day

*Note: $t_{saturation}$ and t_{drying} were determined from water immersion test in 4.2.7.

4.2.9. Scanning Electron Microscopy

Scanning electron microscopy (SEM) was employed to characterise the microstructural morphology and topography of adhesive fracture surfaces and TEMs. SEM works by focusing a beam of accelerated electrons on the specimen in a raster pattern. SEM micrographs are then produced as a result of the electron-specimen interaction on or near the surface of specimen. A variety of scattered electrons can be detected by SEM including secondary electrons, backscattered electrons and characteristic X-rays. Secondary electron detector provides more important specimen information regarding the morphology and topography and therefore was used in this research. Metal specimens require no special preparation. But for non-conductive materials such as adhesive and TEMs, specimens are normally coated with an ultra thin layer of conducting material (e.g. gold, platinum, etc).

SEM imaging of the specimen was conducted at Begbroke Science Park Oxford University using Jeol 5510LV (low vacuum). Samples were gold coated using Cressington Sputter Coater 208HR for 90 seconds at 0.6kV and 18mA. Electron beam energy was set to 20kV.

4.3. Summary

In summary, the whole experimental test programme and test techniques involved at each stage are shown in Figure 4.15 and Table 4.8.

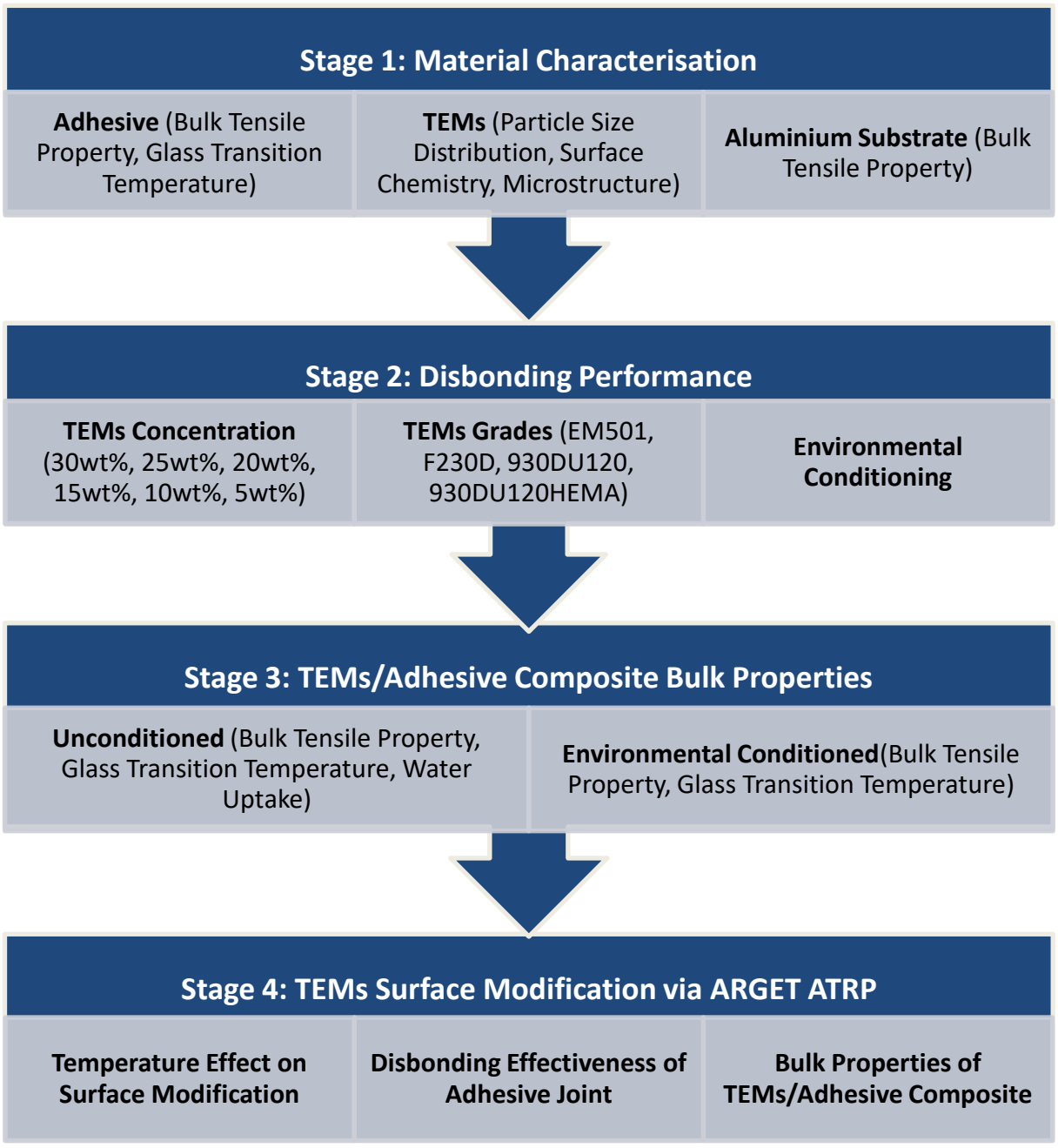

Figure 4.15. Flowchart of Experimental Test Programme.

Table 4.8. Experimental test methods involved at different stages of work.

	Stage 1	Stage 2	Stage 3	Stage 4
Particle Size Distribution Analysis	√			
Fourier Transform Infrared Spectroscopy	√			√
Tensile Lap Shear Test		√		√
Bulk Tensile Test	√		√	√
Dynamic Mechanical Thermal Analysis	√			√
Scanning Electron Microscopy	√	√		√
Disbonding Effectiveness Test		√		√
Water Immersion Test			√	
Environmental Conditioning Test		√	√	√

Chapter 5. Experimental Results

In this chapter, the experimental results are presented in the sequence of four stages of work as structured in Chapter 4.

5.1. Stage 1: Characterisation of Test Materials

In stage one, all the test materials were characterised with respect to their key relevant properties as stated in Chapter 4. The results for the aluminium substrate and TEMs are shown below. For a better comparison, the adhesive test results (DMTA, bulk tensile test) are presented along with TEMs/adhesive composite characterisation results in section 5.3.

5.1.1. Aluminium Substrate

The test results obtained for aluminium substrate (EN AW-6082 T6, thickness: 2mm), Table 5.1 and Figure 5.1, showed acceptable repeatability and were in good agreement with the data provided by the manufacturer, Table 3.1. The measured yield stress of the aluminium substrate (310 MPa) exceeded the minimum required value of 262.5MPa identified in the material selection process. This verified the suitability of using EN AW-6082 T6 as the substrate material in this research.

Table 5.1. Summary of aluminium substrate properties.

Property	Average Value	Standard Deviation
Ultimate Tensile Stress (MPa)	350	6.8
Tensile stress at Yield (MPa) (0.2% offset)	310	3.8
Tensile strain at Yield (MPa) (0.2% offset)	1%	0.01
Young's modulus (GPa)	78	5.8

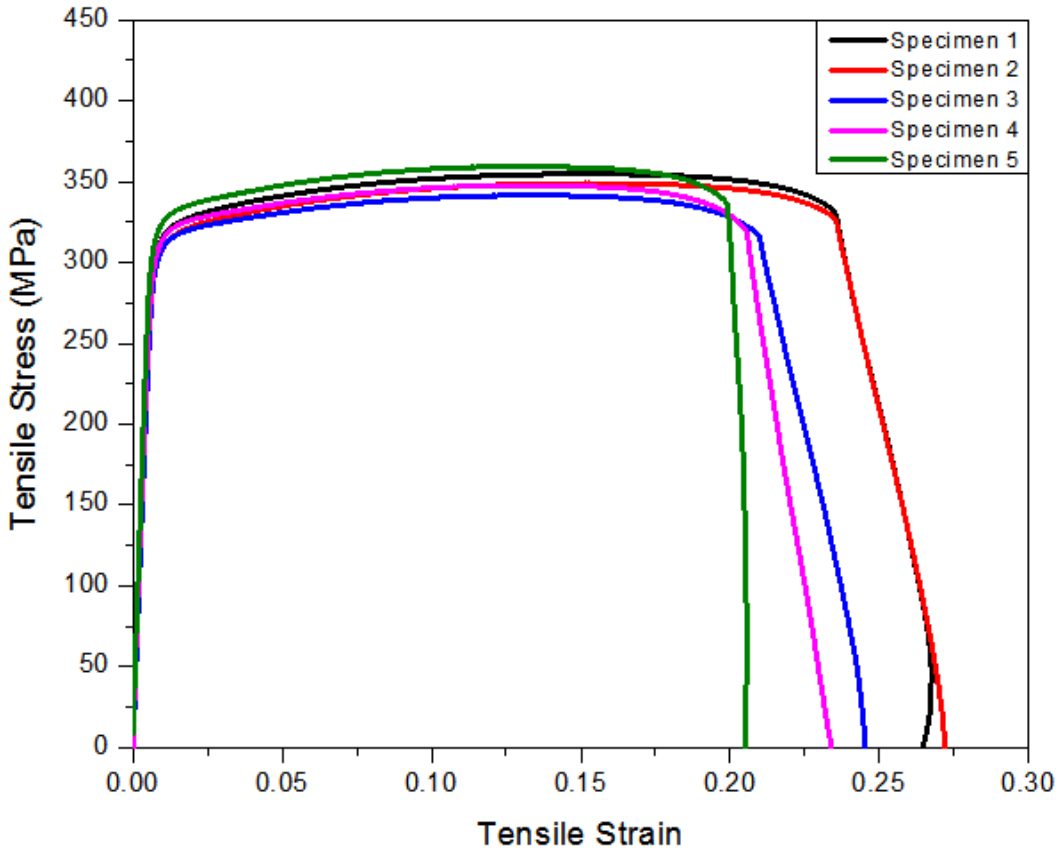

Figure 5.1. Tensile stress-strain curve of aluminium substrate.

5.1.2. Thermally Expandable Microspheres

Particle size distribution (PSD) analysis, Fourier transform infrared (FTIR) spectroscopy analysis and scanning electron microscopy (SEM) were conducted to assess the potential influences of the size, surface chemistry and microstructure of TEMs on TEMs/adhesive SLJs and bulk properties.

5.1.2.1. Particle Size Distribution

A summary of data is presented in Table 5.2. Detailed particle size distribution data are shown from Figure 5.2 to Figure 5.5 for each grade of TEMs (see section 4.2.1 for data definition). All TEMs grades exhibited a monomodal pattern (single peak). It was noticed that TEMs grades from Matsumoto and Sekisui have a smaller span (0.96 and 0.77) and sharper distribution curves compared to the two TEM grades from AkzoNobel. These results generally confirmed the data offered in the

datasheet, see Appendix. Sharper distribution could potentially increase expansion efficiency and reduce the dosage.

Table 5.2. Summary of PSD analysis data for all TEMs grades.

TEMs Grade	D(0.1) (um)	D(0.5) (um)	D(0.9) (um)	Span	D [4, 3] (um)
EM501	13.72	22.22	35.08	0.96	24.02
F230D	15.65	23.10	33.52	0.77	23.99
930DU120	19.46	37.14	70.04	1.36	41.74
930DU120HEMA	18.80	32.43	54.84	1.11	35.00

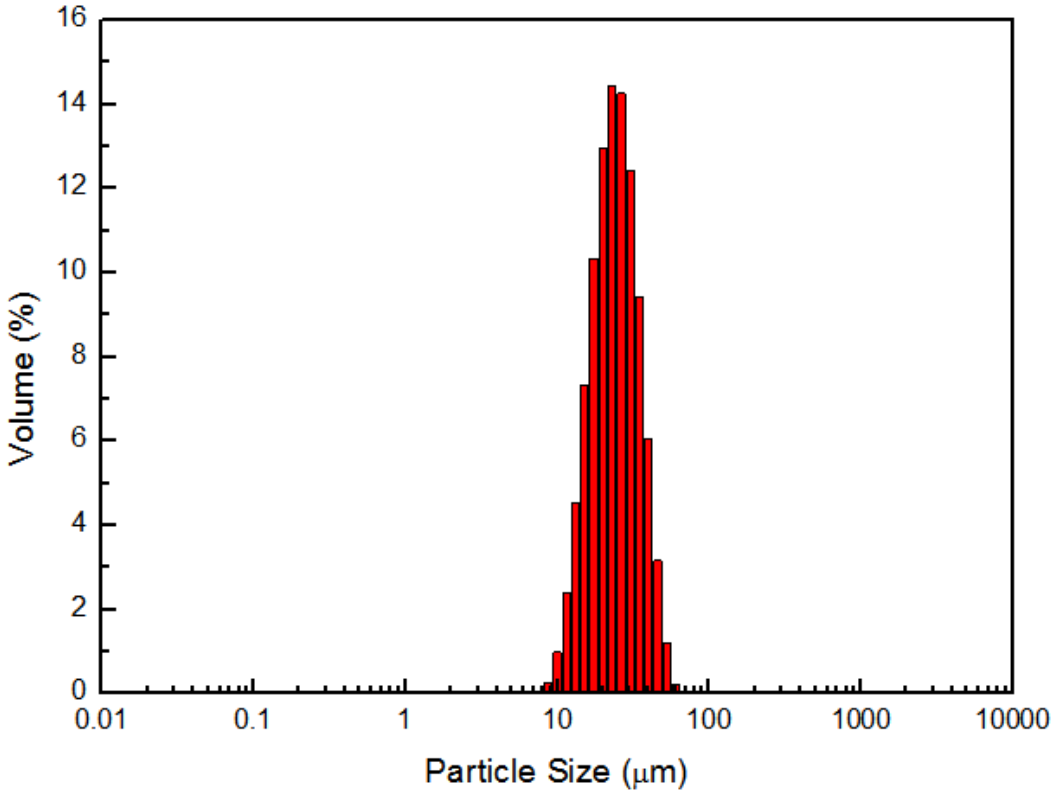

Figure 5.2. Particle size distribution of EM501 (Advancell).

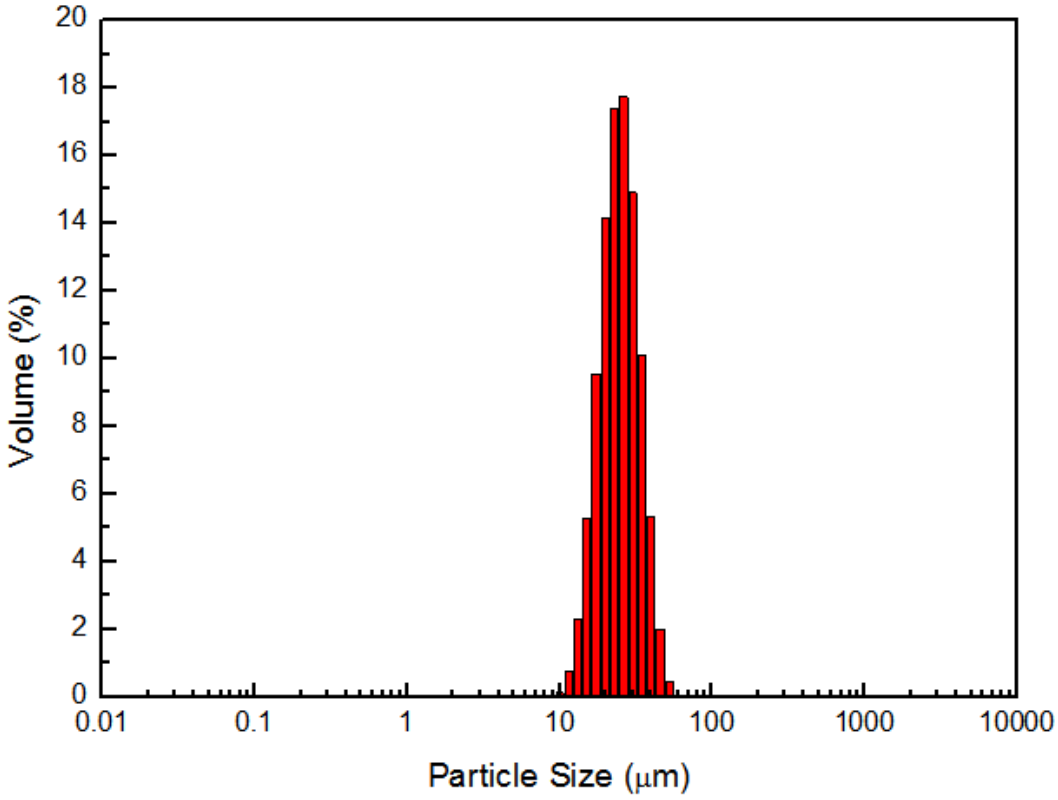

Figure 5.3. Particle size distribution of F230D (Matsumoto).

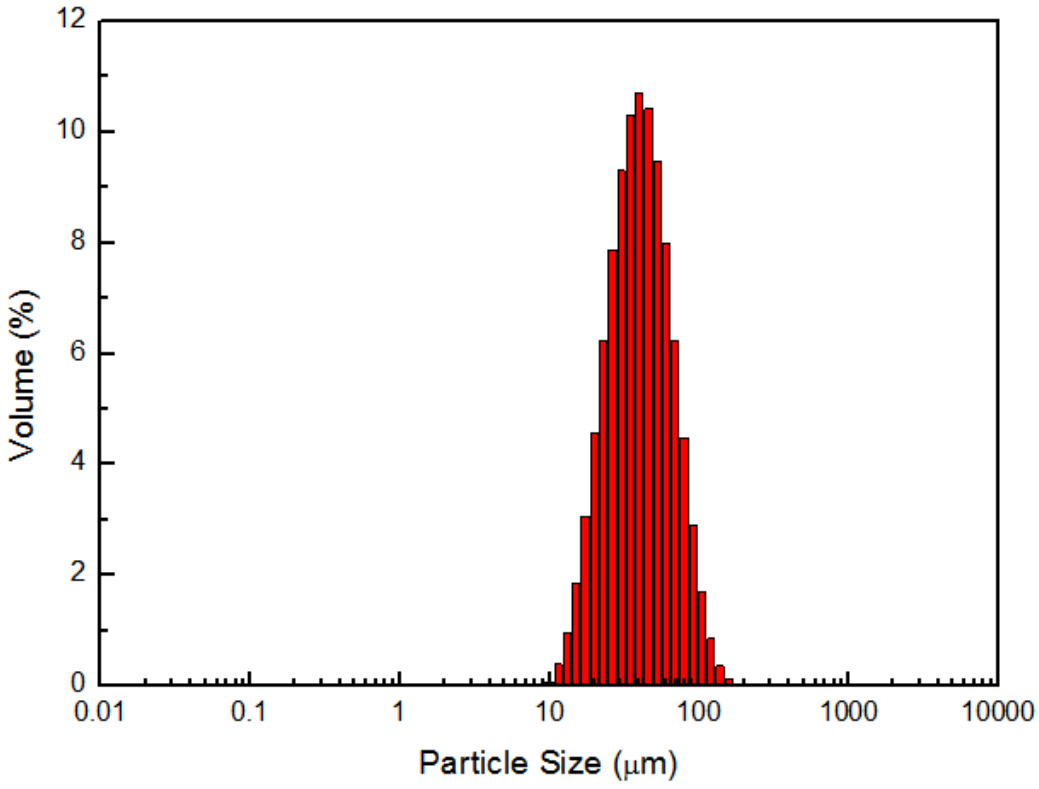

Figure 5.4. Particle size distribution of 930DU120 (Expancel).

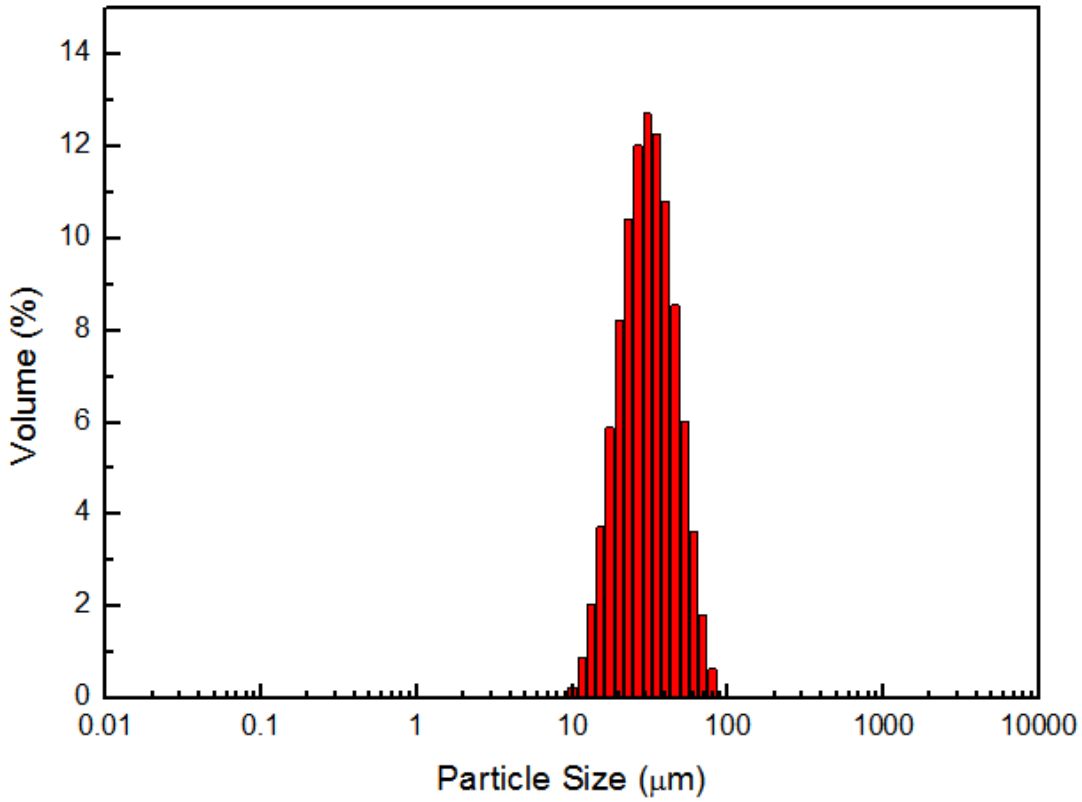

Figure 5.5. Particle size distribution of 930DU120HEMA (Expancel).

5.1.2.2. Fourier Transform Infrared Spectroscopy Results

FTIR results of each grade of TEMs are shown from Figure 5.6 to Figure 5.9. It is noted that the Expancel grade TEMs, both 930DU120 and 930DU120HEMA, showed single sharp peaks at 3600 cm^{-1} which indicates the presence of free or non-hydrogen-bonded hydroxyl groups. This was attributed to the Magnesium hydroxide (0wt% to 20wt%) contained in Expancel grades TEMs, see Appendix. As was introduced in Chapter 3, TEMs shell material is composed of a copolymer of acrylonitrile, methacrylonitrile and methyl methacrylate. Major peaks are all caused by the vibration of –CH, -C≡N, -OH, C=O and C-O-C bonds. Peaks at 2952 cm^{-1} and 1451 cm^{-1} are ascribed to –CH vibration. The peak at 2238 cm^{-1} is assigned to the -C≡N stretching vibration. Compared with 930DU120 grade, 930DU120HEMA grade TEMs showed a stronger peak at 1724.6 cm^{-1} which is attributed to the carbonyl groups as a result of the 15wt% HEMA addition in the shell composition.

It is worth noting that TEMs grades from Sekisui and Matsumoto (EM501 and F230D) showed quite similar FTIR spectra, which indicates similar shell compositions. Broad peak from 3200 cm^{-1} to 3550 cm^{-1} can be attributed to the alcohol OH stretching and N-H stretching. The strong peak at 1724.6 cm^{-1} indicates that EM501 and F230D grades of TEMs contained more carbonyl groups than Expancel grades. The small peak at 2238 cm^{-1} is also assigned to -C≡N stretching vibration but showed much weaker intensity compared with Expancel TEMs. This is possibly due to the fact that Expancel grades contain methacrylonitrile in shell composition while EM501 and F230D grades do not. The strong peak between 1000 cm^{-1} and 1200 cm^{-1} was quite noticeable for EM501 and F230D. This may be attributed to the C-C rocking, -COCN stretching and C-O stretching vibrations in the structure.

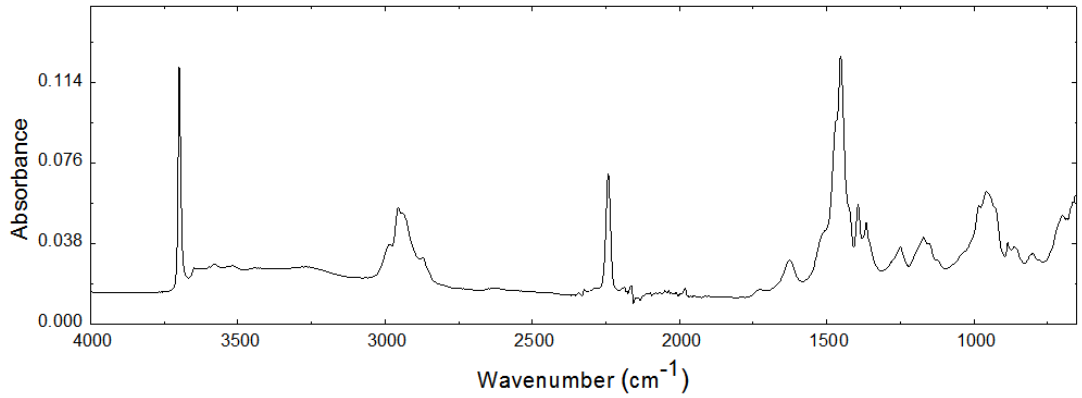

Figure 5.6. FTIR spectrum of 930DU120 grade TEMs.

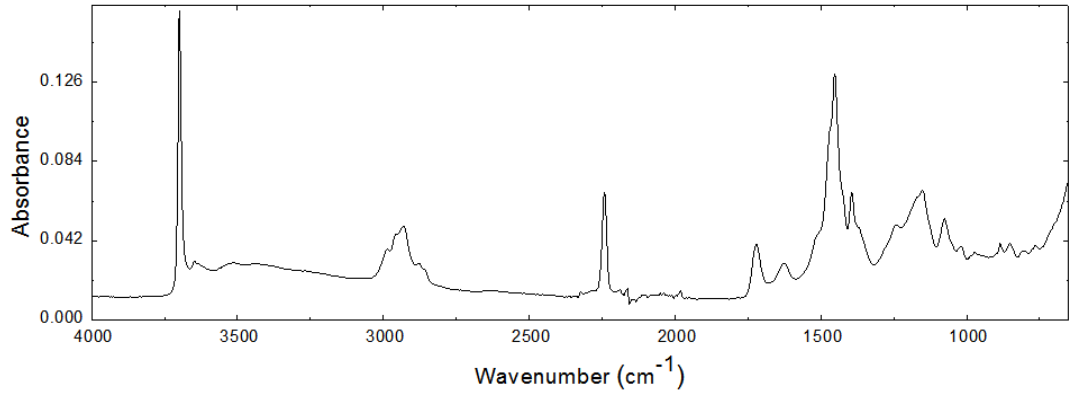

Figure 5.7. FTIR spectrum of 930DU120HEMA grade TEMs.

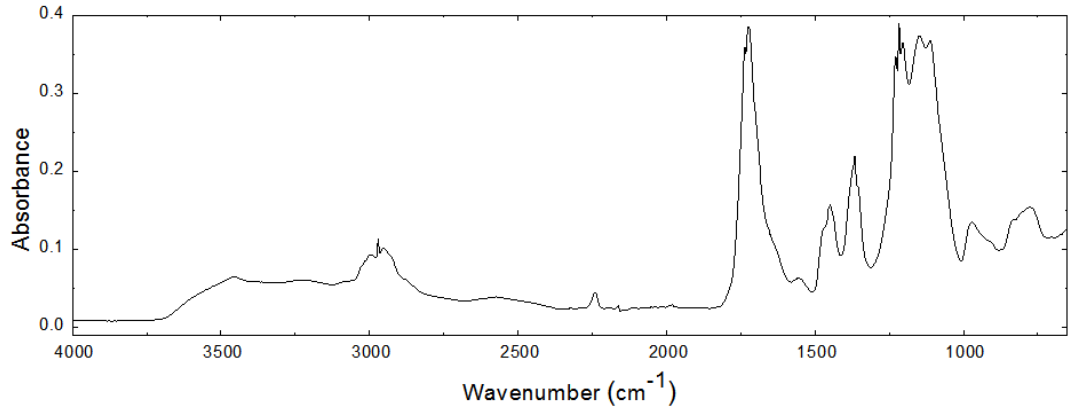

Figure 5.8. FTIR spectrum of EM501 grade TEMs.

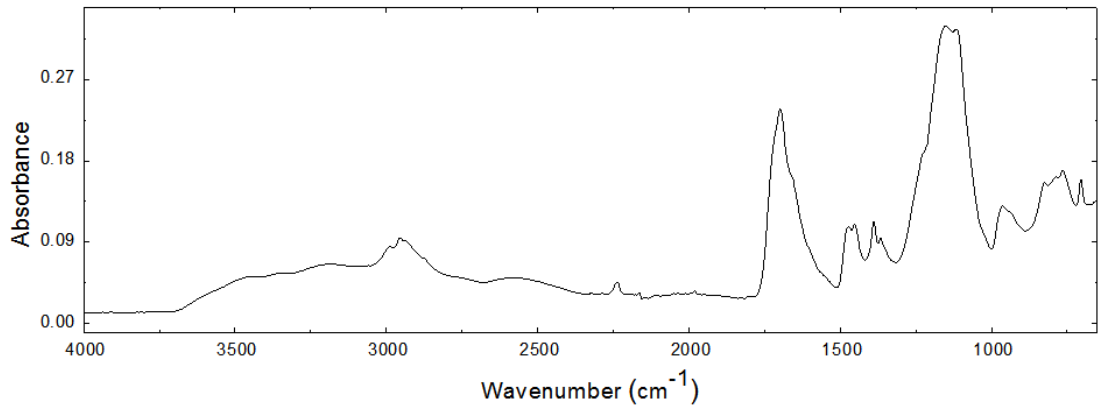

Figure 5.9. FTIR spectrum of F230D grade TEMs.

5.1.2.3. Scanning Electron Microscopy Imaging Results

SEM micrographs, Figure 5.10 to Figure 5.13 indicate that TEMs from Matsumoto and Sekisui generally showed similar morphology and differed from the Expancel grades of TEMs.

It was noted that EM501 and F230D grade TEMs generally had smoother shell morphology whereas 930DU120 and 930DU120HEMA grades TEMs from Expancel showed more buckled surfaces with small particles attached to large microspheres. Expancel grades also showed poorer particle size distribution which confirmed the results in the particle size distribution analysis. SEM micrographs implied that different TEMs manufactures used different methods or special procedures to manufacture the TEMs.

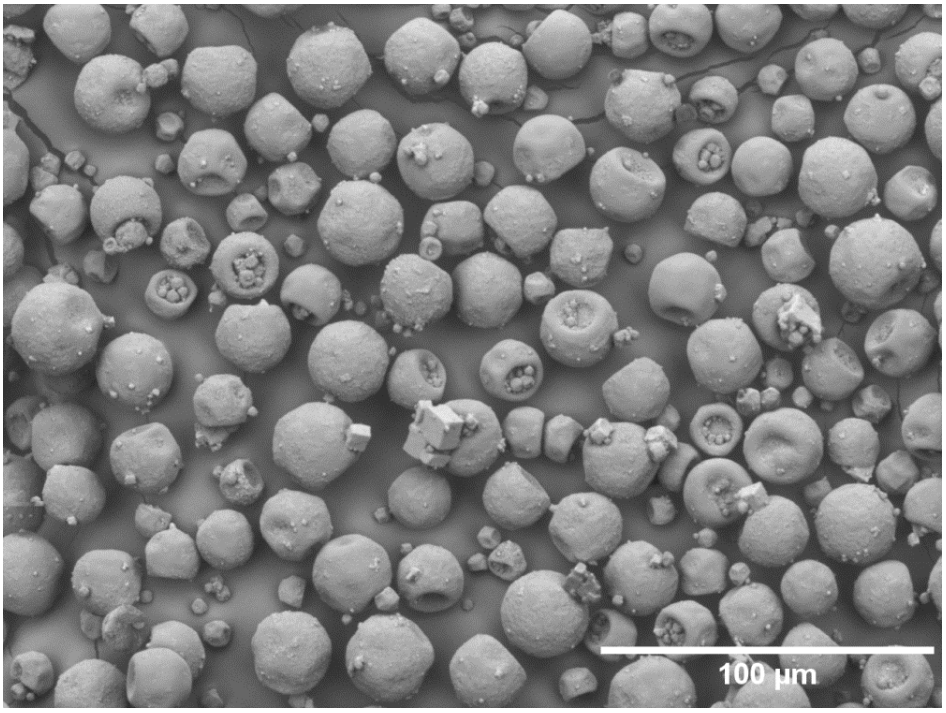

Figure 5.10. SEM micrograph of F230D (Matsumoto).

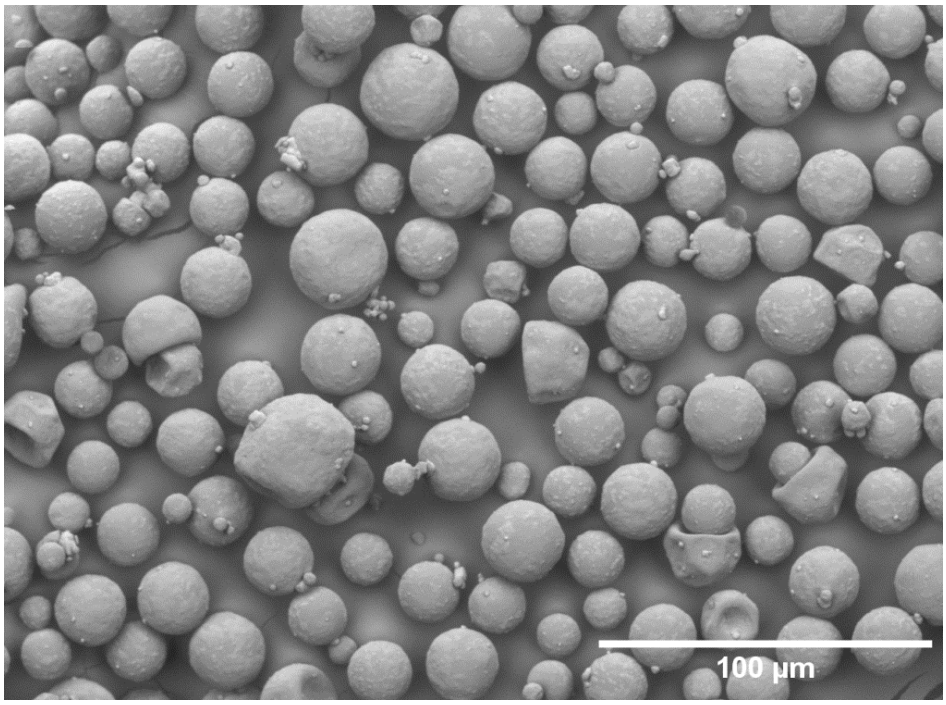

Figure 5.11. SEM micrograph of EM501 (Advancell).

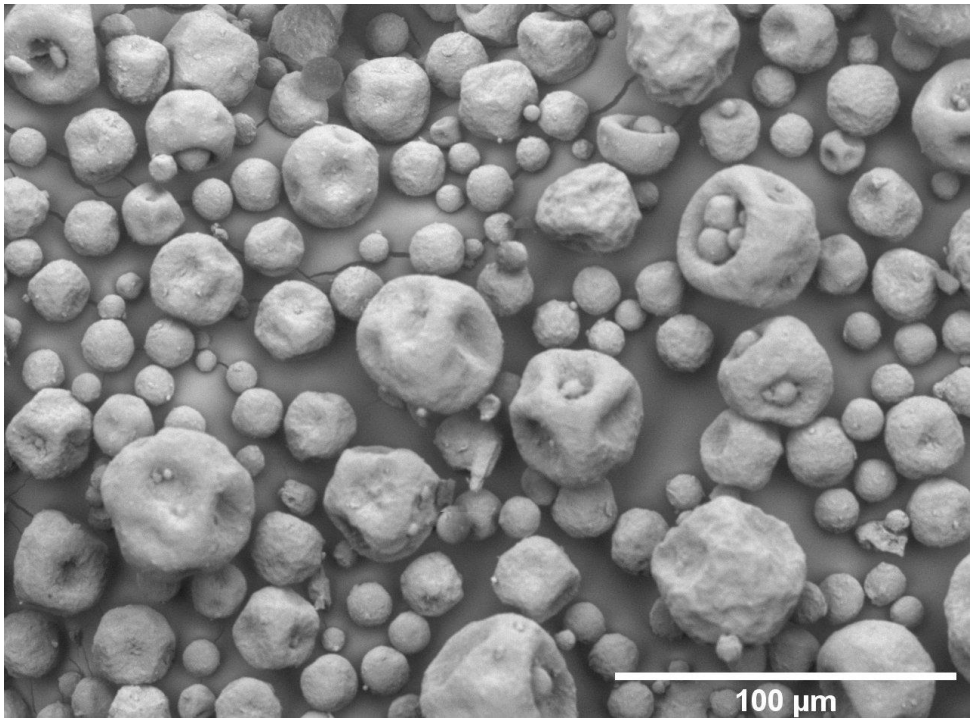

Figure 5.12. SEM micrograph of 930DU120 (Expancel).

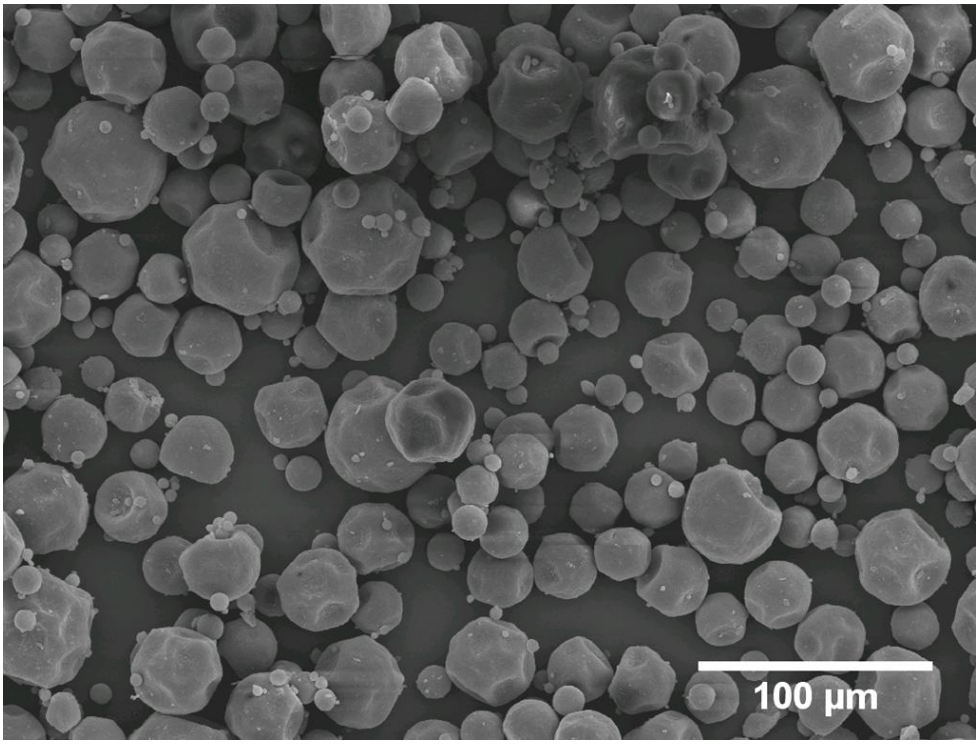

Figure 5.13. SEM micrograph of 930DU120HEMA (Expancel)

5.2. Stage 2: Disbonding Performance of Adhesive SLJs Incorporated with TEMs

The disbonding performance of TEMs incorporated in adhesive joints was evaluated consecutively on 6 levels of TEMs concentrations, four TEMs grades and after environmental conditioning. The two most promising formulations were selected through the test programme for TEMs/adhesive composite characterisation.

5.2.1. Pure Adhesive

The pure adhesive bonded SLJs were tested for disbonding effectiveness to examine effect of the temperature effect on pure adhesive joints. Test results in Table 5.3 show that there was a 23.9% reduction in tensile lap shear strength after heat activation in disbonding effectiveness test. This reduction in strength has to be considered when evaluating TEMs' sole contribution to the disbonding performance of adhesive system. All fracture surfaces of the pure adhesive bonded SLJs showed cohesive failure for specimens both before and after heat activation, featured in Figure 5.14. This validated the suitability of surface treatment procedures in preparation of SLJ specimens.

Table 5.3. Tensile lap shear strength of pure adhesive at room temperature.

Specimen No.	Before Heat Activation	After Heat Activation
1	30.2	22.7
2	30.6	22.9
3	29.4	23.1
Average (MPa)	30.1	22.9
Standard Deviation	0.58	0.17

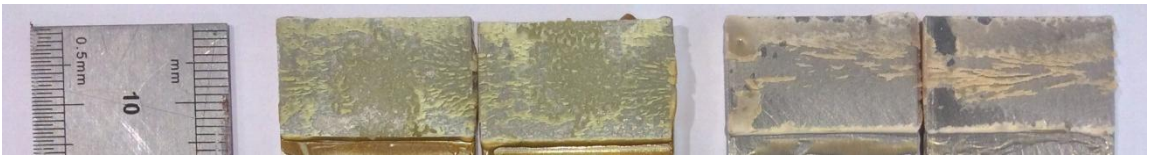

Figure 5.14. Featured fracture surfaces of pure adhesive bonded SLJs. Left: after heat activation; Right: before heat activation.

5.2.2. Different TEMs Concentrations

To determine the optimum concentration of TEMs to achieve the best disbonding performance in SLJs, six levels of TEMs concentrations (5wt%, 10wt%, 15wt%, 20wt%, 25wt%, 30wt%) were examined on EM501 grade of TEMs. Only EM501 grade of TEMs was used based on the assumption that all TEMs grades exhibit approximately identical behaviour in terms of different levels of concentrations.

Table 5.4 shows a negative correlation between the TEMs concentration and tensile lap shear strength of SLJs before heat activation. For heat activated SLJs, the residual strength and TEMs concentration displayed a similar trend up to 25wt% while exhibited an appreciable increase at 30wt%. It is also noted that there was a significant decrease in tensile lap shear strength at 30wt% compared with results at 25wt%. Photographs of SLJs fracture surfaces, Figure 5.15, also show consistent results up to 25wt% TEMs incorporation: cohesive failure was observed for specimens before heat activation and a certain degree of adhesive failure after heat activation. For 30wt% specimens however, only cohesive failure was observed for both before and after heat activation scenarios. The fracture surface of adhesive with 30wt% incorporation of EM501 was characterised by SEM and is shown in Figure 5.16. The reasons for these aberrant results and relatively large standard deviation at 30wt% are discussed in section 6.2.1.

In determination of the optimum TEMs concentration for further investigation, it was noted that the lowest strength after heat activation (4.7MPa) was achieved with 25wt% TEMs incorporation. However the corresponding strength before activation was 16.1 MPa. During specimen preparation process, it was also noticed

that with the increase of TEMs concentration, there was an increase in the viscosity of TEMs/adhesive mixture before curing. This caused difficulties in the specimen preparation process.

In comparison, SLJs containing 20wt% TEMs exhibited the second lowest value of the residual strength, 4.9MPa with less reduction in the strength before heat activation 17.4MPa. No difficulties were encountered in the specimen preparation process. In addition, the 20wt% TEMs formulation showed the highest disbonding effectiveness compared with all other concentrations as shown in Table 5.5. Therefore, it was decided that 20wt% TEMs concentration was selected for further investigation.

Table 5.4. Tensile lap shear strength of different concentrations of EM501 grade TEMs; (A) before heat activation, (B) after heat activation.

(A)

Specimen No.	30wt%	25wt%	20wt%	15wt%	10wt%	5wt%	0wt%
1	8.5	16.1	18.4	19.3	19.9	23.1	30.2
2	8.6	15.6	17.0	18.6	21.0	22.3	30.6
3	9.2	16.7	16.7	18.9	20.7	24.0	29.4
Average (Mpa)	**8.8**	**16.1**	**17.4**	**18.9**	**20.5**	**23.1**	**30.1**
Standard Deviation	**0.35**	**0.55**	**0.91**	**0.36**	**0.58**	**0.84**	**0.58**

(B)

Specimen No.	30wt%	25wt%	20wt%	15wt%	10wt%	5wt%	0wt%
1	6.0	4.9	4.8	5.4	5.6	10.1	22.7
2	8.6	4.1	4.8	5.7	6.7	10.3	22.9
3	7.9	5.0	5.2	5.5	7.1	10.3	23.1
Average (Mpa)	**7.5**	**4.7**	**4.9**	**5.5**	**6.5**	**10.2**	**22.9**
Standard Deviation	**1.35**	**0.51**	**0.24**	**0.19**	**0.78**	**0.13**	**0.17**

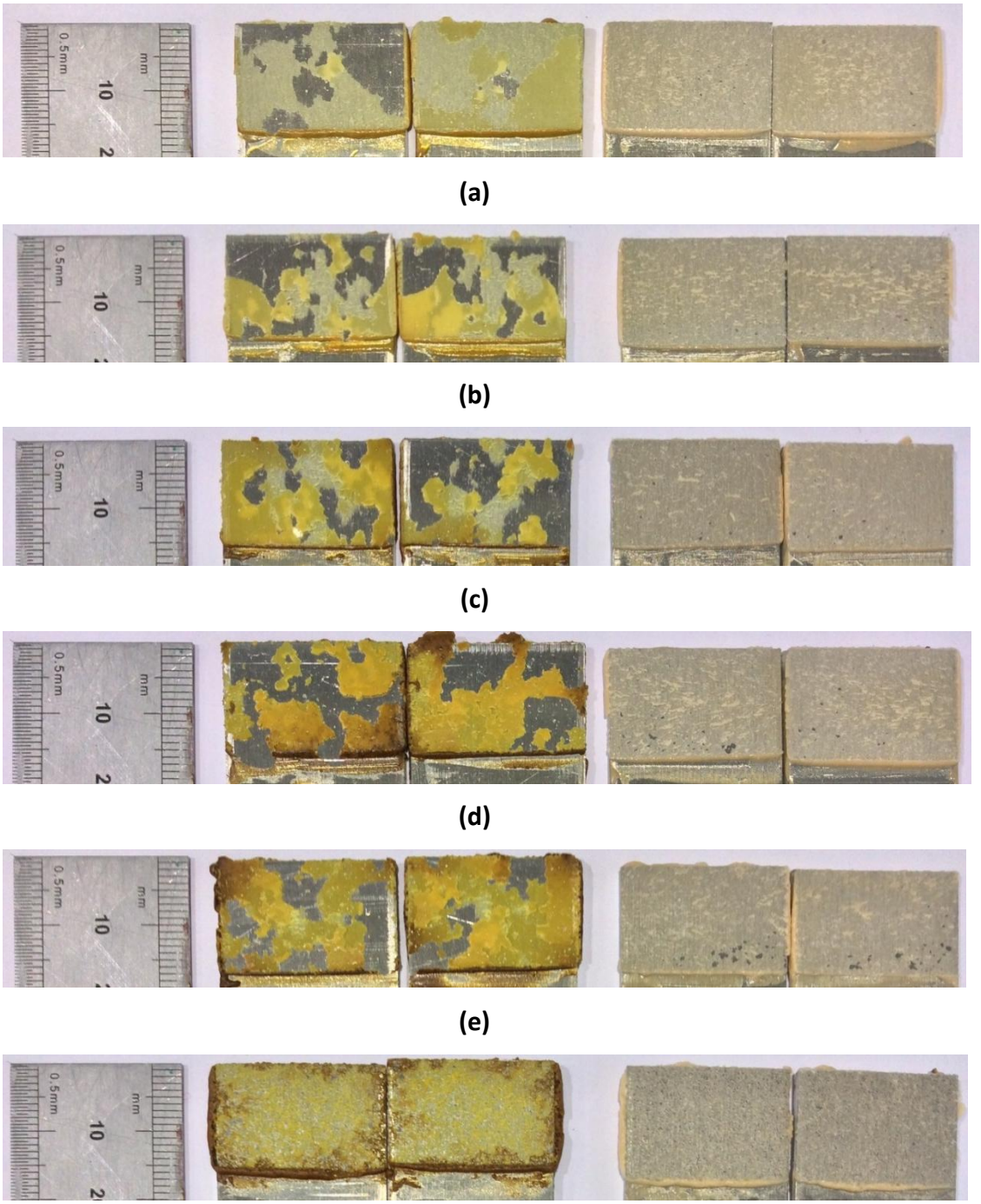

(a)

(b)

(c)

(d)

(e)

(f)

Figure 5.15. Featured fracture surfaces of adhesive SLJs with EM501 incorporation.

Left: after heat activation; Right: before heat activation.

(a) 5wt%; (b) 10wt%; (c) 15wt%; (d) 20wt%; (e) 25wt%; (f) 30wt%.

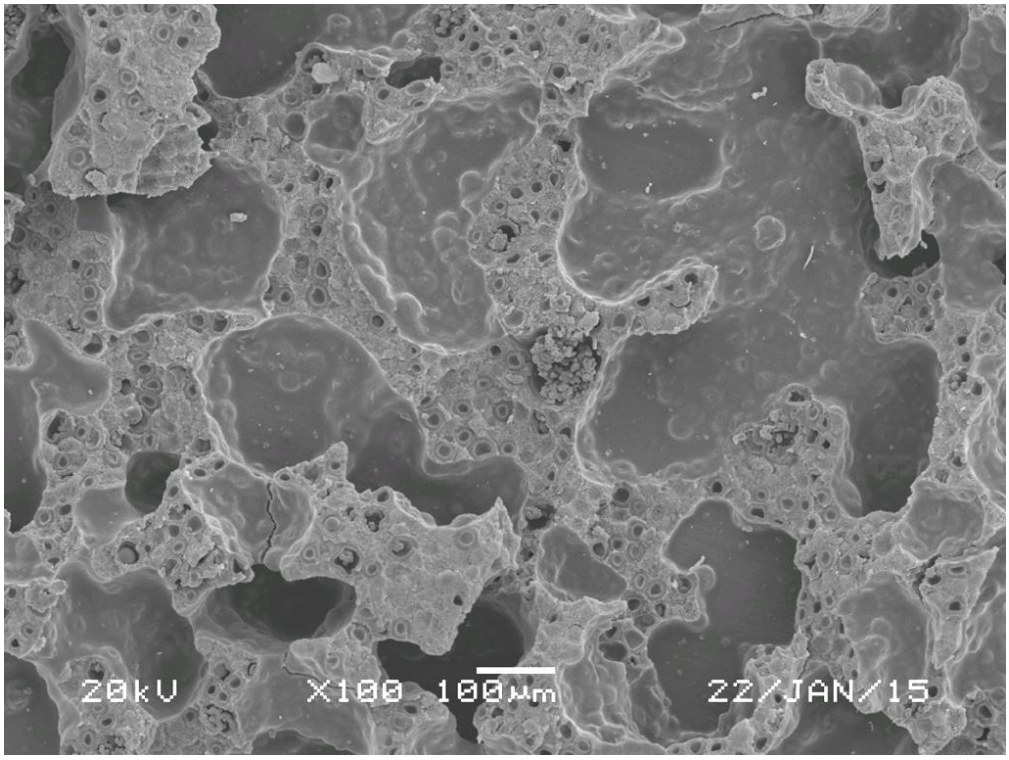

Figure 5.16. SEM micrograph of fracture surface of adhesive with 30wt% EM501 incorporation before heat activation.

Table 5.5. Disbonding effectiveness of SLJs with different TEMs concentrations

TEMs Concentration	30wt%	25wt%	20wt%	15wt%	10wt%	5wt%	0wt%
Disbonding Effectiveness (%)	14.8	70.8	71.8	70.9	68.3	55.8	23.9

5.2.3. Four Grades of TEMs

Disbonding effectiveness was evaluated on all four grades of TEMs with 20wt% incorporation in the adhesive system. According to the results shown in Table 5.6, it is clear that EM501 and F230 grades of TEMs showed the lowest strength for SLJs before heat activation while contributing the least to the disbonding performance of SLJs. On the contrary, for 930DU120 and 930DU120HEMA, tensile lap shear strength was less affected by TEMs incorporation and satisfactory disbonding effectiveness values were achieved (86.0% and 84.4%), see Table 5.7. All fracture

surfaces showed mixed mode failure, Figure 5.17. For further environmental conditioning and bulk property characterisation, 930DU120 and 930DU120HEMA grades of TEMs were opted for.

Fracture surfaces of adhesive incorporated with 930DU120HEMA were characterised by SEM for both before and after heat activation scenarios, Figure 5.18 to Figure 5.19. It is interesting to notice the TEMs sized cavities and a tiny amount of fractured TEMs but generally lack of the TEMs themselves for fracture surface before heat activation. It should also be noted that these cavities were well dispersed in the adhesive matrix with no large agglomerations. This indicates that the TEMs/adhesive mixing process was successful. In terms of specimens after heat activation, no intact TEMs can be observed but only some torn structures which seemed to be the wreckage of TEMs after expansion.

Table 5.6. Tensile lap shear strength for different grades of TEMs (20wt% incorporation) (A) before heat activation; (B) after heat activation.

(A)

Specimen No.	EM501	F230D	930DU120	930DU120HEMA
1	18.4	15.0	17.0	19.2
2	17.0	15.6	18.1	19.8
3	16.7	14.8	18.2	19.0
Average (MPa)	**17.4**	**15.1**	**17.8**	**19.3**
Standard Deviation	**0.91**	**0.41**	**0.64**	**0.41**

(B)

Specimen No.	EM501	F230D	930DU120	930DU120HEMA
1	4.8	4.7	3.0	3.0
2	4.8	5.3	1.8	3.2
3	5.2	5.1	2.9	2.8
Average (MPa)	**4.9**	**5.0**	**2.5**	**3.0**
Standard Deviation	**0.24**	**0.34**	**0.68**	**0.23**

Table 5.7. Disbonding effectiveness of SLJs with four grades of TEMs.

TEMs Grade	EM501	F230D	930DU120	930DU120HEMA
Disbonding Effectiveness (%)	71.8	66.9	86.0	84.4

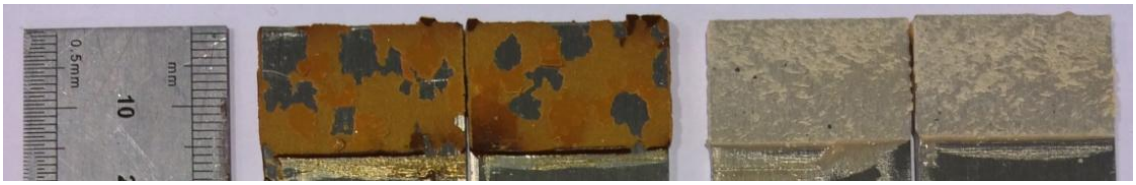

(a)

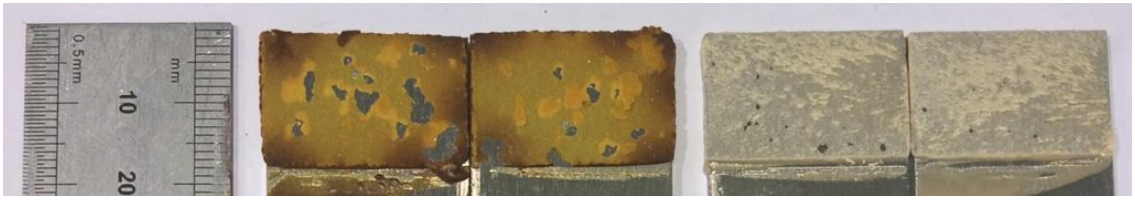

(b)

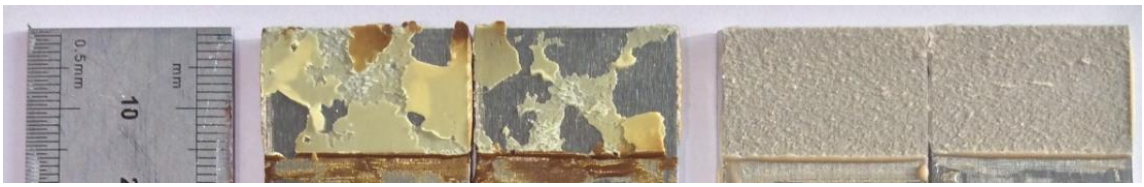

(c)

Figure 5.17. Featured fracture surfaces of adhesive SLJs with different grades of TEMs. Left: after heat activation; Right: before heat activation.

(a) 930DU120, (b) 930DU120HEMA, (c) F230D.

Note: Fracture surface of 20wt%EM501 SLJs was shown in Figure 5.15.

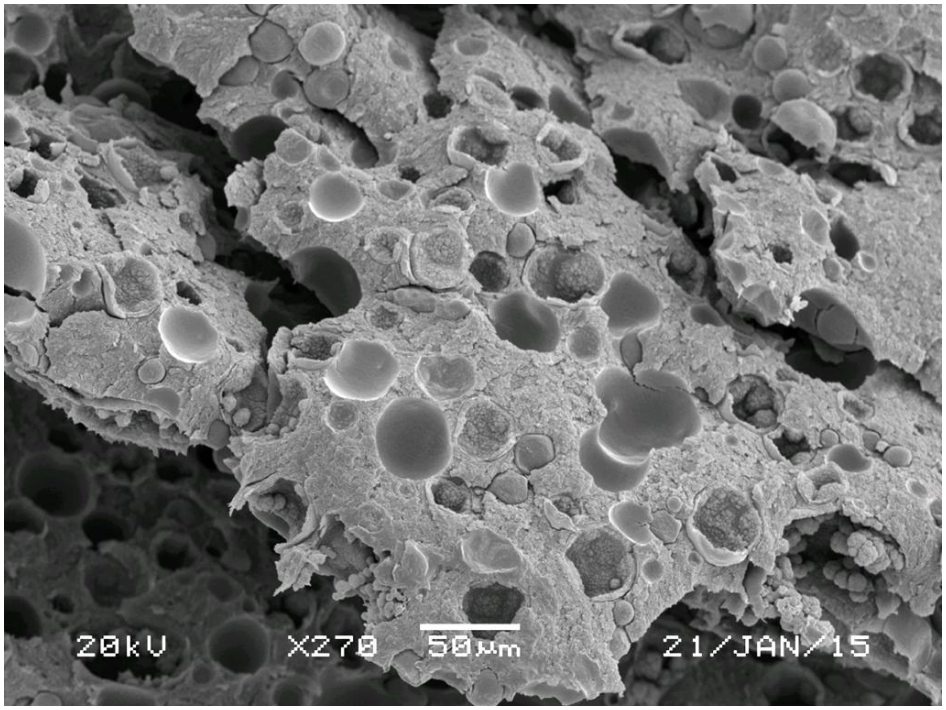

Figure 5.18. SEM micrograph of fracture surface of adhesive with 20wt%930DU120HEMA incorporation before heat activation.

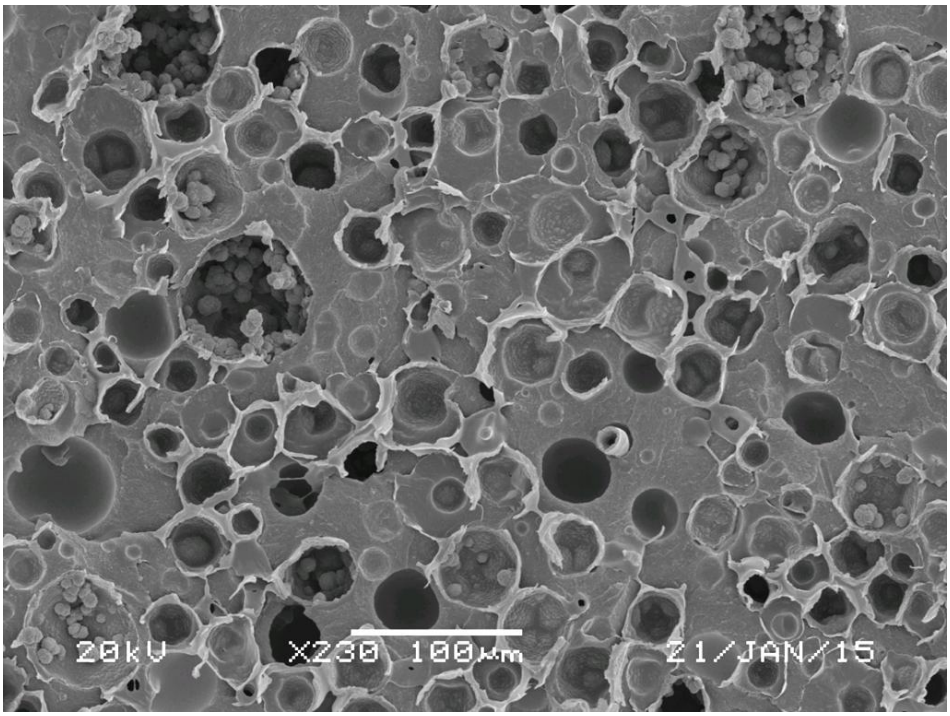

Figure 5.19. SEM micrograph of fracture surface of adhesive with 20wt%930DU120HEMA incorporation after heat activation.

5.2.4. Environmentally Conditioned Single-lap-joint Specimens

SLJ specimens were environmentally conditioned following the procedures detailed in 4.2.8. Tensile lap shear strength of conditioned specimens were measured and displayed in Table 5.8. No significant changes were observed compared with the results of unconditioned specimens in Table 5.3 and Table 5.6. A slight increase (~1MPa) was noted for 930DU120 and 930DU120HEMA grades incorporated SLJs before heat activation. It was suggested that the length of environmental conditioning scheme was not long enough for water ingress to reach the centre of adhesive bond line. The slight increase may be attributed to adhesive post curing or plasticisation caused by water ingress. It was decided to cancel the environmental conditioning test for SLJ specimens for the rest of the test programme.

Table 5.8. Tensile lap shear strength of environmentally conditioned specimens. (A) before heat activation, (B) after heat activation.

(A)

Specimen No.	Pure Adhesive	20wt%930DU120	20wt%930DU120HEMA
1	31.1	18.7	20.5
2	30.2	18.7	19.3
3	30.2	18.5	20.2
Average (Mpa)	**30.5**	**18.6**	**20.0**
Standard Deviation	**0.53**	**0.13**	**0.63**

(B)

Specimen No.	Pure Adhesive	20wt%930DU120	20wt%930DU120HEMA
1	22.9	3.0	2.5
2	23.1	2.3	3.3
3	22.5	2.8	3.1
Average (Mpa)	**22.9**	**2.7**	**3.0**
Standard Deviation	**0.30**	**0.39**	**0.41**

5.3. Stage 3: Characterisation of TEMs/Adhesive Composite

Based on the results from stage 2, 20wt% 930DU120, 20wt% 930DU120HEMA and pure adhesive were selected for the investigation of bulk properties at this stage.

5.3.1. Water Immersion Test

The main objective of the water immersion test was to measure the time taken for the water content to reach a constant value in DMTA and bulk tensile test specimens. Data was collected at time intervals specified in 4.2.7.

TEMs incorporation clearly made the adhesive system more susceptible to water ingress. Adhesive system incorporated with 930DU120HEMA grade TEMs was more prone to water ingress with the end weight of 0.3177g (5.9wt% increase) compared with 0.3154 g (930DU120, 5.1wt% increase) and 0.3147g (Pure adhesive, 4.9wt% increase), Table 5.9. Weight-time curves were created for three different formulations, Figure 5.20.

It was noted that the adhesive systems incorporated with two grades of TEMs and pure adhesive all reached the equilibrium state at approximately same time: 14 days (336 hours). After the water immersion test, specimens were dried in an oven at 80 ^{o}C. No changes in weight measurement were detected after four days of drying. These two values (14 days immersion time and 4 days drying time) were therefore used in the environmental conditioning test of adhesive tensile bars, specified in section 4.2.8.

Table 5.9. Weight measurements at the end of water immersion test.

	Original	930DU120HEMA	930DU120	Pure Adhesive
Average Weight (g)	0.3000	0.3177	0.3154	0.3147
Standard Deviation	0.0005	0.0004	0.0006	0.0004

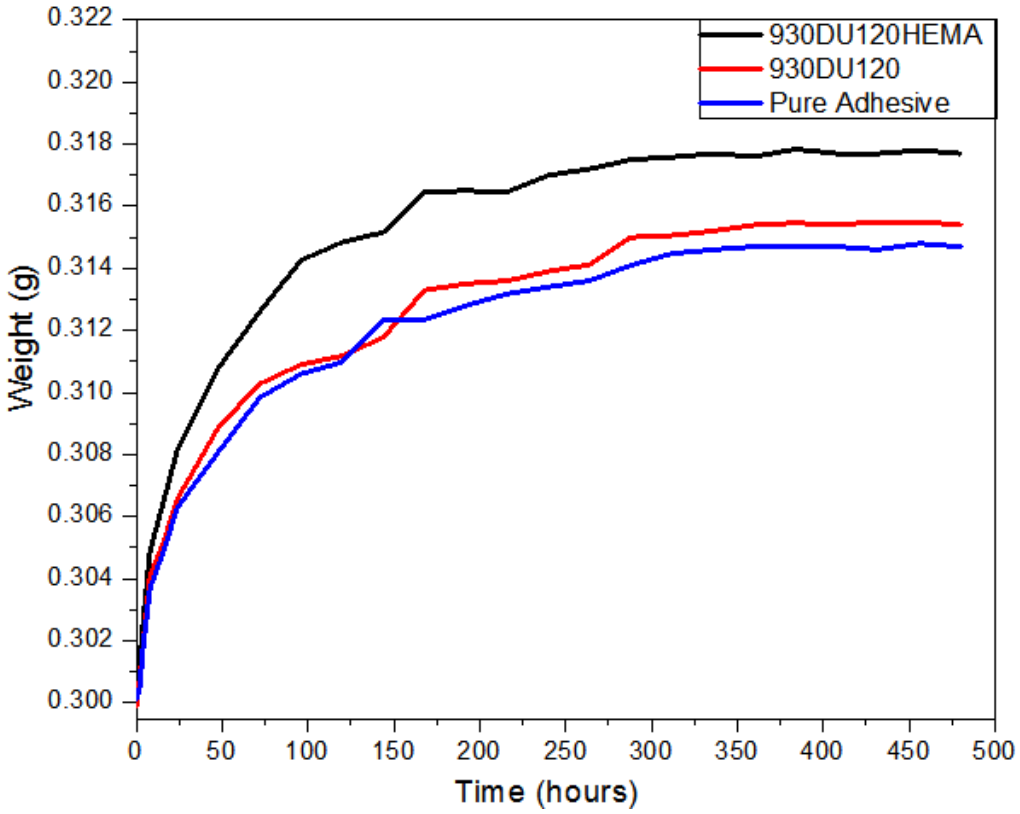

Figure 5.20. Weight versus immersion time for pure adhesive and adhesive incorporated with selected TEMs grades.

5.3.2. Unconditioned Specimens

During bulk tensile specimen preparation, it was found that there was a certain degree of air traps although extra care was taken on mould filling and removal of air bubble. Specimens with visible air bubbles in the gauge length were discounted from further testing. Invisible small bubbles were also found to impair the integrity of adhesive property, resulting in large standard deviations. Therefore, data were excluded from end results if air bubbles were observed in the fracture surface of the tested tensile bars. Generally, 4 to 7 specimens were tested for each formulation to generate more accurate and consistent results. However, the quality of data was still quite poor in terms of tensile strain and tensile modulus measurement. UTS results showed acceptable deviation.

As displayed in Table 5.10, Figure 5.21, Figure 5.22 and Figure 5.23, a significant decrease in UTS was observed for both 930DU120 and 930DU120HEMA grade TEMs

incorporation, from 40.9 MPa to 23.5 MPa and 24.8 MPa, respectively. Comparing two grades of TEMs, 930DU120HEMA grade showed a slightly higher value. The same trend was found when comparing the Young's Modulus values.

In terms of DMTA results, displayed in Table 5.11, Figure 5.24, Figure 5.25 and Figure 5.26, the TEMs/adhesive system showed higher glass transition temperature and lower DMTA modulus and peak tan delta value. There was not much difference between the adhesive formulations incorporated with the two grades of TEMs. For data quality, the DMTA modulus results had comparatively larger deviation which was attributed to the small invisible air bubbles trapped in the specimens. Glass transition temperature measurements showed fair consistency.

Table 5.10. Summary of tensile test results for unconditioned specimens.

Formulation	Ultimate Tensile Strength (MPa)	Young's Modulus (GPa)
Pure adhesive	40.9 ± 0.22	3.2 ± 0.59
20wt% 930DU120	23.5 ± 0.48	2.3 ± 0.46
20wt% 930DU120HEMA	24.8 ± 0.63	2.2 ± 0.09

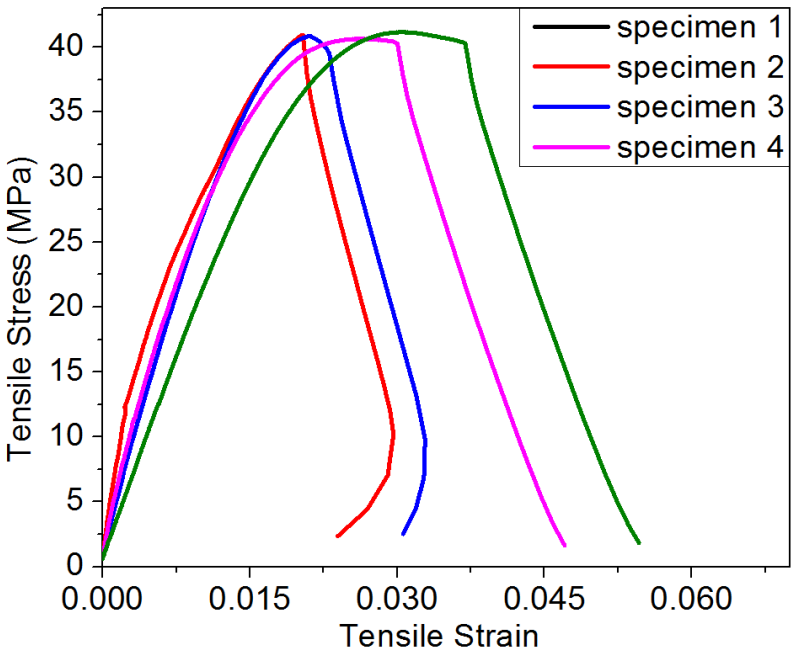

Figure 5.21. Tensile stress-strain curves for unconditioned pure adhesive.

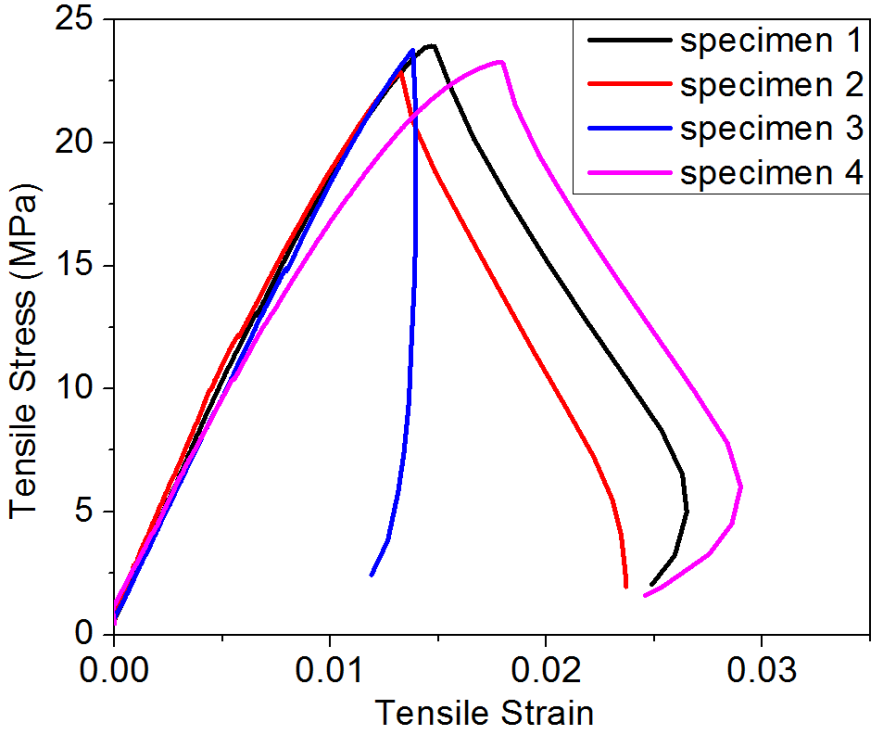

Figure 5.22. Tensile stress-strain curves for unconditioned adhesive with 20wt%930DU120 incorporation.

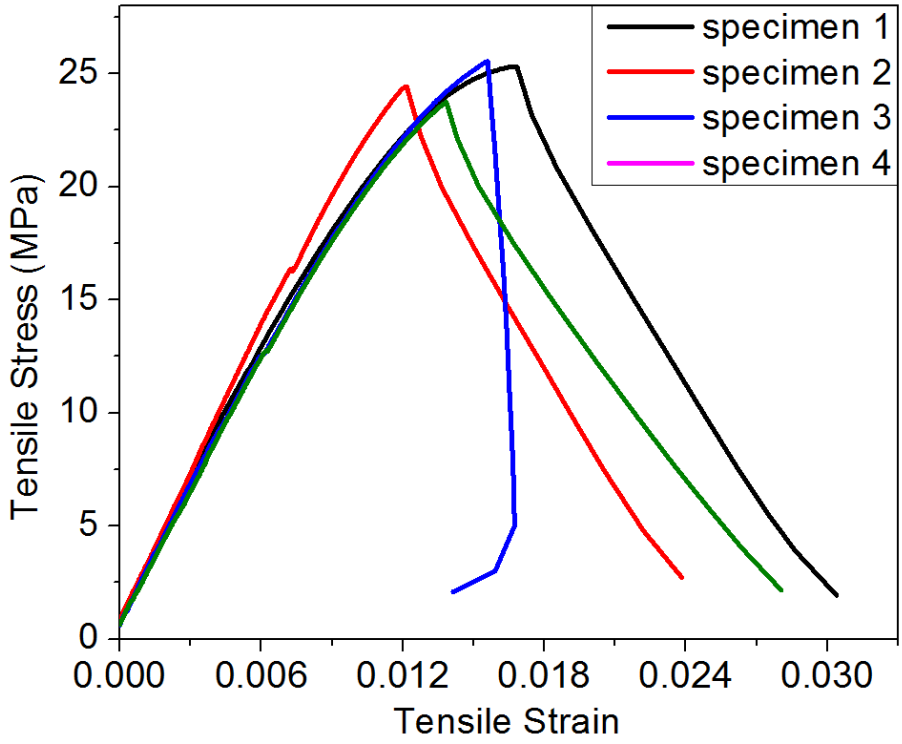

Figure 5.23. Tensile stress-strain curves for unconditioned adhesive with 20wt%930DU120HEMA incorporation.

Table 5.11. Summary of DMTA results for unconditioned specimens.

Formulation	Peak Tan Delta	Tg (°C)	DMTA Modulus (GPa)
Pure adhesive	0.583 ± 0.0276	93.0 ± 0.22	1.9 ± 0.28
20wt% 930DU120	0.489 ± 0.0168	93.9 ± 0.54	1.4 ± 0.17
20wt% 930DU120HEMA	0.520 ± 0.0013	95.0 ± 0.70	1.1 ± 0.45

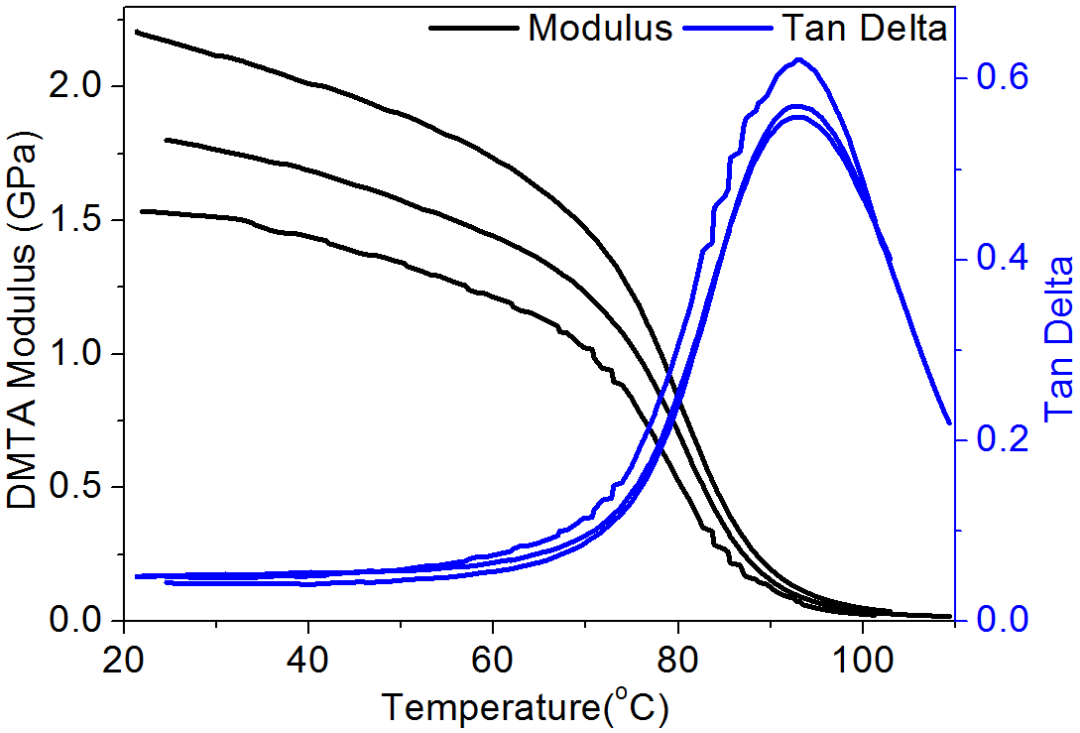

Figure 5.24. DMTA graphs for unconditioned pure adhesive.

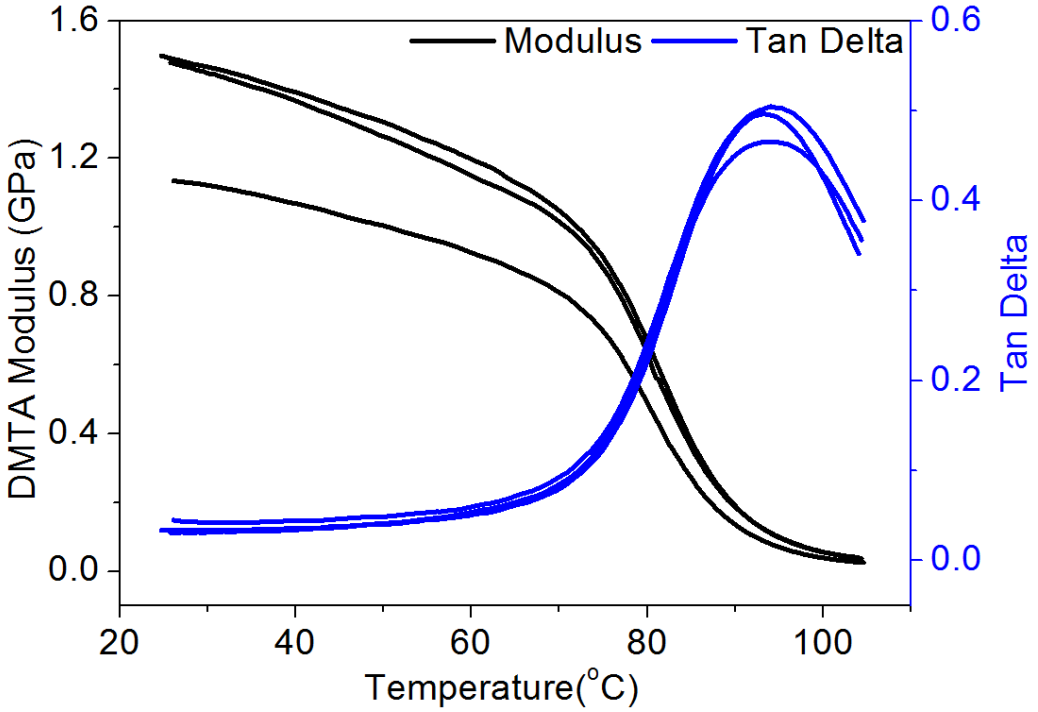

Figure 5.25. DMTA graphs for unconditioned adhesive with 20wt%930DU120 incorporation.

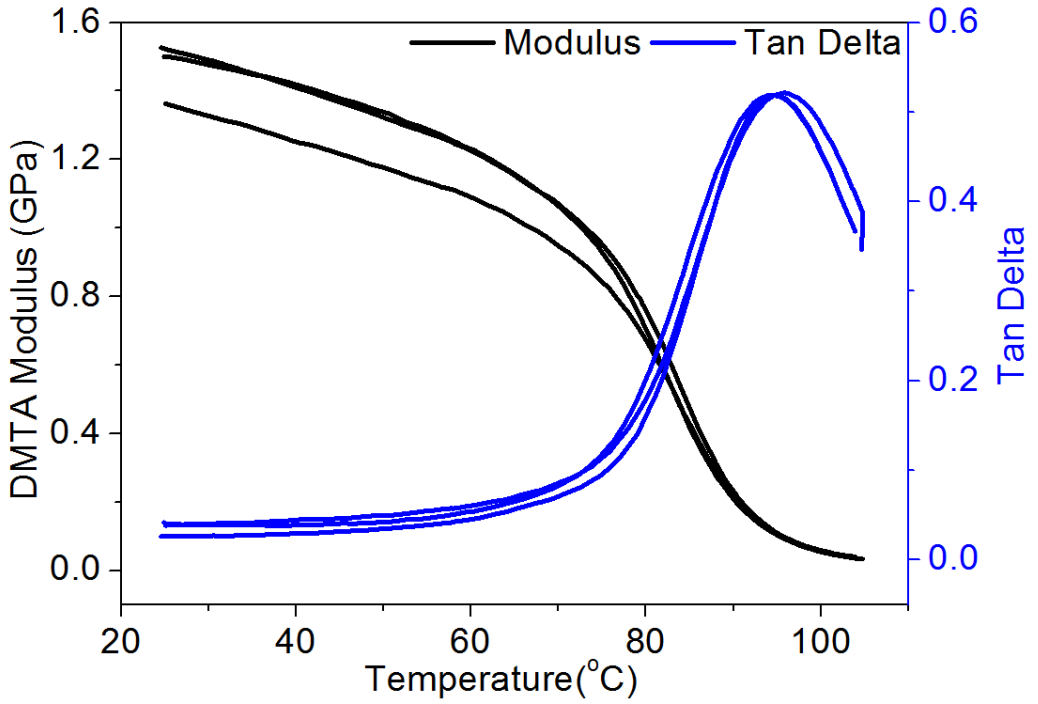

Figure 5.26. DMTA graphs for unconditioned adhesive with 20wt% 930DU120HEMA incorporation.

5.3.3. Environmentally Conditioned Specimens

For bulk tensile test, environmentally conditioned specimens showed an appreciable decrease in UTS but little change in Young's modulus, compared with the results of unconditioned specimens in section 5.3.2. It was observed that the adhesive system with 20wt% 930DU120HEMA incorporation was more susceptible to conditioning -- a 25.4% decrease in UTS while only 7.2% was observed for 20wt%930DU120 formulation. For DMTA results, decreases were observed in peak tan delta value, DMTA modulus as well as glass transition temperature.

UTS measurements showed good consistency. However, data quality was still very poor in terms of Young's modulus and tensile strain measurement. DMTA results of environmentally conditioned specimens all showed good consistency.

Table 5.12. Summary of tensile test results for environmentally conditioned specimens.

Formulation	Ultimate Tensile Strength (MPa)	Young's Modulus (GPa)
Pure adhesive	38.3 ± 0.51	2.1 ± 0.20
20wt% 930DU120	21.8 ± 1.05	2.1 ± 0.58
20wt% 930DU120HEMA	18.5 ± 0.49	2.5 ± 0.44

Table 5.13. Summary of DMTA results for environmentally conditioned specimens.

Formulation	Peak Tan Delta	Tg (°C)	DMTA Modulus (GPa)
Pure adhesive	0.557 ± 0.0026	90.5 ± 0.45	1.7 ± 0.05
20wt% 930DU120	0.482 ± 0.0067	92.3 ± 0.31	1.3 ± 0.06
20wt% 930DU120HEMA	0.500 ± 0.0029	90.2 ± 0.70	1.3 ± 0.06

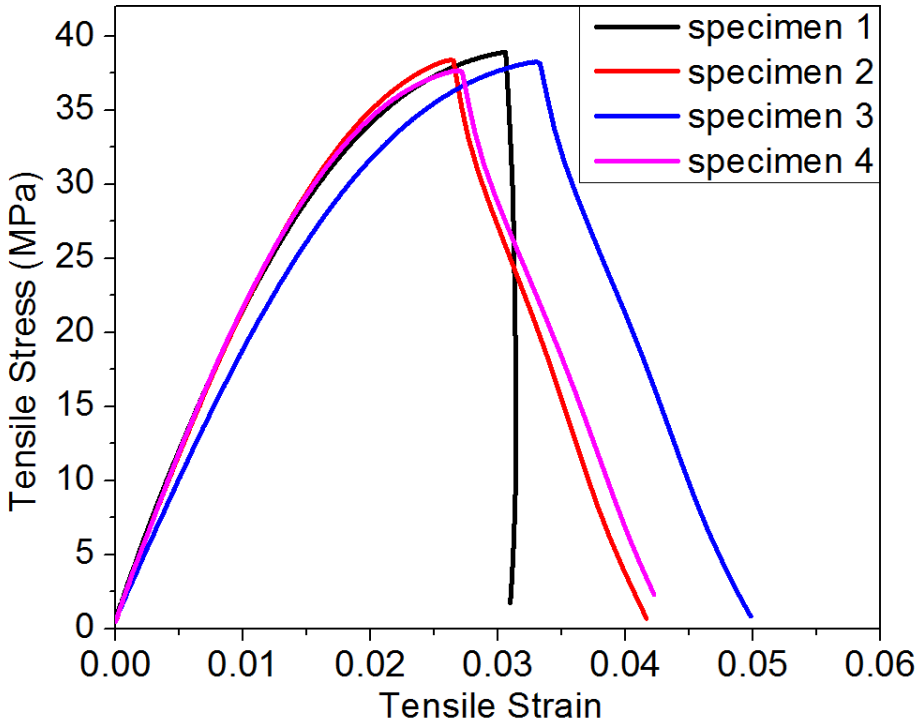

Figure 5.27. Tensile stress-strain curves for environmentally conditioned pure adhesive.

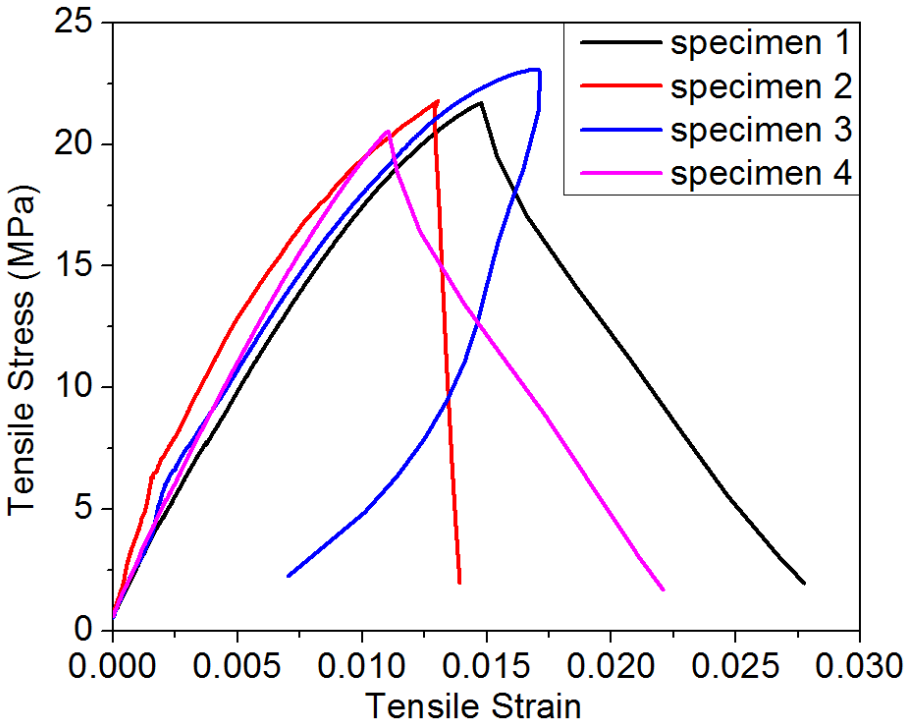

Figure 5.28. Tensile stress-strain curves for environmentally conditioned adhesive with 20wt%930DU120 incorporation.

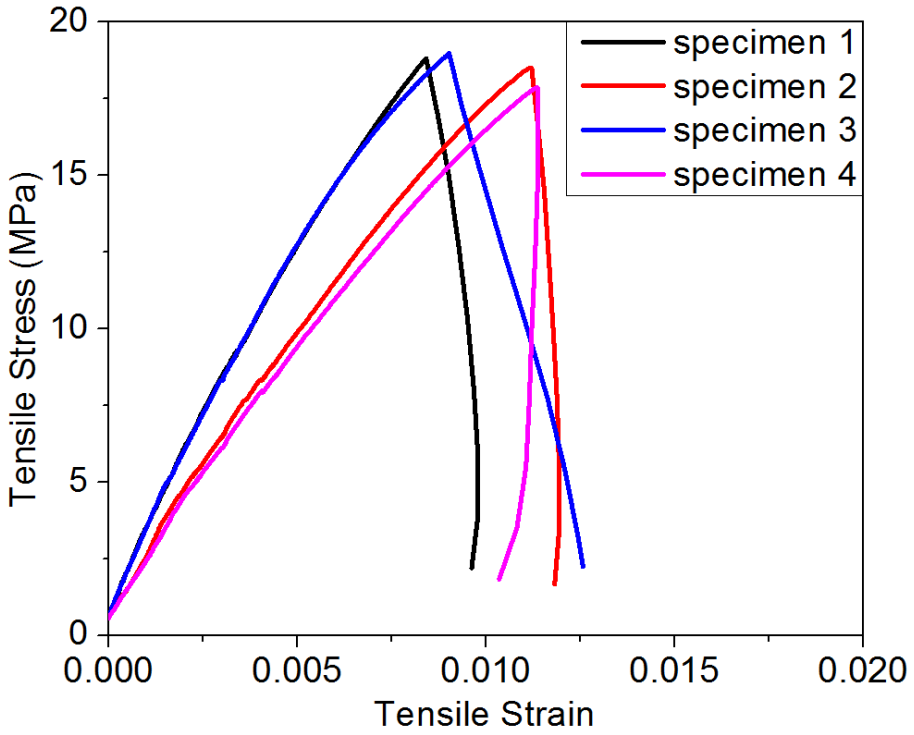

Figure 5.29. Tensile stress-strain curves for environmentally conditioned adhesive with 20wt%930DU120HEMA incorporation.

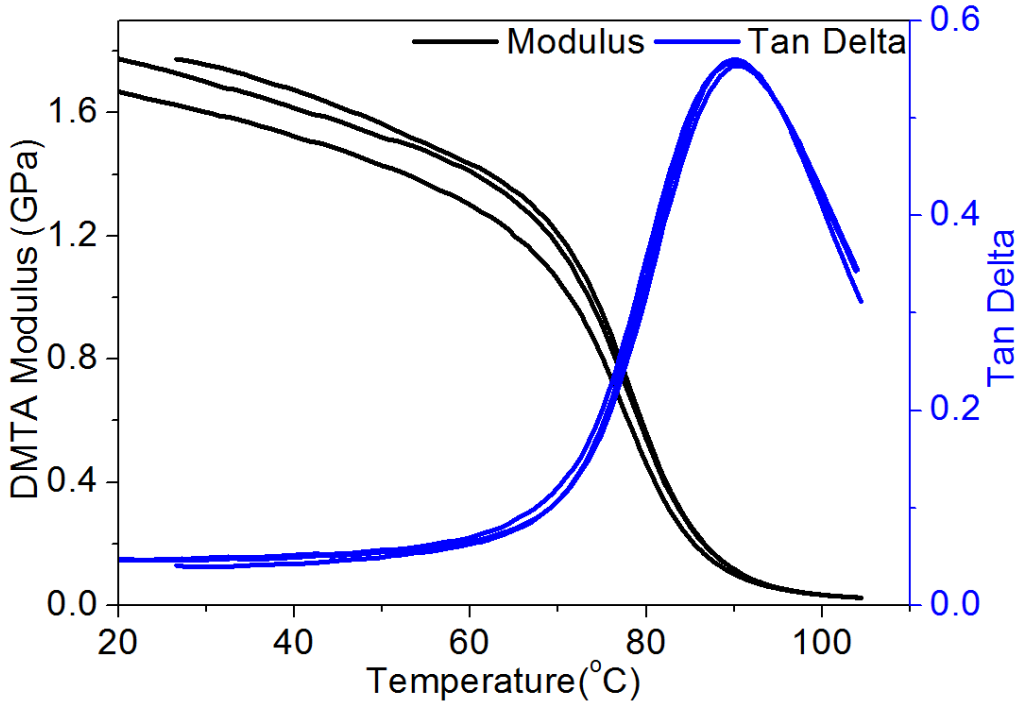

Figure 5.30. DMTA graphs for environmentally conditioned pure adhesive.

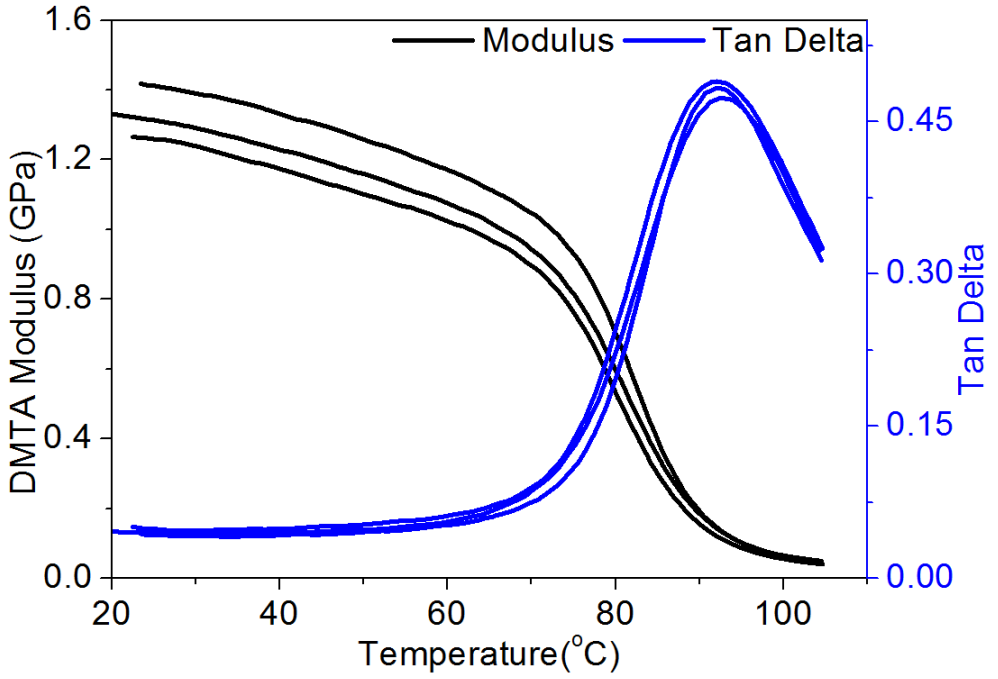

Figure 5.31. DMTA graphs for environmentally conditioned adhesive with 20wt%930DU120 incorporation.

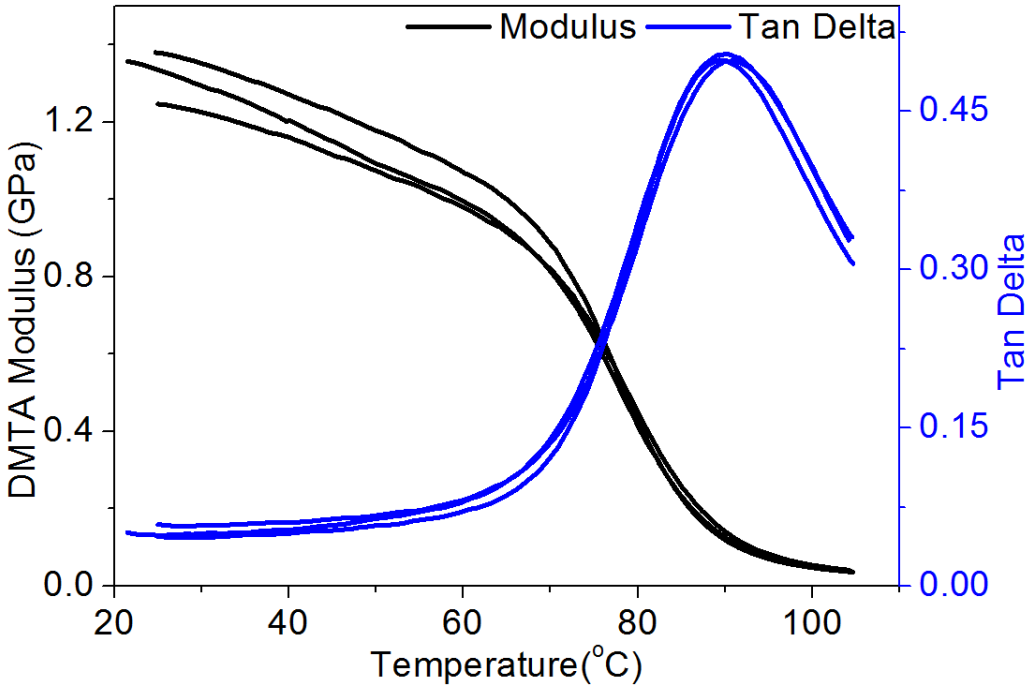

Figure 5.32. DMTA graphs for environmentally conditioned adhesive with 20wt%930DU120HEMA incorporation.

5.4. Results of Stage 4: TEMs Surface Modification via ARGET ATRP

This section is divided into two parts: temperature effect on TEMs modification process and properties of adhesive with modified TEMs incorporation. Optimum surface modification conditions were determined and the influences on TEMs/adhesive system were investigated. Only 930DU120HEMA TEMs grade was used at this stage.

5.4.1. Temperature-Time Effect on TEMs Surface Modification Process

The temperature-time effect on the TEMs surface modification via ARGET ATRP was studied and characterised by FTIR and SEM tests. FTIR spectra were obtained for TEMs at different stages of modification process:

- After acid treatment, Figure 5.34;
- After immobilisation process, Figure 5.35;
- TEMs modified at 23^{o}C for 3 hours, 23^{o}C for 5 hours , 30^{o}C for 3 hours, 30^{o}C for 5 hours, 37^{o}C for 3 hours, 37^{o}C for 5 hours (Figure 5.36 to Figure 5.41);

FTIR spectrum of GMA was also obtained for a better analysis of characteristic peaks, Figure 5.33. It was noticed that the sharp peak at 3600 cm^{-1} (attributed to free or non-hydrogen-bonded hydroxyl groups) disappeared for FTIR spectrum of TEMs after acid treatment. This indicates that the Magnesium hydroxide was successfully removed. It was observed that the major differences between modified TEMs (grafted with PGMA chains) and original TEMs occurred at the peaks in the following wavelength ranges in Table 5.14.

It is apparent that TEMs modified at both 23 ^{o}C 3 hours and 23^{o}C 5 hours did not show significant differences in these main peaks, especially the epoxide ring vibration peaks at 904^{-1}, 847^{-1} and 761cm^{-1}. FTIR spectra are discussed in details in section 6.1 in Chapter 6.

TEMs modified at 30^{o}C 3 hours, 30^{o}C 5 hours, 37^{o}C 3 hours and 37^{o}C 5 hours were characterised by SEM and shown from Figure 5.42 to Figure 5.46. No significant

changes were observed for TEMs modified at 30°C 3 hours and 30°C 5 hours compared with unmodified TEMs in Figure 5.13. For TEMs modified at 37°C 3 hours and 37°C 5 hours, it was apparent that small particulate deposits were attached to the surface of TEMs. For TEMs modified at 37°C 5 hours specifically, large agglomerates were observed under the microscope and more particulate deposits were found attached to the surface of TEMs. It was also observed that large deposits formed during TEMs modification at 37°C 5 hours, see Figure 5.46 and Figure 5.47. This indicates that at 37°C, 5 hours might not be a suitable time for polymerisation. Detailed explanations for these microstructural changes are provided in section 6.4 in Chapter 6.

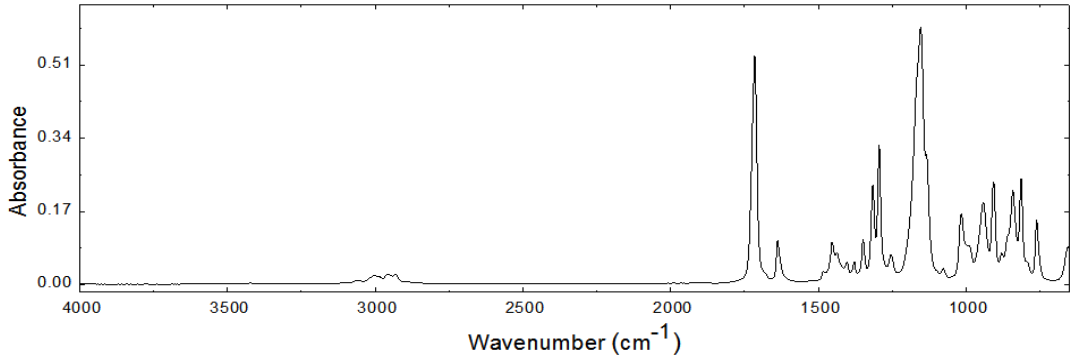

Figure 5.33. FTIR spectrum of glycidyl methacrylate.

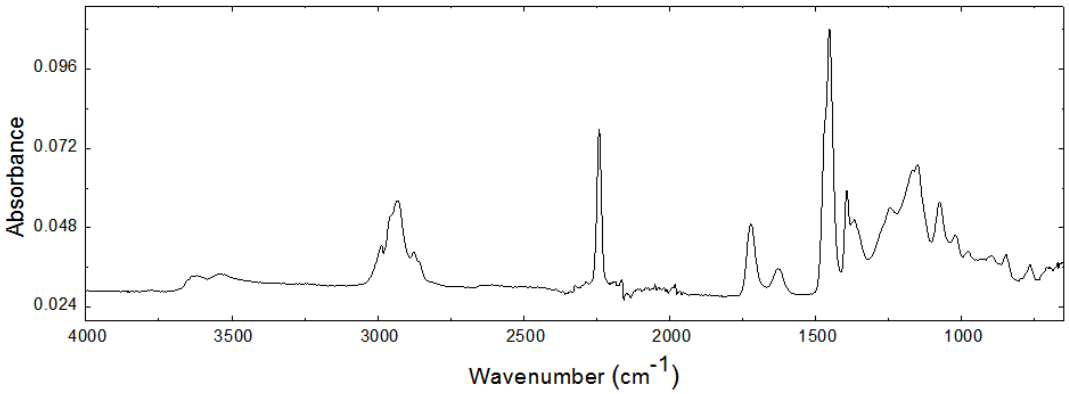

Figure 5.34. FTIR spectrum of acid treated TEMs.

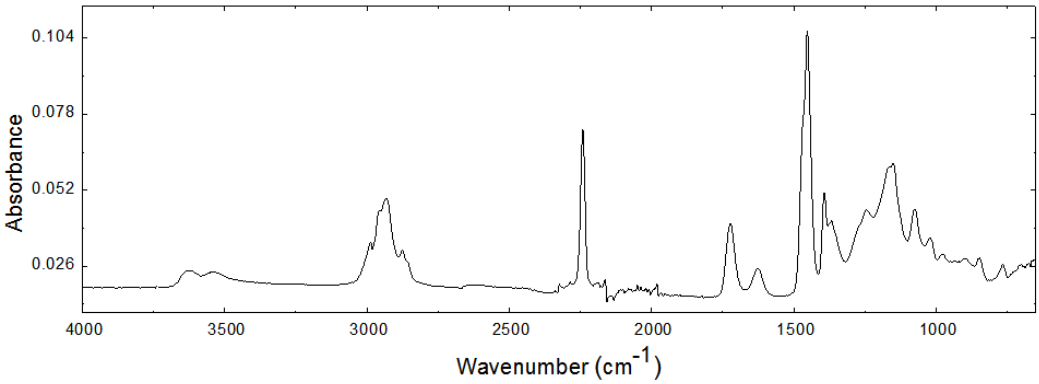

Figure 5.35. FTIR spectrum of α-bromoisobutyryl bromide immobilised TEMs.

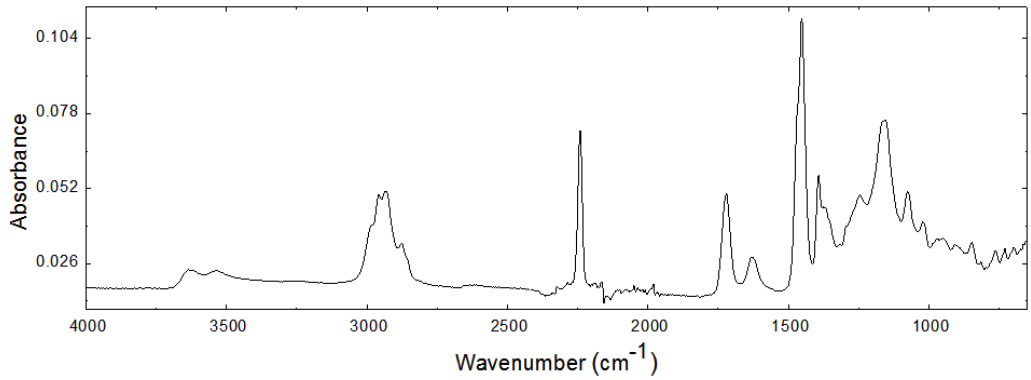

Figure 5.36. FTIR spectrum of TEMs modified at 23°C for 3 hours.

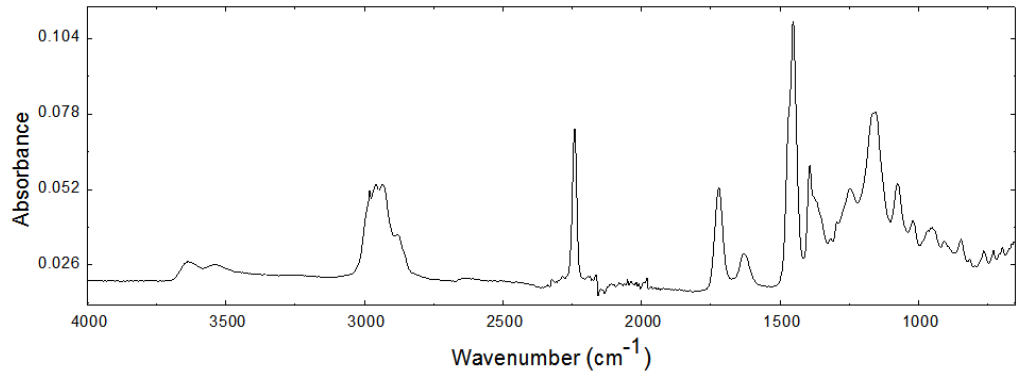

Figure 5.37. FTIR spectrum of TEMs modified at 23°C for 5 hours.

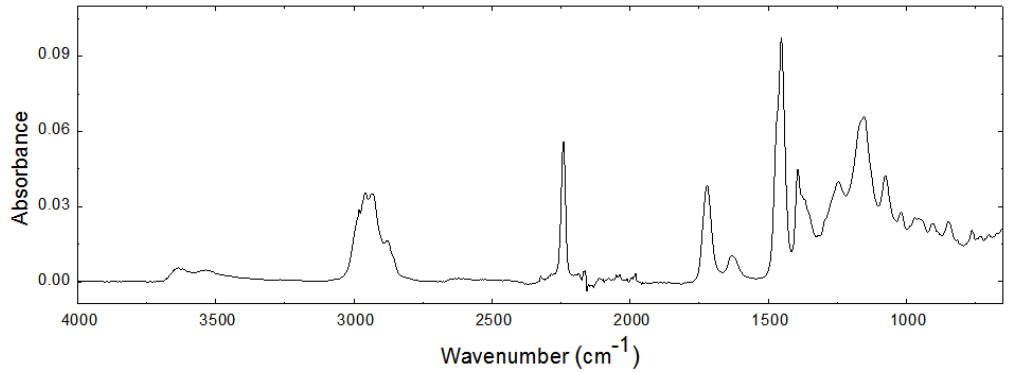

Figure 5.38. FTIR spectrum of TEMs modified at 30°C for 3 hours.

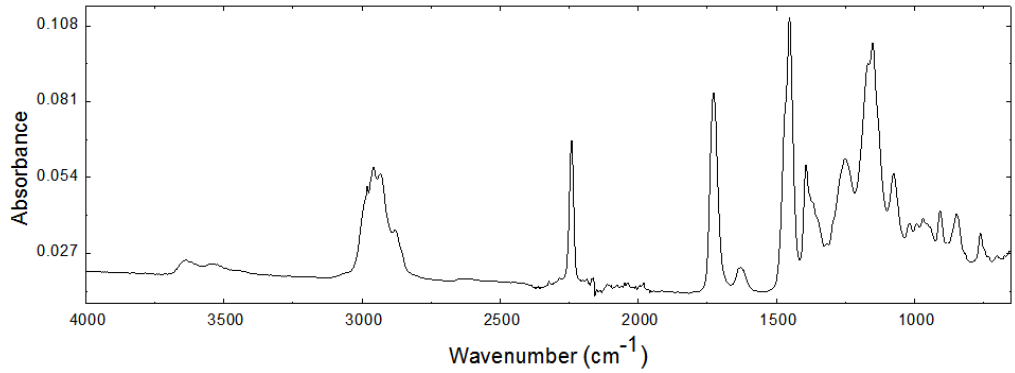

Figure 5.39. FTIR spectrum of TEMs modified at 30°C for 5 hours.

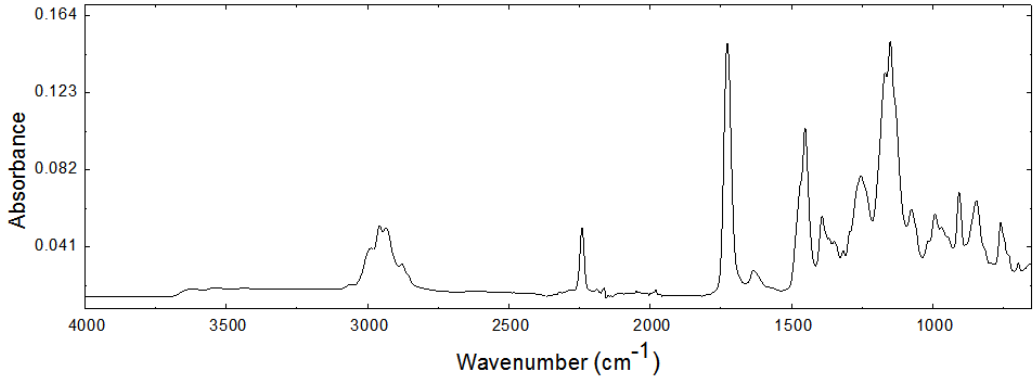

Figure 5.40. FTIR spectrum of TEMs modified at 37°C for 3 hours.

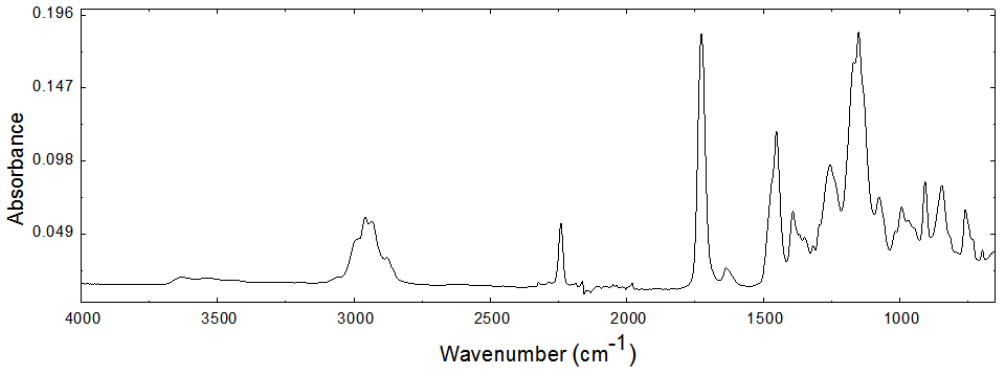

Figure 5.41. FTIR spectrum of TEMs modified at 37°C for 5 hours.

Table 5.14. Wavelength ranges of major differences and main assignments.

Wavelength Ranges (cm^{-1})	Main Assignments
1757 - 1677	C=O stretching
1325 – 1220	-CH in-plane deformation; epoxide ring vibration
1220 - 1035	C-O-C stretching
1035 – 930	C-O stretching
930 – 883	Epoxide ring vibration
883 – 780	Epoxide ring vibration
780 - 720	Epoxide ring vibration

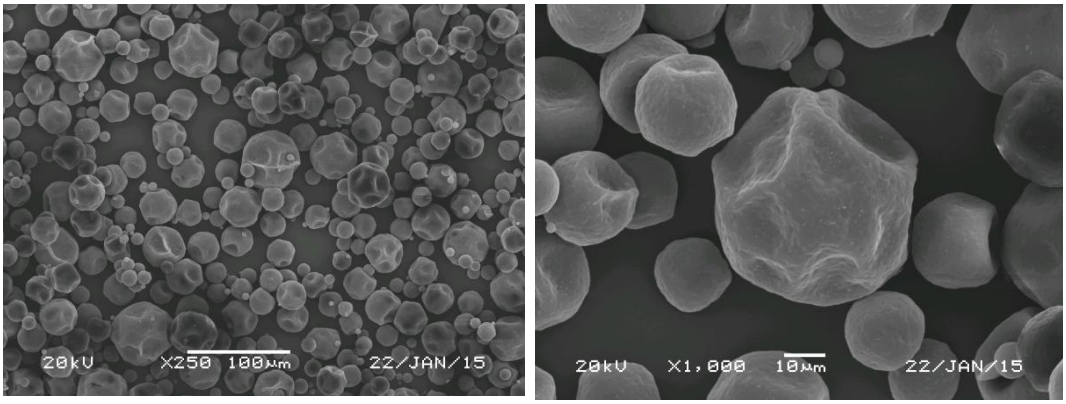

Figure 5.42. SEM micrograph of TEMs modified at 30°C for 3hours.

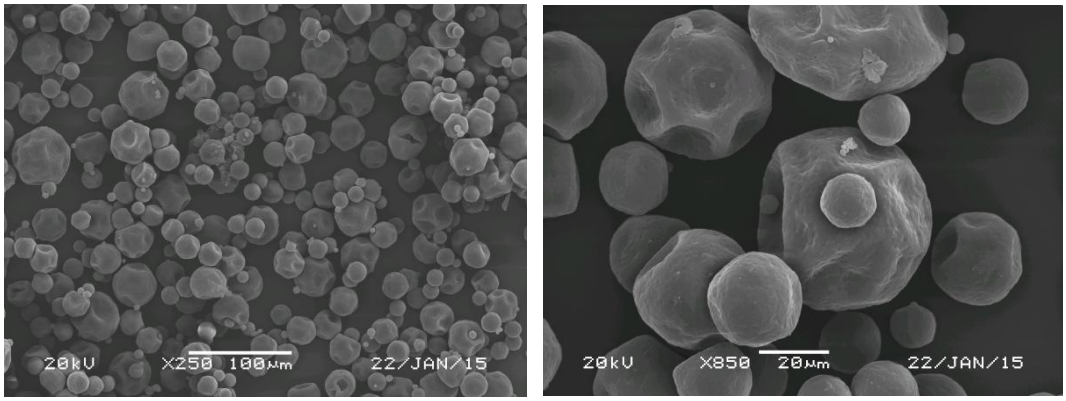

Figure 5.43. SEM micrograph of TEMs modified at 30^{o}C for 5hours.

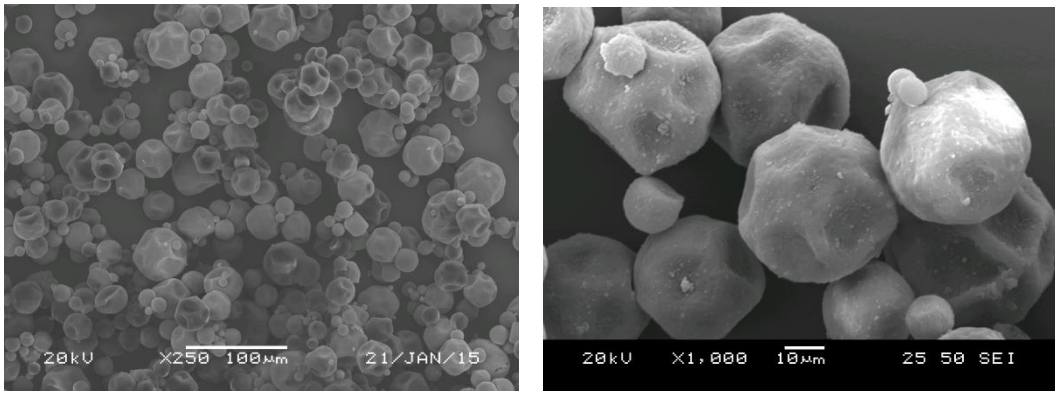

Figure 5.44. SEM micrograph of TEMs modified at 37^{o}C for 3hours.

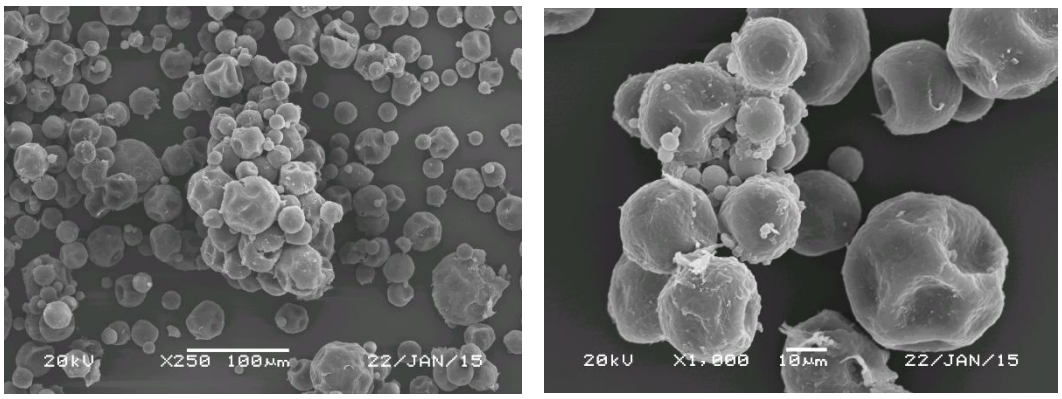

Figure 5.45. SEM micrograph of TEMs modified at 37^{o}C for 5hours.

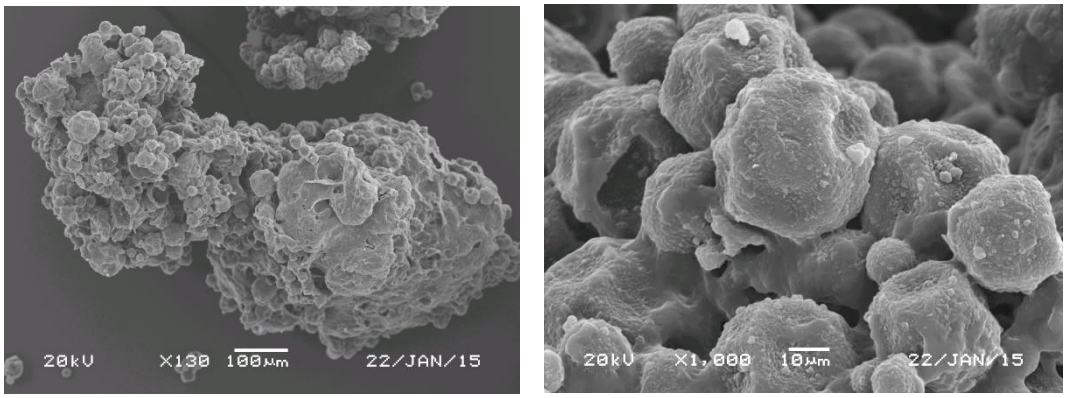

Figure 5.46. SEM micrograph of bulk materials formed during TEMs modification at 37^{o}C for 5 hours.

Figure 5.47 Photograph of bulk materials formed during surface modification.

5.4.2. Adhesive System Incorporated with Modified TEMs

Based on the results from FTIR and SEM, the TEMs modified at 30 ^{o}C for 3 hours, 30^{o}C for 5 hours and 37^{o}C for 3 hours were selected to be incorporated into adhesive single lap joints and evaluated for disbonding effectiveness and improvement in tensile lap shear strength. Modified TEMs with the best performance were further incorporated into the adhesive matrix and tested for bulk tensile test and DMTA test, for both unconditioned specimens and environmentally conditioned specimens. Specimens incorporated with modified TEMs were labelled using the modification condition: Temperature + Time, e.g. 37^{o}C3 h means TEMs modification at 37^{o}C for 3 hours.

5.4.2.1. Disbonding Performance

It can be seen from the results in Table 5.15 and Table 5.16 that the TEMs modified at 30^{o}C 3h and 37^{o}C 3h achieved quite similar disbonding effectiveness while 30^{o}C 5h variation showed slightly lower value. It was noted that for the tensile lap shear strength before heat activation, for adhesive incorporated with 37^{o}C 3h modified, achieved an average of 22.1 MPa, which is 14.5% higher than the 19.3 MPa of the unmodified TEMs (930DU120HEMA). This improvement was also much higher than 30^{o}C 3h and 30^{o}C 5h modified TEMs. Photographs of typical fracture surfaces showed mixed mode failure both before and after heat activation, Figure 5.48. The quality of data showed satisfactory consistency. 37°C 3h modified TEMs were chosen for further bulk tests. Fracture surface of adhesive incorporated with TEMs modified at 37°C 3h was characterised by SEM, Figure 5.49 and Figure 5.50. Similar to the results in Figure 5.18, TEMs sized cavities and fracture TEMs but no intact TEMs were observed on the fracture surface before heat activation.

Table 5.15. Tensile lap shear strength for modified TEMs (A) before heat activation, and (B) after heat activation.

(A)

Specimen No.	30°C 3h	30°C 5h	37°C 3h
1	20.7	20.7	22.1
2	20.4	20.8	22.1
3	20.4	21.1	22.0
Average (MPa)	**20.5**	**20.9**	**22.1**
Standard Deviation	**0.19**	**0.24**	**0.07**

(B)

Specimen No.	30°C 3h	30°C 5h	37°C 3h
1	2.9	4.8	3.9
2	3.5	4.1	3.3
3	3.5	3.6	3.9
Average (MPa)	**3.3**	**4.2**	**3.7**
Standard Deviation	**0.38**	**0.61**	**0.35**

Table 5.16. Disbonding Effectiveness of SLJs with modified TEMs.

Modified TEMs	30°C 3h	30°C 5h	37°C 3h
Disbonding Effectiveness (%)	83.9	80.0	83.3

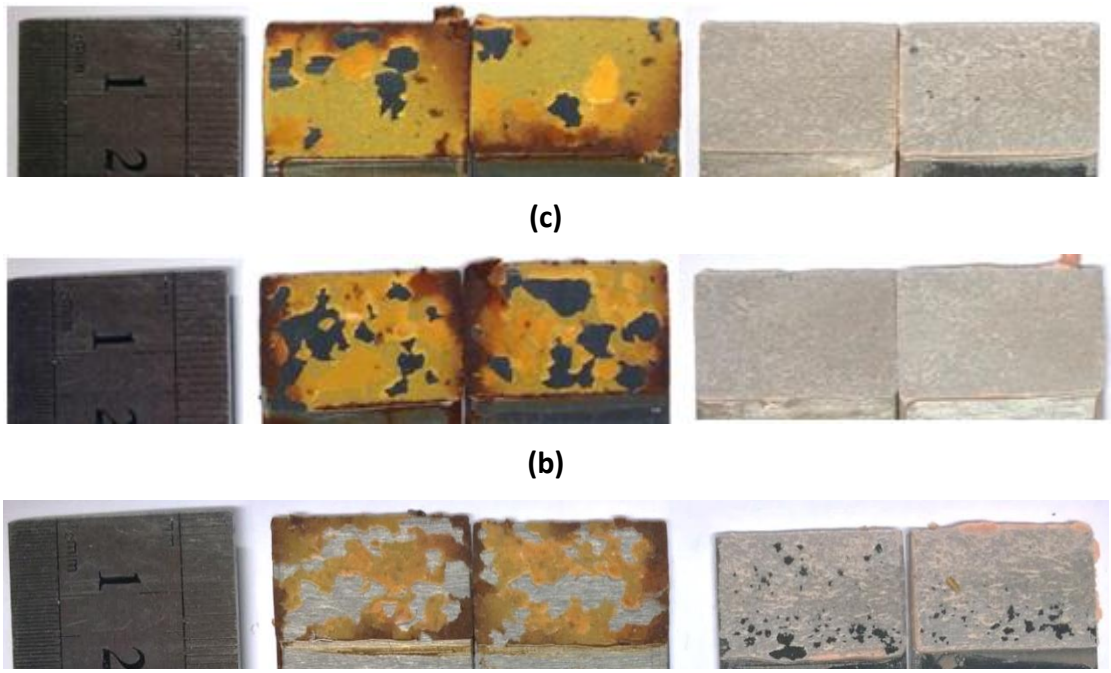

(c)

(b)

(a)

Figure 5.48. Featured fracture surfaces of adhesive SLJs with modified TEMs. Left: after heat activation; Right: before heat activation. (a) 30 °C 3h, (b) 30°C 5h, (c) 37°C 3h.

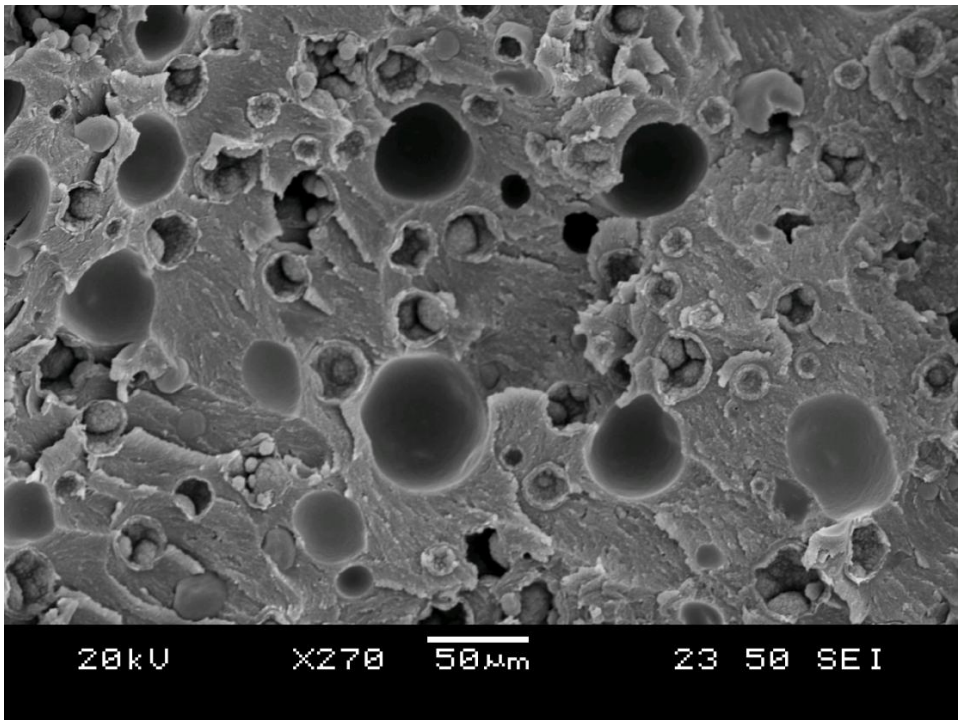

Figure 5.49. SEM micrograph of fracture surface of adhesive with TEMs modified at 37^{o}C 3h before heat activation.

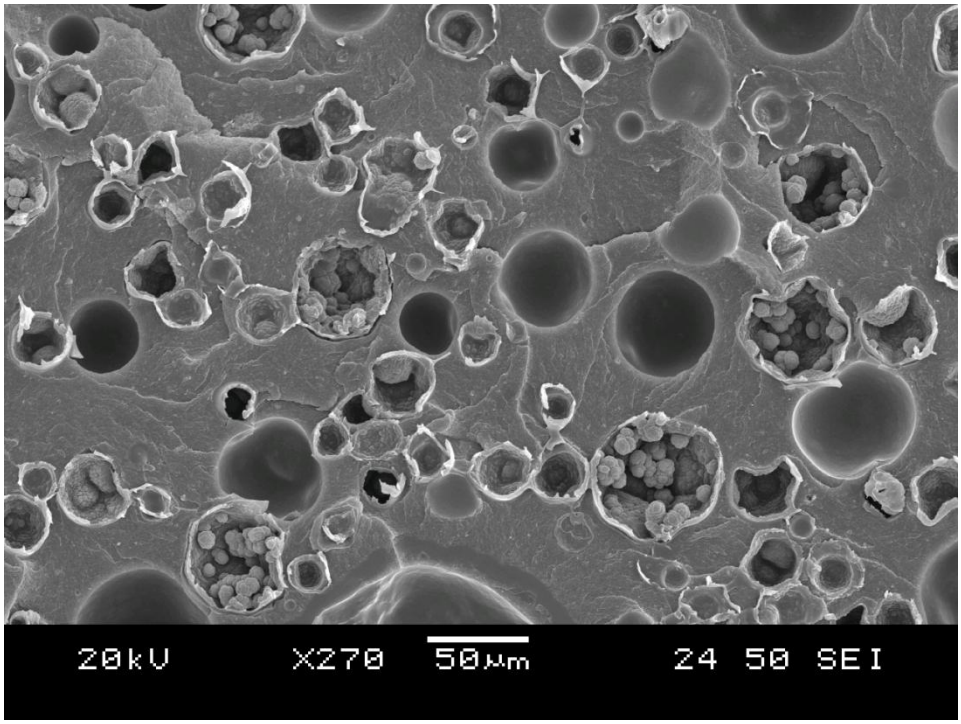

Figure 5.50. SEM micrograph of fracture surface of adhesive with TEMs modified at 37^{o}C 3h after heat activation.

5.4.2.2. Bulk Test Results

Bulk tensile tests of modified TEMs (37°C 3h) achieved an UTS of 30.7 MPa which was 23.8% higher than 24.8 MPa for the unmodified TEMs, see Table 5.10 and Table 5.17. It was also noted that the UTS of environmentally conditioned specimens was 26.94 MPa, which was higher than both the unconditioned and environmentally conditioned specimens of the unmodified TEMs, see Table 5.10, Table 5.12 and Table 5.17. The quality of data was poor for Young's modulus measurement but showed acceptable standard deviation for UTS measurement.

Compared with the results for unconditioned TEMs, DMTA results showed increases in peak tan delta value, Tg and DMTA modulus for adhesive incorporated with modified TEMs before environmental conditioning, See Table 5.11 and Table 5.18. After environmental conditioning, the peak tan delta value, Tg and DMTA modulus all decreased and showed similar results compared with environmentally conditioned specimens with unmodified TEMs, see Table5.13 and Table 5.18. A fairly good data quality was achieved with DMTA tests.

Table 5.17. Bulk tensile test results of adhesive with modified TEMs (37°C 3h) incorporation.

	Ultimate Tensile Strength(MPa)	Young's Modulus(GPa)
Unconditioned	30.7 ± 0.74	2.6 ± 0.33
Environmentally Conditioned	26.9 ± 1.21	2.9 ± 0.84

Table 5.18. DMTA test results of adhesive with modified TEMs (37°C 3h) incorporation.

	Peak Tan Delta	Tg (^oC)	DMTA Modulus (GPa)
Unconditioned	0.561 ± 0.0076	95.9 ± 0.66	1.6 ± 0.16
Environmentally Conditioned	0.498 ± 0.0092	89.9 ± 0.15	1.6 ± 0.06

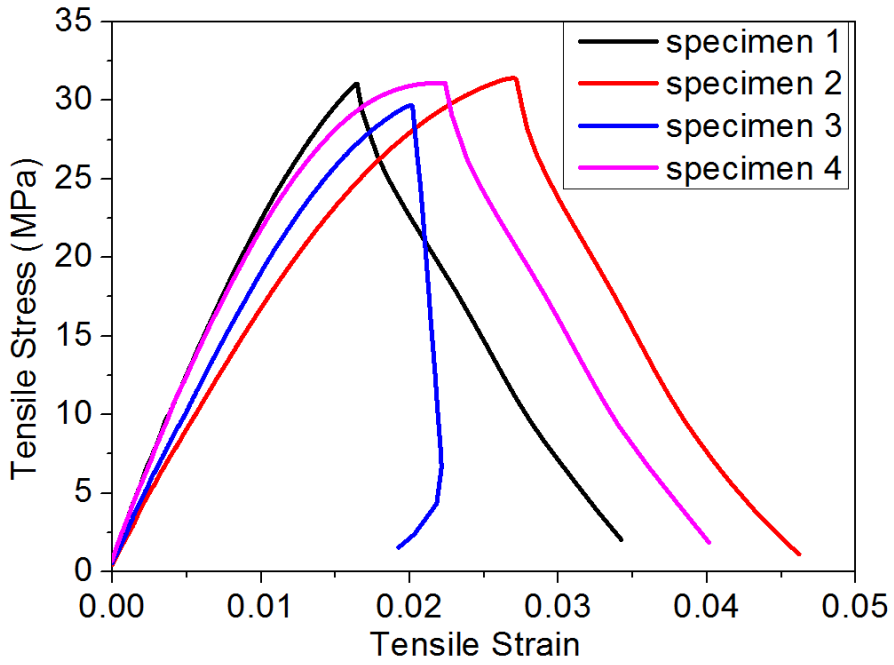

Figure 5.51. Tensile stress-strain curves for unconditioned adhesive with modified TEMs (37^{o}C3h) incorporation.

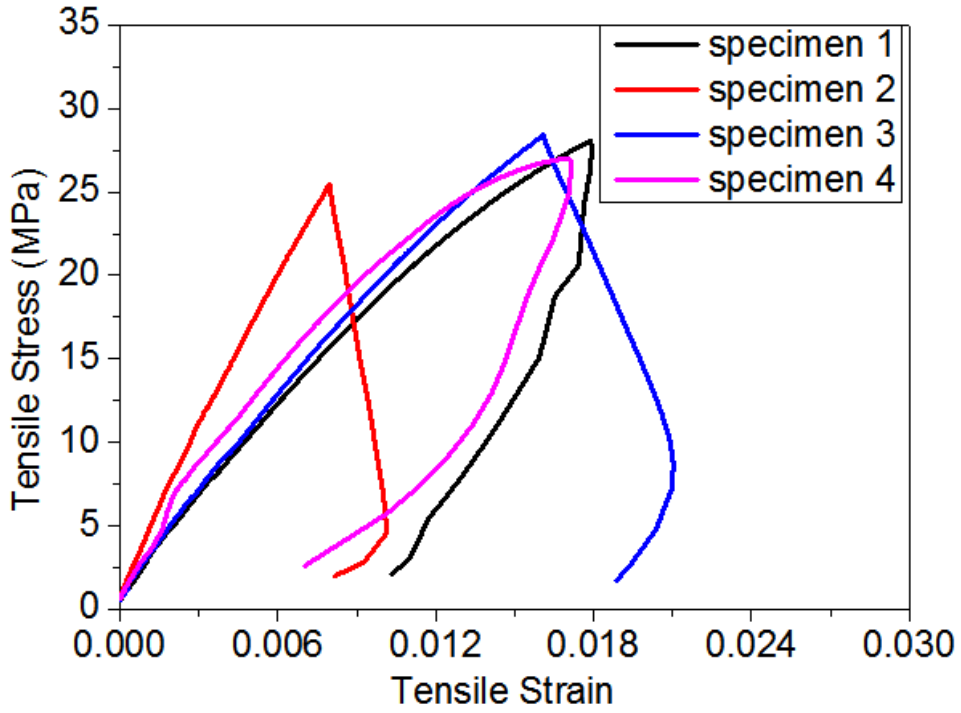

Figure 5.52. Tensile stress-strain curves for environmentally conditioned adhesive with modified TEMs (37°C3h) incorporation.

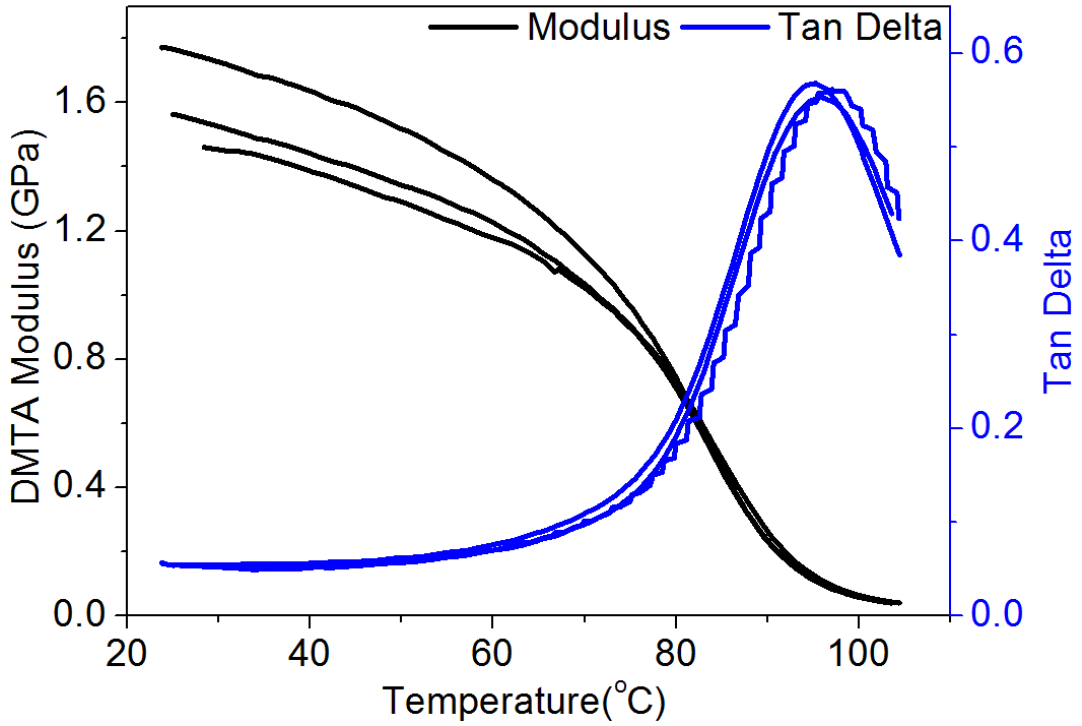

Figure 5.53. DMTA graphs of unconditioned adhesive with modified TEMs (37°C3h) incorporation.

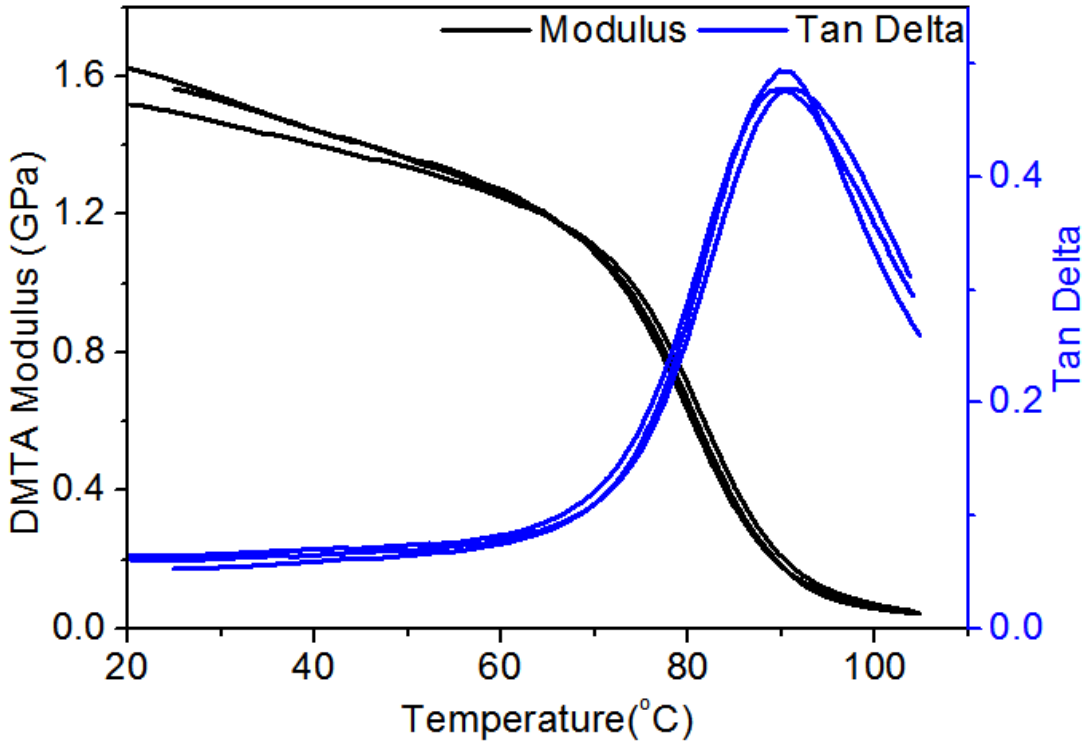

Figure 5.54. DMTA graphs of environmentally conditioned adhesive with modified TEMs (37°C3h) incorporation.

5.5. Summary

In summary, key properties of each test materials (adhesive, TEMs, aluminium substrate) were successfully characterised in Stage 1.

For stage 2, the optimum TEMs concentration was identified as 20wt% and the optimum TEMs grades were identified as 930DU120 and 930DU120HEMA.

For stage 3, TEMs/adhesive system showed higher weight gain in water immersion test. Mechanical properties were generally reduced by TEMs incorporation. Also, TEMs/adhesive system was found more vulnerable to water ingression.

For Stage 4, TEMs surface modification via ARGET ATRP was proved to be successful. Adhesive incorporated with modified TEMs showed improvement in mechanical properties as well as water resistance.

Chapter 6.Discussion

6.1. Introduction

In the search for a disbondable adhesive system suitable for automotive applications, the TEMs approach was identified as one of the most promising systems with satisfactory disbonding performance observed in previous research conducted within JTRC (McCurdy, 2011).

However, the major limitation of the TEMs approach was poor TEMs/adhesive compatibility which weakened the mechanical properties and long term durability of the original adhesive system. Therefore, the primary concern for this project was to address this compatibility issue. On the basis of this, experimental test programme was established in Chapter 4.

A better understanding of this compatibility issue was achieved from the experimental studies on both TEMs/adhesive joints and bulk material properties. The disbonding performances of different TEMs concentrations and four grades of TEMs were also studied to understand the disbonding mechanism.

To improve the TEMs/adhesive compatibility, the ARGET ATRP technique was employed for TEMs surface modification. As a simple and controlled polymerisation technique, ARGET ATRP has been successfully applied as a surface modification technique for both flat and spherical surfaces. Its relatively high tolerance to oxygen and impurities also indicate a greater potential for industrial application. The temperature effect on TEMs surface modification via ARGET ATRP was investigated for an optimum modification condition. The improvement on adhesive joint and bulk properties of the modified TEMs system was evaluated by comparing the results with that of unmodified TEMs system. Only 930DU120HEMA grade of TEMs were used in the surface modification work.

6.2. Disbonding Performance of TEMs/Adhesive system

The disbonding performance of adhesive SLJs with TEMs incorporation was evaluated using the SLJ configuration from two aspects: TEMs concentrations and TEMs grades.

6.2.1. Effect of TEMs Concentrations

The effect of TEM concentration was investigated on six different concentrations of EM501 grade TEMs. Based on the results obtained, Figure 6.1 illustrates the relationship found between TEMs concentration and tensile lap shear strength. 0wt% TEMs concentration represents the pure adhesive.

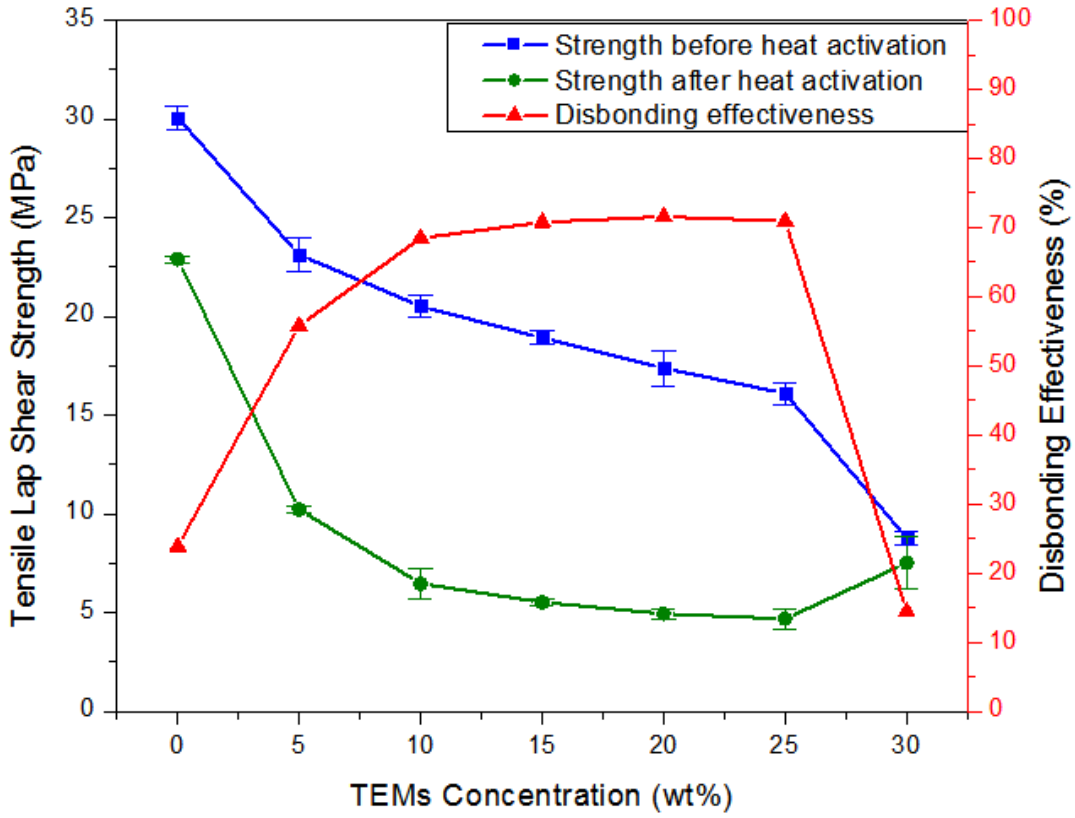

Figure 6.1. TEMs (EM501) concentration vs tensile lap shear strength.

It is obvious that the incorporation of TEMs lowered the tensile lap shear strength of adhesive joints. This negative correlation followed an approximately linear relationship between 5wt% and 25wt% for specimens both before and after heat

activation. The principal reason for this reduction in strength was attributed to the weak interaction between the TEMs and adhesive matrix. SEM micrograph of SLJ fracture surface which showed TEMs sized cavities but no intact TEMs, see Figure 5.18. Also, it was noted that the cavities, unlike the rest of fracture surface, exhibited a relatively clean and smooth texture. This implies that the TEMs were separated from the adhesive matrix upon fracture leaving behind the smooth cavities. Another possible reason for this reduction was ascribed to the weak structure of TEMs. This is supported by the small amount of fractured TEMs structure shown in Figure 5.18.

At 30wt% concentration, the tensile lap shear strength exhibited a sharp decrease prior to heat activation and an apparent increase once subject to heat activation. The sharp decrease is ascribed to poor mixing at higher concentrations. The viscosity of TEMs/adhesive mixture before curing increased with TEMs concentration, which led to problems encountered during SLJs preparation process. This poor mixing increases the chance of TEMs clustering and air entrapment between the TEMs, as illustrated in Figure 6.2. The existence of air entrapment can also be confirmed in the SEM micrograph in Figure 6.3 (edited from Figure 5.16). The slight increase in residual strength after heat activation was unexpected. It is possible that due to the presence of large amount of TEMs, at a temperature above T_3, the TEMs thermoplastic shell material melted and sealed some of the cracks, producing a slight increase in residual strength. This phenomenon could also happen at low concentrations of TEMs albeit with negligible effect.

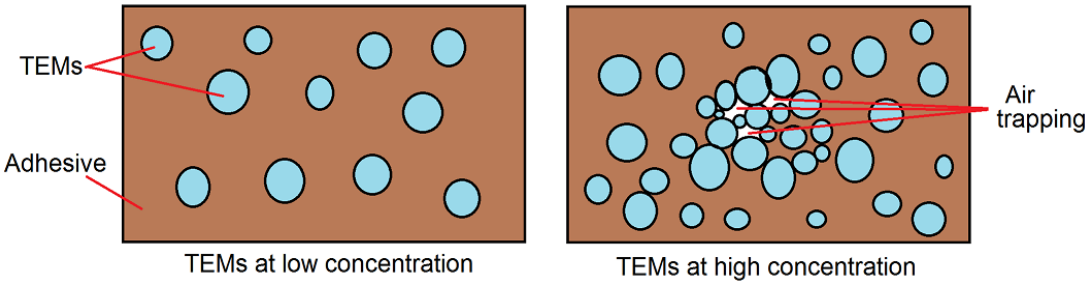

Figure 6.2. Schematic illustration of air trapping at high TEMs concentration.

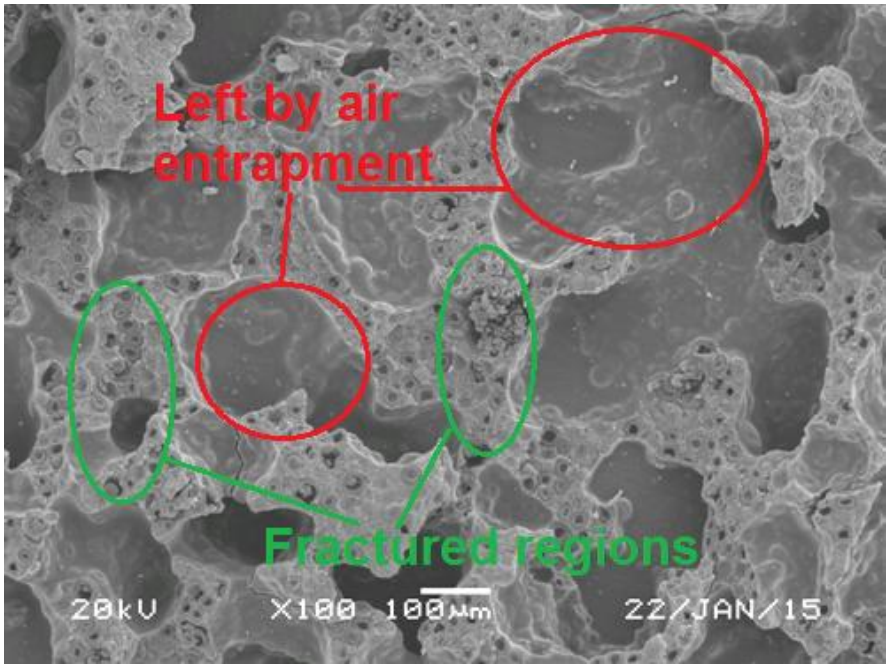

Figure 6.3. Marked: SEM micrograph of fracture surface of adhesive incorporated with 30wt% EM501 before heat activation.

6.2.2. Effect of Different TEMs Grades

Adhesive joints incorporated with different grades of TEMs were investigated for disbonding performance using the optimum concentration 20wt% identified from earlier results. Figure 6.4 and Figure 6.5 re-depict the results in 5.2.3 for a better illustration. As was shown in 5.1.2, the four TEMs grades differ from each other mainly in the following ways:

i. **Chemical composition:** core and shell material;
ii. **Particle size distribution**: compared with 930DU120 and 930DU120HEMA, EM501 and F230D showed sharper distribution;
iii. **Microstructure**: EM501 and F230D grade showed smoother morphology while the other two grades exhibited different levels of roughness.

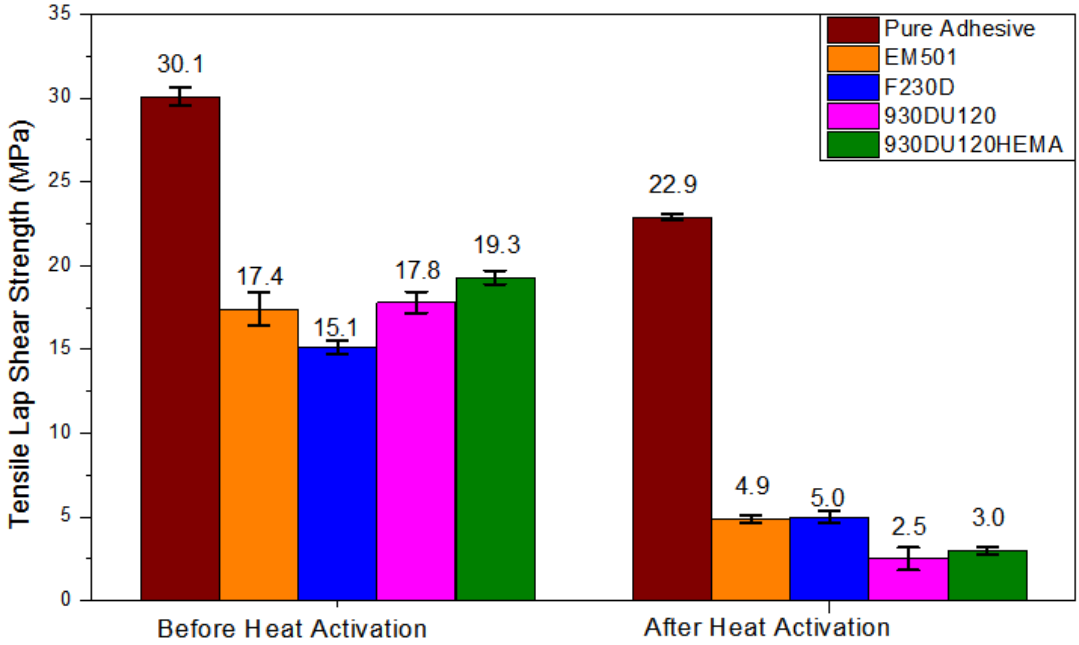

Figure 6.4. Tensile lap shear strength of four grades of TEMs before and after heat activation.

It was found that the sharper PSD and smoother morphology of EM501 and F230 did not play a decisive role on the disbonding effectiveness of TEMs/adhesive system. Compared with 930DU120 and 930DU120HEMA grades, EM501 and F230D grades showed slightly lower tensile lap shear strength prior to heat activation and also a higher residual strength after heat activation. It is possible that smooth morphology and narrow PSD contributed to a better disbonding performance due to a better mixing. However, these two effects (morphology and PSD) cannot be validated from current experimental results as they were either too weak or masked by other more dominant factors such as the TEMs' material composition (both hydrocarbon core and thermoplastic shell).

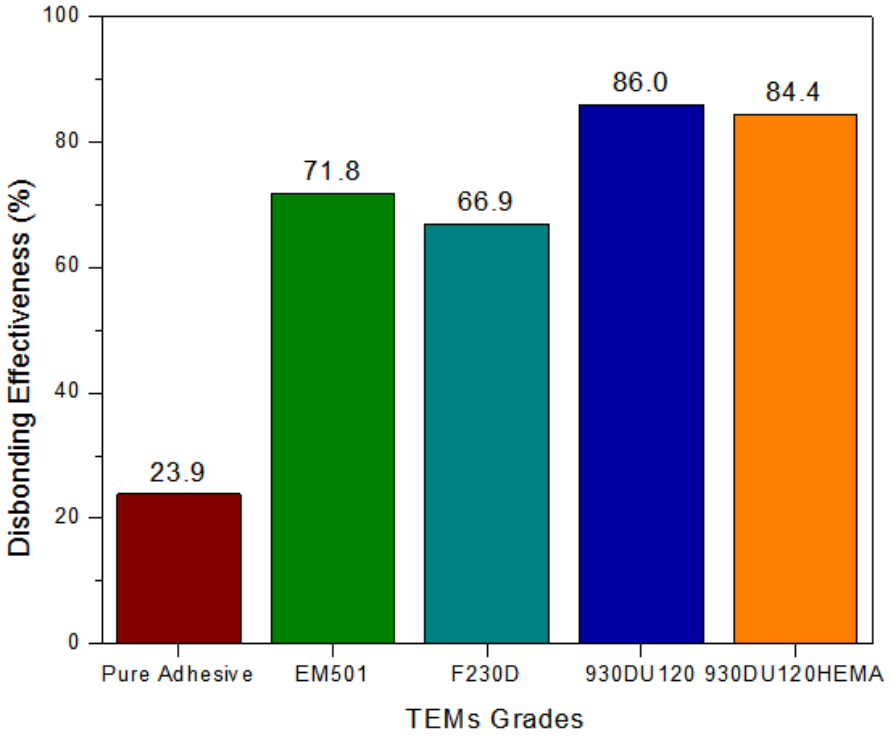

Figure 6.5. Disbonding effectiveness of adhesive incorporated with four grades of TEMs.

The importance of TEMs chemical composition and the difference between 930DU120 and 930DU120HEMA grade TEMs are further discussed in relation to the bulk test results in 6.3.

6.2.3. Disbonding Mechanism of TEMs/Adhesive System

Previous research in the literature has given several explanations regarding the disbonding mechanisms of adhesive joints incorporated with foaming agents, including:

- Adhesive softening at higher temperature, which inevitably weakens joint integrity;
- Migration of additives to adhesive/substrate interface, then foaming and expansion exerts pressure to disbond;
- Crack propagation caused by additive expansion. (McCurdy, 2011)

To understand the disbonding mechanism of TEMs/adhesive system, oven heating was used as a better controlled method to activate adhesive joint disbonding. SLJ specimens were allowed to cool down to room temperature prior to testing. This was designed to preclude the effect of adhesive softening at higher temperature and focus only on the TEMs' role in the disbonding process.

Based on the results and observations in this research, the disbonding mechanism of TEMs/adhesive system was dependent on the following three aspects, each supported with evidence:

A. Crack propagation

Crack propagation was identified as the principal cause for the disbonding mechanism of TEMs/adhesive system. As can be observed from SEM micrographs in Figure 5.19, there are no intact TEMs on the fracture surfaces of SLJs after heat activation. This is attributed to the fact that TEMs shell structures were ruptured by the hydrocarbon gases upon full heat activation at T_3 temperature. Internal stresses caused by TEMs expansion led to the formation of cracks in the adhesive matrix. Although no concrete proof was found, it was speculated that the crack propagation in the bond line might be further promoted by the leaked hydrocarbon gases. This transformation upon heat activation is illustrated in Figure 6.6.

As was noticed from the photographs (see Figure 5.17) of almost every SLJ fracture surface, mixed mode failure was observed as the predominant failure mode. Poor surface treatment can be ruled out as a contributing factor to this phenomenon since all SLJs before heat activation exhibited 100% cohesive failure. A more convincing explanation would be that cracks initially propagated in all directions in the adhesive matrix but were deflected along the adhesive-aluminium interface upon reaching the aluminium substrate. The one exception to this was adhesive system with 30wt% EM501 incorporation (100% cohesive failure). In this case, it is believed that TEMs shell material melted and blocked the passage for crack propagation resulting in a relatively confined structure for voids and cracks left by TEMs expansion.

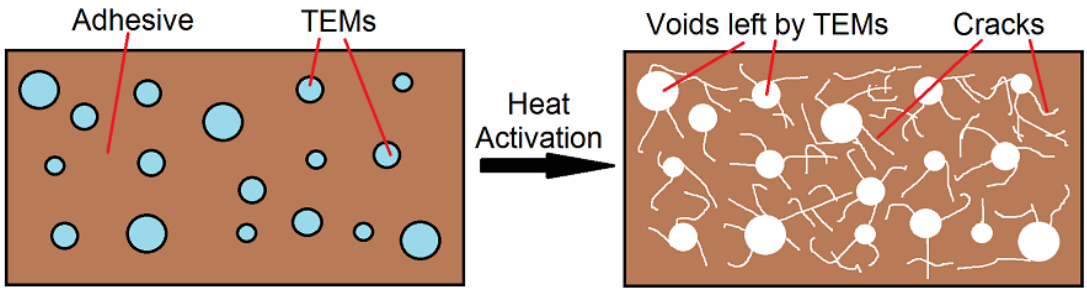

Figure 6.6. Schematic illustration of crack propagation in the adhesive after heat activation.

B. Differential thermal expansion coefficient

The linear thermal expansion coefficient of EN AW-6082 T6 alumnium is $24*10^{-6}$ K^{-1}. For the epoxy adhesive, the linear thermal expansion coefficient is approximately $(50\sim60)*10^{-6}$ K^{-1} for temperatures below Tg and $(170\sim190)$ $*10^{-6}$ K^{-1} for temperatures above Tg (Adams et al., 1997). For epoxy adhesive with TEMs incorporation, this value is supposed to be higher than pure adhesive.

This difference in thermal expansion coefficient means a 7 to 8 times' difference in expansion ratio above glass transition temperature. Therefore, during the disbonding effectiveness test, differential thermal expansion and shrinkage stresses were unavoidably incurred which would further weakened the integrity of joint and contribute to the disbonding performance.

C. Adhesive degradation

As can be observed from the photographs of SLJ fracture surface (see Figure 5.17), there was some degree of colour change for specimens before and after heat activation. The fracture surfaces of specimens after heat activation had generally darkened in colour. For the adhesive joints incorporated with TEMs, this could be ascribed to the degradation of TEMs, as shown in Figure 4.2. However, this change was also observed on the pure adhesive joints. This colour change indicated some oxidation reaction or other forms of adhesive degradation that could potentially affect the mechanical properties of adhesive joints.

6.3. TEMs/Adhesive Composite Bulk Properties

The third stage's work was to examine the influence of TEMs incorporation on adhesive bulk properties both for unconditioned and environmentally conditioned scenarios. According to the results from Stage 2, adhesive system with only 20wt% 930DU120 and 20wt% 930DU120HEMA incorporation were studied and compared with pure adhesive specimens.

6.3.1. Unconditioned TEMs /Adhesive System

The incorporation of TEMs clearly weakened the mechanical performance (ultimate tensile strength and Young's modulus) of the adhesive system. The ultimate tensile strength of TEMs/adhesive system decreased by 42.5% and 39.4% for 930DU120 and 930DU120HEMA, see Table 5.10. This degradation in mechanical property is in line with the tensile lap shear strength results obtained in Stage 2. Reasons for this degradation are also attributed to the TEMs' poor compatibility with the adhesive matrix. The TEMs acted as weak links, susceptible to interfacial disbonding, and were pulled out from adhesive matrix during necking of the tensile bar. The interfacial disbonded regions can also promote crack propagation, leading to adhesive failure. Figure 6.7 illustrates the interfacial disbonding of TEMs/adhesive system under tensile stress.

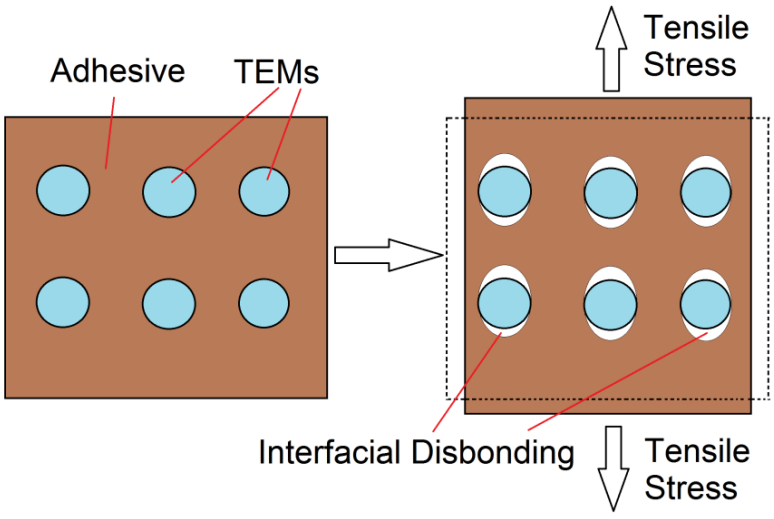

Figure 6.7. Schematic illustration of TEMs/adhesive interfacial disbonding.

Apart from this weakening effect on mechanical properties, incorporation of TEMs also increased the glass transition temperature and reduced peak tan delta value. Peak tan delta (defined as the ratio of loss modulus to elastic modulus) indicates the material's damping capacity (ability to absorb and dissipate energy). The decrease in peak tan delta measurement (from 0.584 to 0.489 and 0.520, see Table 5.11) showed that the TEMs lowered the damping capacity of the adhesive system. This may be explained by the increased restrictions on the movement of molecular chains as a result of TEMs incorporation. This increased restriction of chain movement can also be used to explain the increase in glass transition temperature.

It was noted that 930DU120HEMA showed slightly higher ultimate tensile strength as compared with 930DU120 grade, Table 5.10. This is in accord with the higher tensile lap shear strength discussed in section 6.2. As was noted in Chapter 3 and Chapter 5, 930DU120 and 930DU120HEMA are essentially two very similar TEMs grades. The major difference lies in their shell composition. 930DU120HEMA grade contains 15wt% 2-hydroxyethyl methacrylate (HEMA) in the shell composition.

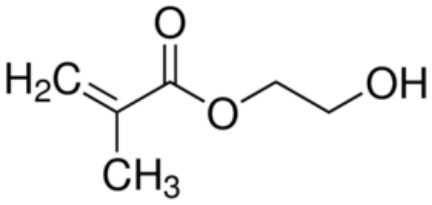

Figure 6.8. Molecular structure of 2-hydroxyethyl methacrylate.

The slight difference in strength can be ascribed to the hydroxyl group on each HEMA molecule, see Figure 6.8. The addition of HEMA molecules in the TEMs' shell composition introduced numerous hydroxyl groups, which in turn could strengthen the TEMs/adhesive system by enhancing TEMs/adhesive interfacial adhesion. This was achieved by the formation of intermolecular hydrogen bonds between hydroxyl groups and functional groups in the adhesive matrix, such as epoxy groups, carbonyl groups, amine groups and hydroxyl groups, etc. From this point of view, it is also worth pointing out that the increased TEMs/adhesive interaction, due to the hydrogen bonds, led to higher peak tan delta value and glass transition

temperature compared with TEMs without hydroxyl groups. The incorporation of TEMs could possibly introduce three new damping mechanisms which differ from pure adhesive systems:

- Friction among TEMs agglomerates in the matrix;
- Friction between TEMs and adhesive matrix;
- Damping near TEMs/adhesive interface as a result of thermal stresses (caused by difference in thermal expansion coefficient). (Landel and Nielsen, 1993)

Therefore, due to the presence of hydrogen bonds, 930DU120HEMA TEMs should interact with adhesive matrix, creating more molecular frictions and resulting in higher energy dissipation and consequently a higher intensity of peak tan delta.

6.3.2. Environmentally Conditioned TEMs/Adhesive System

As explained in Chapter 4, the water immersion tests were first conducted to measure the saturation time for each formulation. It was clear that incorporation of TEMs facilitated water ingress into adhesive joint. This was attributed to the poor interfacial adhesion which left spaces between TEMs and adhesive matrix for water ingression. Adhesive system with 930DU120HEMA incorporation achieved the highest weight gain. This was mainly attributed to the addition of hydroxyl groups on 930DU120HEMA grade TEMs. Hydroxyl groups could form hydrogen bonds with water molecules, making TEMs/adhesive system more hydrophilic and vulnerable to water attack.

The bulk tensile tests showed irreversible reduction in both ultimate tensile strength and Young's modulus. During environmental conditioning, water can swell and damage the adhesive system by crazing, cracking and hydrolyse chemical bonds. As can be observed in Figure 6.9, the 930DU120HEMA grade of TEMs, although achieved a slightly higher ultimate tensile strength in the unconditioned tests, showed a greater reduction after environmental conditioning.

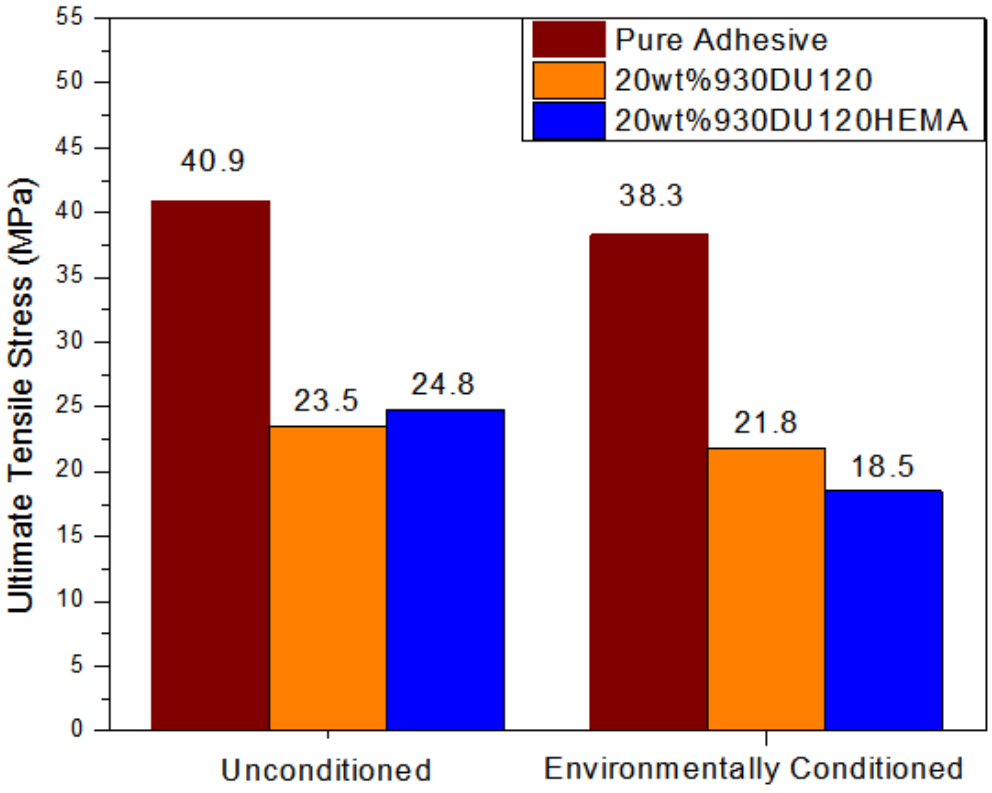

Figure 6.9. Comparison of ultimate tensile strength for both unconditioned and environmentally conditioned specimens.

The impact of water exposure on the TEMs/adhesive system can also be observed from the DMTA results. Compared with the results of unconditioned specimens, there was an appreciable decrease in glass transition temperature. The micro cracks and crazes, as well as the hydrolysis of chemical bonds, all contributed to more free volume and polymer chain mobility, which therefore led to the decrease in glass transition temperature. It is very interesting to note that the decrease of the intensity of peak tan delta was more noticeable for adhesive incorporated with 930DU120HEMA and 930DU120 grade TEMs, see Figure 6.10. The main reason is ascribed to the fact that more cracks and crazes formed in the region of TEMs/adhesive interface due to higher water absorption of 930DU120HEMA grade TEMs. The TEMs therefore had less contact with the adhesive matrix and thereby reducing the TEMs/adhesive friction.

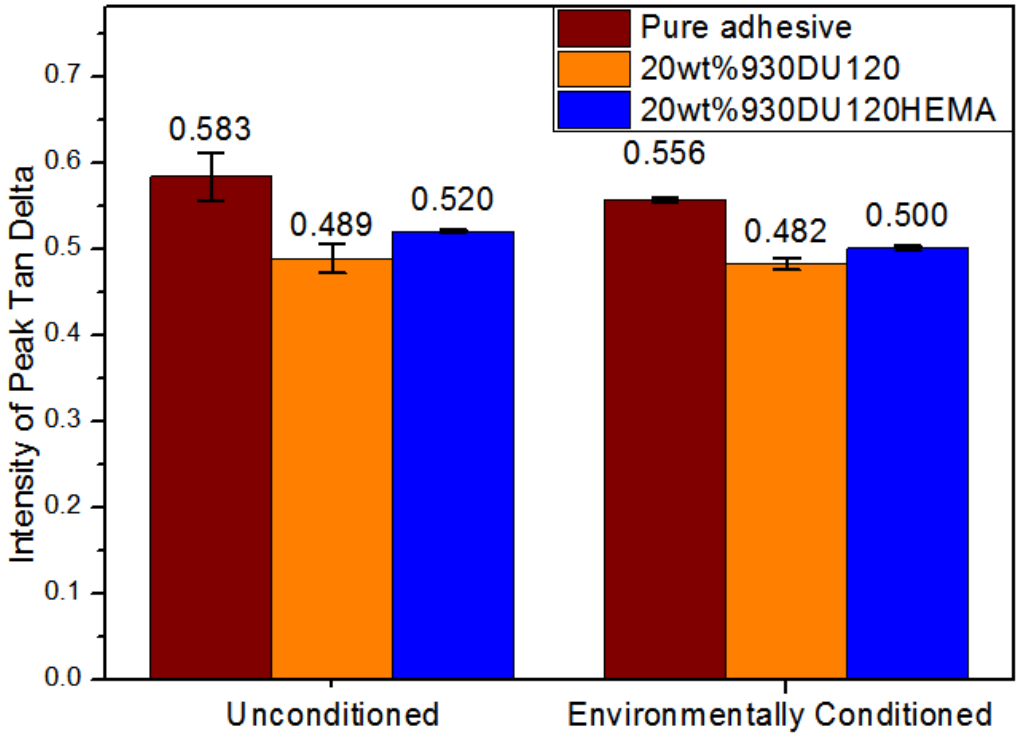

Figure 6.10. Comparison of peak tan delta for both unconditioned and environmentally conditioned specimens.

6.4. Temperature-Time Effect on TEMs Surface Modification

The TEMs surface modification was carried out at three temperature sets (23^{o}C, 30^{o}C, 37^{o}C) and two time sets (3 hours and 5 hours). As was observed from FTIR spectra of these six variations of modified TEMs, major changes occurred at 7 peaks within the 5 wavelength ranges listed in Table 5.14. These 7 peaks matched the major characteristic peaks of GMA, see Figure 5.33. This indicates that PGMA chains were successfully grafted from the TEMs surface. It is still worth noting that the increases of the three peaks at 904 cm^{-1}, 847 cm^{-1}, and 761 cm^{-1} confirmed the presence of the grafted epoxy rings on the modified TEMs, see Figure 6.13 and Figure 6.14.

It can be observed from Figure 6.11 to Figure 6.14 that the intensities of all those 7 peaks according to different modification conditions generally followed the same

trend (from high intensity to low intensity): 37^{o}C 5h > 37^{o}C 3h > 30^{o}C 5h > 30^{o}C 3h > 23^{o}C 5h ≈ 23^{o}C 3h > Immobilised TEMs ≈ Acid treated TEMs. The intensity differences in characteristic peaks were more noticeable at 37^{o}C. It is clear that temperature has a dramatic effect on the growth of the PGMA chains on the TEMs. This positive correlation is generally consistent with other relevant studies regarding the temperature effect in ARGET ATRP process (Zhu, 2012) (Tanaka and Matyjaszewski, 2008). The temperature effect can be correlated with the Arrhenius empirical equation,

$$k = Ae^{-Ea/RT} \quad \text{.....Equation 6.1.}$$

where A is the pre-exponential factor (constant), k is the reaction rate constant; Ea is the activation energy, T is the temperature (in Kelvin) and R is the universal gas constant.

It is also interesting to note that the increase of peak intensity from 30^{o}C to 37^{o}C was more substantial than from 23^{o}C to 30^{o}C. Also, the difference of peak intensity between 23^{o}C 3h and 23^{o}C 5h was insignificant compared with the differences at 37^{o}C and 30^{o}C as a result of reaction time. This indicated that the rate of polymerisation was more accelerated at 37^{o}C. Recent research on surface initiated ARGET ATRP of PHEMA-b-PDMAEMA copolymers from silicon wafers showed very similar acceleration at a temperature of 40^{o}C (Zhu, 2012).

SEM micrographs of modified TEMs (from Figure 5.42 to Figure 5.46) suggested a general trend that with the increase of polymerisation temperature and time, an increasing amount of small particulate deposits was found attached to the surfaces of TEMs. This might be attributed to the following two reasons:

- Once a certain chain length was achieved, the polymer chains would intertwine with each other forming larger particulates;
- At a certain chain length, interchain termination also led to the formation of larger particulates.

It should also be noted that these two reasons can have combined effect leading to large agglomerations or gel formation, as was observed for TEMs modified at 37°C for 5 hours, see Figure 5.47. It is therefore suggested that an optimum chain length could be determined for the best TEMs surface modification.

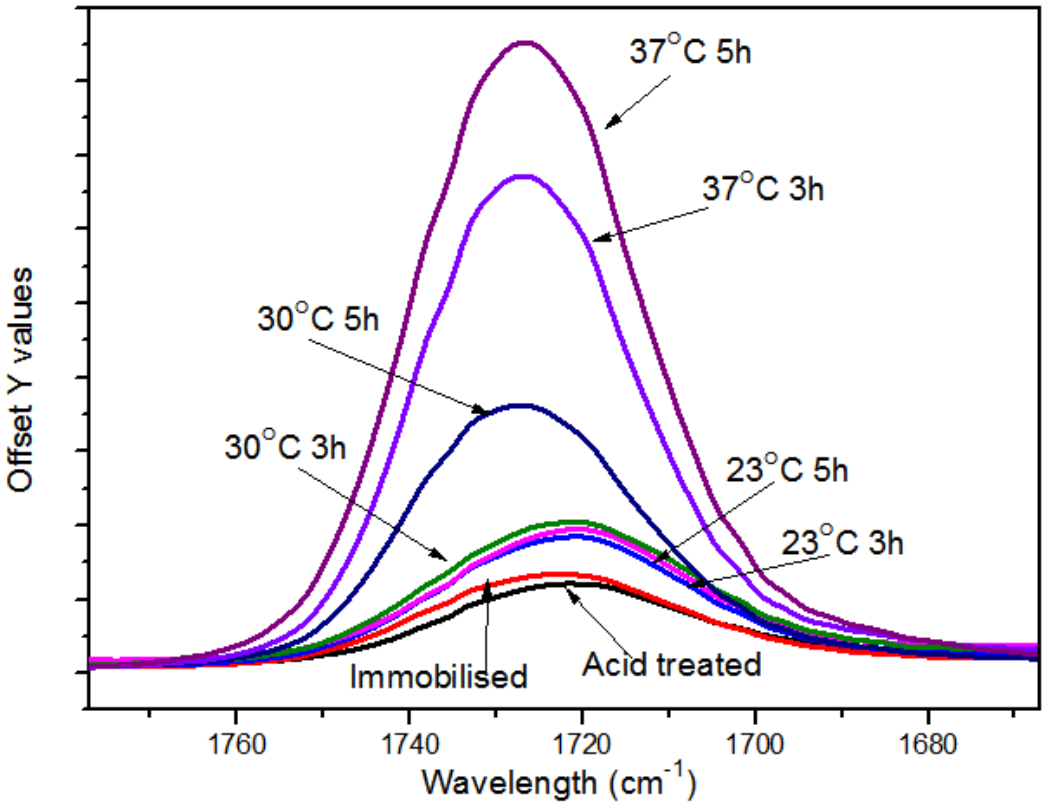

Figure 6.11. FTIR spectra of modified TEMs at wavelength ranges 1757-1677 cm^{-1}.

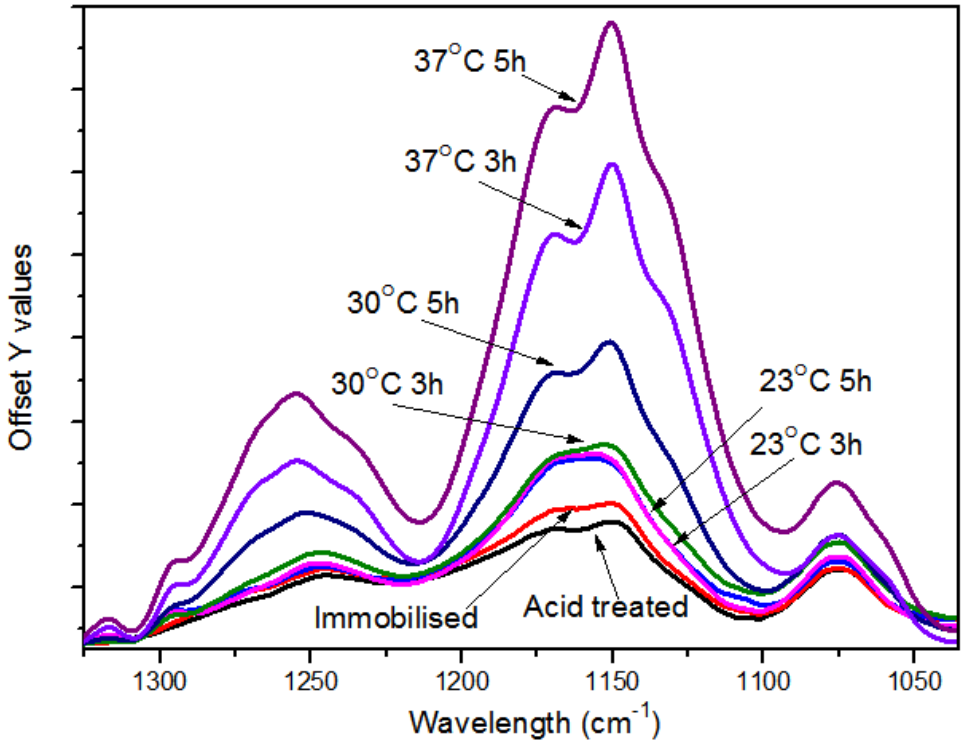

Figure 6.12. FTIR spectra of modified TEMs at wavelength ranges 1325-1035 cm^{-1}.

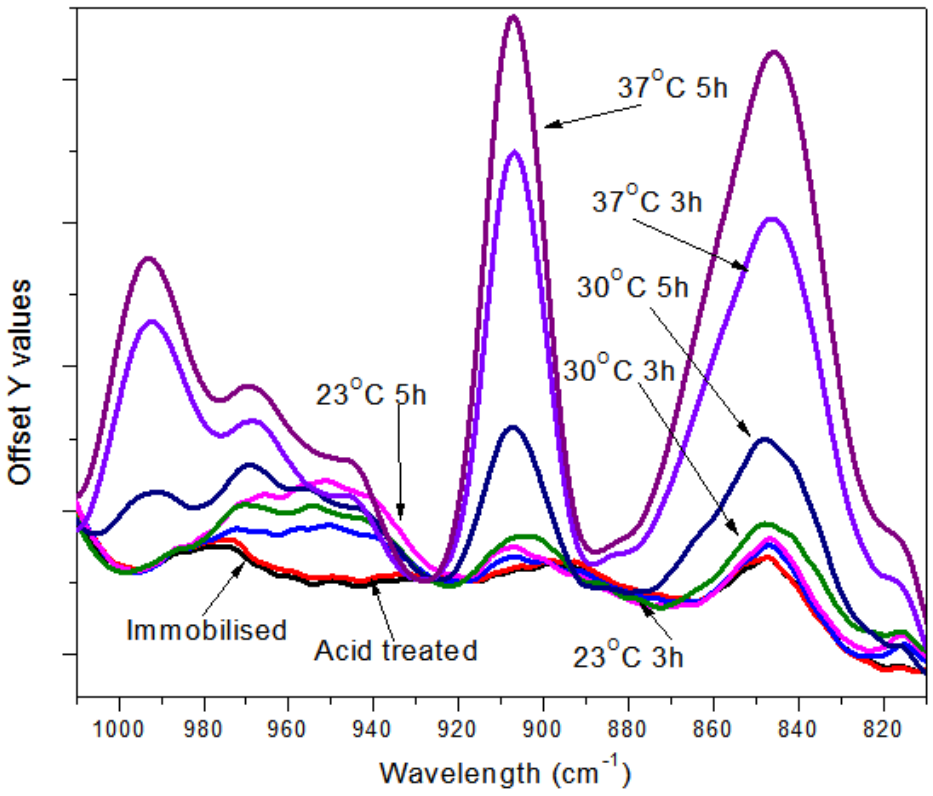

Figure 6.13. FTIR spectra of modified TEMs at wavelength ranges 1010-810 cm^{-1}.

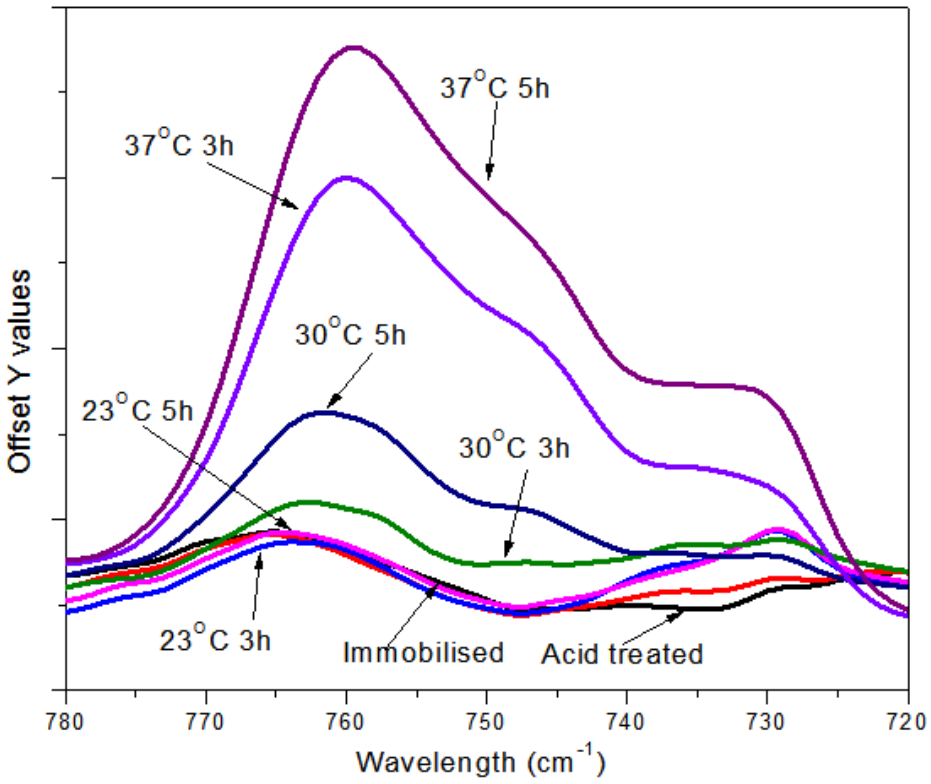

Figure 6.14. FTIR spectra of modified TEMs at wavelength ranges 780-720 cm^{-1}.

6.5. Properties of Adhesive Incorporated with Modified TEMs

6.5.1. Disbonding Performance of Adhesive Joint with Modified TEMs Incorporation

Based on the results from FTIR and SEM, three variations of modified TEMs (30°C 3h, 30°C 5h and 37°C 3h) were chosen from six variations and evaluated for TEMs/adhesive SLJs disbonding performance. It was noted that modified TEMs resulted in a higher tensile lap shear strength compared with the unmodified TEMs. As was noted in 5.4.2, the highest improvement in strength of 14.5% was achieved using the 37°C 3h process. This confirmed the FTIR and SEM characterisation discussed in section 6.4. In addition, the difference of improvement between 30°C 3h and 37°C 3h variations indicated that TEMs grafted with longer PGMA chains are likely to have greater improvement. However, as was observed during the modification process, gel formation was unavoidable when PGMA chains grew to a certain length. This infers that an optimum length of PGMA chains could be determined.

The residual tensile lap shear strength after heat activation showed slight increases compared with the TEMs/adhesive system before modification. The decrease in the disbonding performance of TEMs/adhesive system was attributed to the reduction in TEMs' expansion property. Although TEMs generally have good chemical resistance, long time immersion in solvents during surface modification can plasticise or even degrade the TEMs' shell composition leading to hydrocarbon leakage and thereby affecting TEMs' expansion property. It was for this reason that the adhesive system incorporated with 5 hours modified TEMs (30^{o}C 5h) showed the highest residual strength after heat activation and lowest disbonding effectiveness whereas 3 hours modified TEMs (30^{o}C 3h and 37^{o}C 3h) showed similar strength, see Table 5.15 and Figure 6.15.

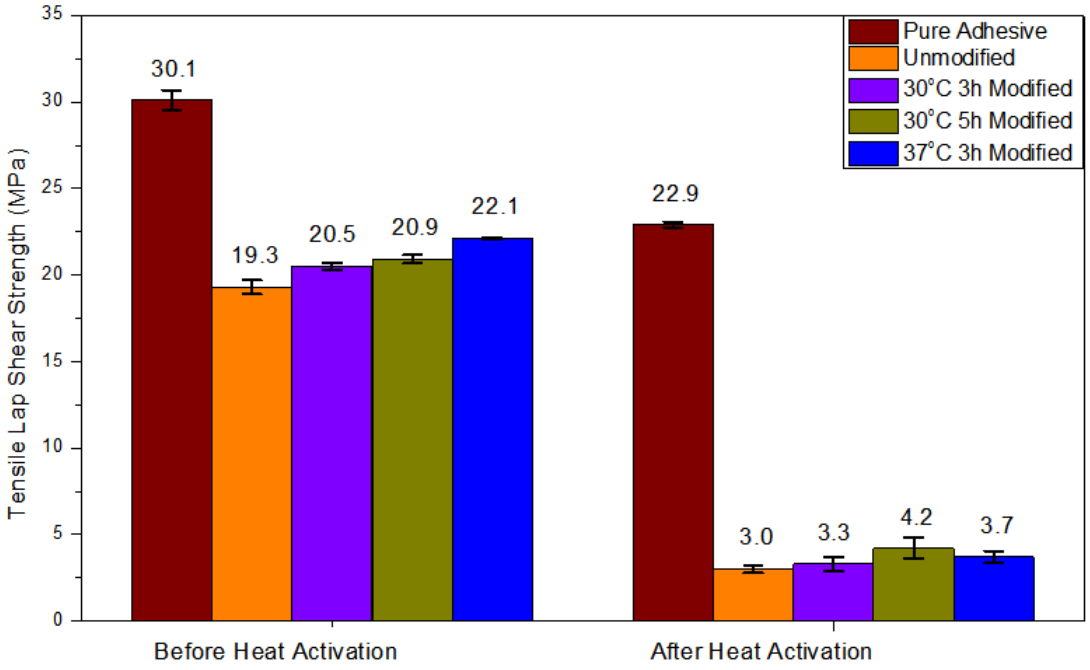

Figure 6.15. Tensile lap shear strength of different variations of modified TEMs before and after heat activation.

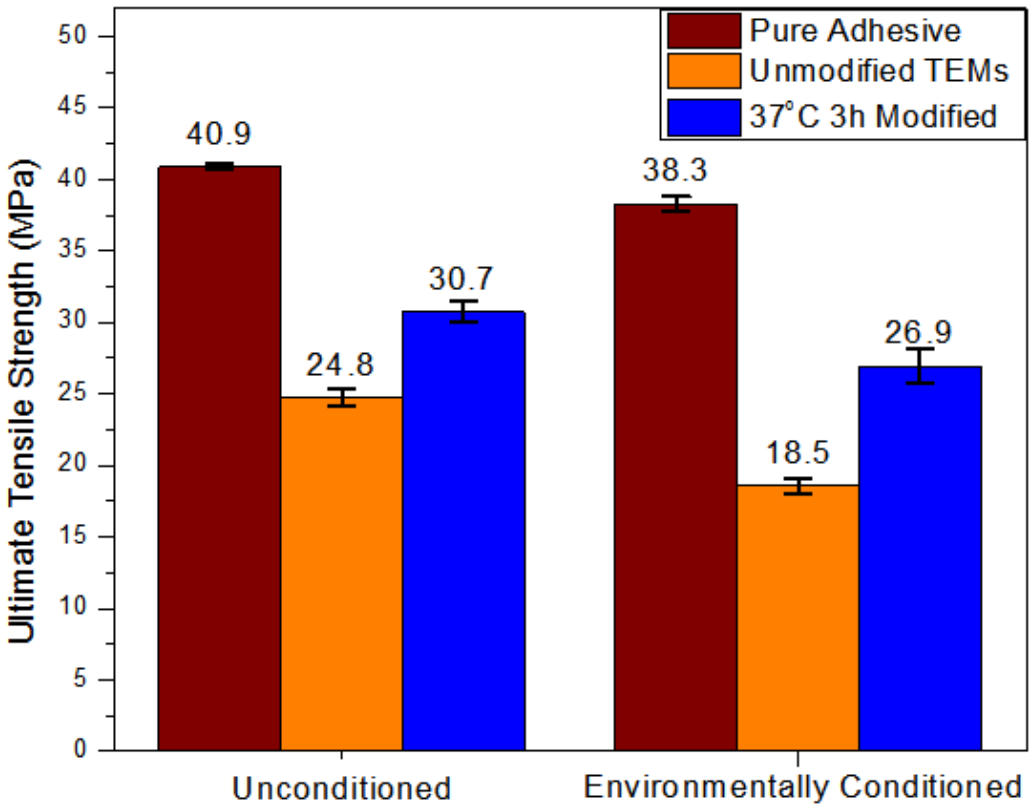

Figure 6.16. Ultimate tensile strength of adhesive incorporated with 37°C 3h modified TEMs in comparison with pure adhesive and unmodified TEMs system.

6.5.2. Bulk Properties of Adhesive System with Modified TEMs Incorporation

The modified TEMs adhesive system achieved an UTS of 30.7 MPa which was 23.7% higher than that of the unmodified TEMs before environmental conditioning. It is also very interesting to point out that the UTS of modified TEMs system post environmental conditioning was still 8.5% higher than the unmodified TEMs system before environmental conditioning, Figure 6.16. Though the quality of data was poor for Young's modulus measurement, a similar trend can also be observed comparing the results in Table 5.10, Table 5.12 and Table 5.17. The improvement in UTS and Young's modulus clearly demonstrated that the TEMs had been successfully modified and the current modification approach can improve the TEMs/adhesive compatibility. Modified TEMs were grafted with long PGMA chains which can extend well into the adhesive system and form covalent bonds by reacting epoxy groups with the Part A amine curing agent of the 2K Scotch-Weld

9323 epoxy adhesive. A schematic illustration of adhesive incorporated with modified TEMs was shown in Figure 3.6 in Chapter 3.

Results from the DMTA tests further support the success of TEMs surface modification and indicated the strengthening mechanism of the modified TEMs system. The PGMA chains, containing numerous epoxy groups contributed to a more cross-linked network which also led to an increase in glass transition temperature. For the unconditioned specimens, the adhesive system with 37^{o}C 3h modified TEMs showed a 7.9% increase in peak tan delta value (0.561) compared with the unmodified TEMs (0.520), which indicated a higher damping capacity, see Figure 6.17. This could be mainly attributed to the following reasons:

- Modified TEMs had a better interaction with adhesive matrix which led to increased TEMs/adhesive friction and higher energy dissipation;
- Energy can be transferred via grafted PGMA chains and consumed by TEMs;
- The strong covalent bonds between TEMs and adhesive also intensified chain motions locally near the TEMs/adhesive interface local area which resulted in more adhesive chain friction and therefore a better dissipation of energy.

Apart from these changes on bulk properties, another interesting point worths noticing is that the introduction of PGMA chains into the adhesive system would have consumed a certain amount of the curing agent. It is therefore likely that the adhesive system with modified TEMs incorporation could achieve a more substantial improvement in mechanical performance if extra curing agents are added as compensation.

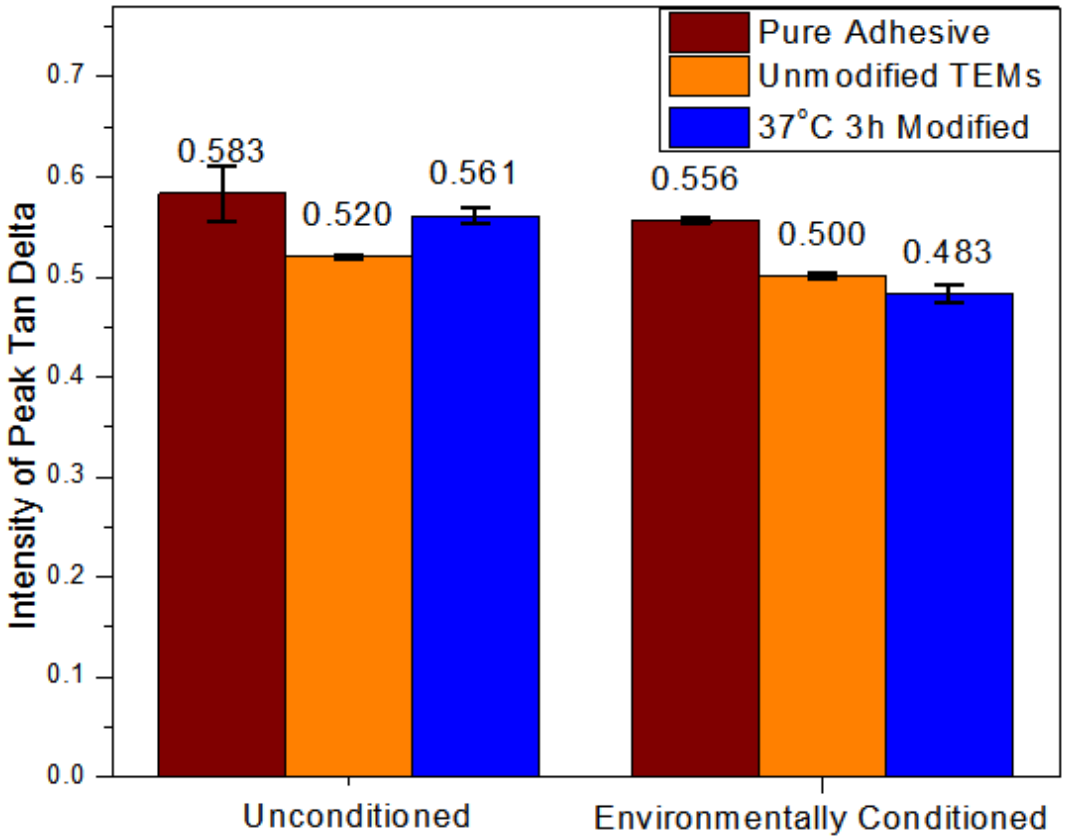

Figure 6.17. Intensity of peak tan delta of adhesive incorporated with 37°C 3h modified TEMs in comparison with pure adhesive and unmodified TEMs system.

6.6. Suitability of Test Methods

The test methods chosen and designed in this research provided satisfactory information in achieving the project objectives. An alternative method for evaluating disbonding effectiveness of adhesive joints was proposed. SLJ specimens were cooled down to room temperature prior to the measurement of residual strength after heat activation in the oven. This process helped to preclude the effect of temperature and focused more on the TEM's role in achieving adhesive joints disbonding. However, for practical applications, it would be more effective at temperatures higher than room temperature, especially above Tg. It is therefore suggested that a parallel study of TEMs/adhesive joints disbonding at higher temperatures (e.g. TEMs' T_3 temperature) would be interesting for practical purposes.

The environmental conditioning test on SLJ specimens was not successful due to the project time constraints and therefore removed from the latter part of the project. The environmental conditioning test on bulk materials compensated for this by removing the added complication of substrate interfacial effect. Nevertheless, it is suggested that environmental conditioning test on SLJ specimens with longer time or more cycles to be used for future evaluation.

In terms of bulk material property tests (tensile and DMTA tests), the quality of data was sometimes less reliable due to larger experimental scatter, compared with results from joint tests. Although extra care was taken in the specimen preparation process, air entrapment was found unavoidable during the moulding process. As was stated, specimens with large voids were cancelled from testing. However, small voids are likely to have contributed to the scatter.

Chapter 7. Conclusions and Future Work

7.1. Summary of Research Findings

This research aimed to evaluate suitable joining solutions which enable rapid disassembly process of bonded automotive vehicle for maintenance or end-of-life recycling purposes. Upon reviewing the project objectives set in Chapter 2 and key research findings (summarised as follows), all the three objectives were satisfactorily achieved.

7.1.1. Critical Review of the Innovations in Adhesive Disbonding Technologies

Due to the ever growing concerns over the recycling, reuse and recovery issues of end-of-life vehicles, a high demand for the development of a disbondable joining solution was identified from both practical and legislative perspectives. The lightweight multi material trend in the automotive industry further motivated the design requirements for an ease of disassembly process. The literature research critically reviewed the recent innovations in the disassembly technologies of adhesive bonding, which has been increasingly and extensively used in automotive applications.

It was found that the most promising adhesive disbonding technologies involve an addition of functional additives, which can be activated via heat, electric current, electro-magnetic field, etc. This approach generally outperformed the other two major approaches for automotive applications mainly because of its cost-effectiveness, as current OEMs approved adhesives can be employed without the need to invest in the development of new adhesive systems. The use of thermally expandable microspheres (TEMs) has attracted much attention recently and achieved one of the highest ratings comparing with other adhesive disbonding techniques in the literature review. However, TEMs/adhesive compatibility issue which led to the reduction of adhesive integrity was revealed as one of the major

limitations of this technique. Consequently, this led to the programme of work for this thesis.

7.1.2. Disbonding Performance and General Properties of TEMs/Adhesive System

A better understanding of TEMs/adhesive compatibility issue has been obtained. The incorporation of TEMs generally weakened the mechanical properties (e.g. ultimate tensile strength, tensile lap shear strength, and modulus) of the adhesive system. The main reason was ascribed to the poor interfacial adhesion, which led to TEMs/adhesive interfacial disbonding upon deformation. This poor interfacial adhesion also contributed to higher water absorption due to the presence of spaces between TEMs and adhesive matrix.

It was found that the TEMs' chemical compositions had a dominant effect on the behaviour of TEMs/adhesive composite. The influences of particle size distribution and microstructural morphology of the TEMs however were not validated in this research. 930DU120HEMA grade TEMs achieved higher mechanical strength due to the hydrogen bonds formed between the hydroxyl groups of TEMs and adhesive matrix. The hydroxyl groups also made the TEMs/adhesive system more hydrophilic and vulnerable to water attack.

In terms of TEMs concentration effect, a higher concentration resulted in higher disbonding effectiveness but a general reduction in mechanical properties of adhesive joints. Also, when the TEMs concentration exceeded a certain value 30wt% (EM501 grade), the properties and rheology of TEMs/adhesive system were dramatically affected as a result of the TEMs clustering or agglomeration during mixing.

The disbonding mechanism was mainly attributed to the crack propagation caused by the TEMs expansion. Additionally, adhesive degradation and the different thermal coefficients of the adhesive and metal substrate would also contribute to the disbonding process.

7.1.3. TEMs Surface Modification for Improved TEMs/Adhesive Compatibility

It has been demonstrated that PGMA chains can be grown from the surfaces of TEMs using ARGET ATRP technique. Modified TEMs were characterised by FTIR and SEM. It was found that temperature can significantly accelerate the rate of polymerisation and hence the length of PGMA chains, which also increased with polymerisation time. The large bulk materials observed during polymerisation indicated that modified TEMs can form gels when the grafted chain is allowed to grow beyond a certain length.

The modified TEMs produced substantial improvements in tensile lap shear strength and ultimate tensile strength. DMTA test also indicated an increase in Tg and damping capacity compared with an unmodified TEMs system. These improvements were all attributed to the formation of strong covalent bonds and the grafted polymer chain length resulting in a stronger interaction between TEMs and adhesive matrix.

Also, it was shown that the modified TEMs system obtained better water resistance. Most notably, the ultimate tensile strength of adhesive system with the modified TEMs after environmental conditioning was even higher than the strength of unmodified TEMs before environmental conditioning.

7.2. Recommendations for Future Work

Apart from the issues identified, this research also sparked a number of interesting topics for future work, exploring which could facilitate a more reliable disbondable adhesive solution readily to be applied in the automotive industry:

- Investigate a range of TEMs with different particle size distributions or microstructural morphology for a more comprehensive understanding of TEMs/adhesive performance;
- Conduct a parallel disbonding effectiveness test which allows the joint properties to be measured at the TEMs/adhesive activation temperature for an understanding of practical adhesive disbonding scenarios;
- Investigate the disbonding performance of other joint types (e.g. butt joint) and non-metal substrates;
- Investigate the long-term durability, fracture toughness and toughening mechanism of TEMs/adhesive system, especially for modified TEMs;
- Increase the amount of curing agents during mixing to accommodate the increase of epoxy groups from modified TEMs;
- Tailor the current ARGET ATRP system for a better TEMs surface modification by changing catalyst, solvent, initiator and other key parameters;
- Investigate a suitable method to measure or estimate the length of grafted chains;
- Determine the optimum chain length for the best improvement in TEMs/adhesive properties.

7.3. Novelty of Research

The novelty of this research can be attributed to the following contributions:

- A critical review of the innovations in adhesive disbonding technologies for automotive applications;
- The investigation of a range of TEMs grades with high initiation temperature from three major TEMs manufacturers;
- A better understanding of the disbonding mechanism and compatibility issues of TEMs/adhesive system;
- An investigation of the temperature effect on TEMs surface modification via ARGET ATRP technique;
- Demonstration that modified TEMs improved the strength and water resistance of the TEMs/adhesive systems.

References

Abrego, J.F. (2010) 'Carbon dioxide dissociation and capture by means of ultrasound', *Journal of Applied Sciences Research*, 6(5), pp.469-472.

Adams, R.D. (2005) Adhesive Bonding: science, technology and applications, England: Woodhead Publishing Limited.

Adams, R.D., Comyn. J. and Wake, W.C. (1997) Structural Adhesive Joints in Engineering, London: Chapman and Hall.

Adderley, C.S. (1988) Adhesive bonding, Material and Design, 9, pp.287-293.

Akcora, P., Liu, H., Kumar, S.K. et al (2009) 'Anisotropic self-assembly of spherical polymer-grafted nanoparticles', *Nature Materials*, 8, pp.354-359. doi:10.1038/nmat2404.

Alcorta, J., Papon, E. and Dalet, P. (2006) Method of assembling two substrates by means of bonding and method of disassembling said bonded assembly by means of migration, Patent Number WO 2006/048585 A1.

Anderson, S.M. (2004) Adhesives in Automotive Interiors - Versatile and Economical Bond Solutions. Available at: http://www.chemquest.com/PDF-files/Adhesives_in_Automotive_Interiors.pdf. (Accessed 22 Nov 2014)

Antrekowitsch, H., Hanko, G., and Paschen, P., 'Recycling of Aluminium and Magnesium Parts from Used Cars: Legislative Frame and Consequences for Metallurgy and Material Design', SAE Technical Paper. doi:10.4271/2001-01-3778.

Ardakani, A.A., Buchwalter, S.L., Gelorme, J.D., Kosbar, L.L., Newman, B.H. and Pompeo, F.L. (1996) Cleavable diepoxide for removable epoxy compositions, Patent Number US 5560934.

Aubert, J.H. (2010) 'Thermally removable epoxy adhesives incorporating thermally reversible diels-alder adducts', *Journal of Adhesion*, 79(6), pp.609-616.

Augustin, D., Leriche, C. and Poisson, P. (1988) Bonding method employing thermo reversible crosslinking adhesives, Patent Number US 4744852.

Bansal, A., Yang, H., Li, C., Benicewicz, B.C., Kumar, S.K. and Schadler, L.S. (2006) 'Controlling the thermomechanical properties of polymer nanocomposites by tailoring the polymer-particle interface', *Journal of Polymer Science Part B: Polymer Physics*, 44(20), pp.2944-2950. doi:10.1002/polb.20926.

Barbey, R., Lavanant, L., Paripovic, D., Schuwer, N. et al (2009) 'Polymer brushes via surface-initiated controlled radical polymerisation: synthesis, characterisation, properties, and applications', *Chemical Reviews*, 109(11), pp.5437-5527. doi:10.1021/cr900045a.

Barnes, T.A. and Pashby, I.R. (2000) 'Joining techniques for aluminium spaceframes used in automobiles Part II adhesive bonding and mechanical fasterners', *Journal of Material Processing Technology*, 99(1-3), pp.72-79. doi: 10.1016/S0924-0136(99)00361-1.

Baeyens, J., Brems, A. and Dewil, R. (2010) 'Recovery and recycling of post-consumer waste materials. Part 1. Generalities and target wastes (paper, cardboard and aluminium cans)', International Journal Sustainable Engineering, 3(3), pp.148-158. doi:10.1080/19397038.2010.498529

Baeyens, J., Brems, A. and Dewil, R. (2010) 'Recovery and recycling of post-consumer waste materials Recovery and recycling of post-consumer waste materials. Part 2. Target wastes (glass beverage bottles, plastics, scrap metal and steel cans, end-of-life tyres, batteries and household hazardous waste)', International Journal Sustainable Engineering, 3(4), pp.232-245. doi:10.1080/19397038.2010.507885.

Becher, B., Flegel, H., Herrmann, M. et al. (2004) Adhesive system for form reversible glued joints, Patent Number US 6764569B1.

Bencherif, S.A., Gao, H., Srinivasan, A., Siegwart, D.J., Hollinger, J.O., Washburn, N.R. and Matyjaszewski, K. (2009) 'Cell-adhesive star polymers prepared by ATRP', Biomacromolecules, 10(7), pp.1795-1803. doi:10.1021/bm900213u.

Bergenudd, H. (2011) Understanding the mechanism behind atom transfer radical polymerisation – exploring the limit of control. PhD Thesis. KTH Royal Institute of Technology.

Bogue, R. (2011) 'Recent developments in adhesive technology: a review', *Assembly Automation*, 31(3), pp.207-211.

Bombalski, L., Min, K., Dong, H., Tang, C. and Matyjaszewski, K. (2007) 'Preparation of Well-Defined Hybrid Materials by ATRP in Miniemulsion', *Macromolecules*, 40, pp.7249-7432.

Brady, G.S., Clauser, H.R. and Vaccari, J.A. (1997) Materials Handbook, 14th Ed., USA: The McGraw-Hill Companies.

Braunecker, W.A. and Matyjaszewski, K. (2007) 'Controlled/living radical polymerisation: Features, developments, and perspectives', *Progress in Polymer Science*, 32(1), pp.93-146. doi:10.1016/j.progpolymsci.2006.11.002

Brown, D. and Kaufman, H. (2005) Reversible adhesive, Patent Number US 20050159521.

Carter, S. (2008) Preparation and analysis of polypyrrole-coated TEM particles, Classified Report by De-Bonding Ltd.

Carlmark, A. (2002) Atom transfer radical polymerisation from multifunctional substrates. PhD Thesis. KTH Royal Institute of Technology.

Carlmark, A. and Malmstrom, E. (2002) 'Atom Transfer Radical Polymerization from Cellulose Fibers at Ambient Temperature', *Journal of the American Chemical Society*, 124(6), pp.900-901. doi:10.1021/ja016582h.

Cheesman, B., Neilson, A.J.G., Willott, J.D., Webber, G.B., Edmondson, S. and Wanless, E.J. (2013) 'Effect of colloidal substrate curvature on pH-responsive polyelectrolyte brush growth', *Langmuir*, 29(20), pp.6131-6140. doi:10.1021/la4004092.

Cheng, Z., Zhu, X., Kang, E.T. and Neoh, K.G. (2006) 'Modification of poly(ether imide) membranes via surface initiated atom transfer radical polymerisation', Macromolecules, 39(4), pp.1660-1663. doi:10.1021/ma0520601

Chino, K., Ikawa, M. and Natori, J. (2004) Methods of making and recycling rubber bodies bonded with a thermo-reversible, crosslinkable elastomer, Patent Number US 6746562.

Coates, G. and Edwards, C. (2006) Cost-orientated approach to design and recovery of vehicles to meet the requirements for the end-of-life vehicle (ELV) Directive, Available at: http://www.centreforsmart.co.uk/publications/cost-oriented-approach-to-design-and-recovery-of-vehicles-to-meet-the-requirements-for-the-end-of-life-vehicle-elv-directives. (Accessed 13 Dec 2014)

Correia, J.R., Almeida, N.M. and Figueira, J.R. (2011) 'Recycling of FRP Composites: Reusing Fne GFRP Waste in Concrete Mixtures', Journal of Cleaner Production, 19(15), pp1745-1753. doi:10.1016/j.jclepro.2011.05.018

Crolla, D.A. (2009) Automotive engineering: powertrain, chassis system and vehicle body, Oxford: Elsevier.

Cook, M.S. (1976) Adhesive system, Patent Number US 3938266.

Daoud, M. and Cotton, J.P. (1982) 'Star shaped polymers: a model for the conformation and its concentration dependence', *Journal de Physique Archives*, 43(3), pp.531-538.

DC Polymers (2011) Available at: http://masschallenge.org/profile/dc-polymers. (Accessed 4 May 2012)

Department for Business, Innovation and Skills (2012) 'Vehicle manufacturers and importers: end-of-life vehicles regulations'. Available at: http://www.environment-agency.gov.uk/business/regulation/65470.aspx. (Accessed: 5 June 2013)

Dukes, D., Li, Y., Lewis, S., Benicewicz, B., Schadler, L. and Kumar, S.K. (2010) 'Conformational Transitions of Spherical Polymer Brushes: Synthesis, Characterization, and Theory', *Macromolecules*, 43(3), pp1564-1570. doi:10.1021/ma901228t.

Ebnesajjad, S. (2008) Adhesive Technology Handbook, 2nd Ed, William Andrew.

Edwards, C., Coates, G., Leaney, P.G. and Rahimifard, S. (2006) Implications of the end-of-life vehicles directive on the vehicle recovery sector, *Proceedings of the Institution of Mechanical Engineers, Part B: Journal of Engineering Manufacture*, 220 (7), pp.1211-1216

Edmondson, S., Vo, C.D., Armes, S.P., Unali, G.F., Weir, M.P. (2008) 'Layer-by-layer deposition of polyelectrolyte macroinitiators for enhanced initiator density in surface-initiated ATRP', *Langmuir*, 24(14), pp.7208-7215. doi:10.1021/la7039898.

Edmondson, S. and Armes, S.P. (2009) 'Synthesis of surface-initiated polymer brushes using macro-initiators', *Polymer International*, 58(3), pp.307-316. doi:10.1002/pi.2529.

Elwell, J.L. (1981) Solvent mixture for dissolving and removing epoxy resinous compounds, Patent Number US 4278557.

Environment and labour committee of the national assembly of Korea (2007) 'Act for resource recycling of electrical and electronic equipment and vehicles'. Available at: http://www.rsjtechnical.com/images/Documents/Korea_RoHS_ELV_April_2007_EcoFrontier.pdf (Accessed 15 Jan 2015)

Essig, O., Hartweg, M., Keller, A. and Tomaschko, S. (2004) Methods and apparatuses for detaching components adhesively bonded to one another, Patent Number US 20030127174.

European Commision (2000) 'Directive 2000/53/EC'. Available at: http://ec.europa.eu/environment/waste/elv_index.htm (Accessed 5 March 2012)

European Commission, (2008) Available at http://epp.eurostat.ec.europa.eu/portal/page/portal/waste/. (Accessed 3 Mar 2012)

Evonik, (no date) Available at: http://nano.evonik.com/sites/nanotechnology/en/technology/applications/magsilica/pages/default.aspx. (Accessed 3 Mar 2012)

Foulc, M.P., Bergara, T. and Olive, M. (2012) Assembly of two substrates bonded by a rigid polymer, and methods for assembly and dismantling by means of migration of said bonded assembly, Patent Number US 20120258315 A1.

Friese, C., Unger, L., Kirsten, C., Huver, T. and Ferencz, A. (2001) Lösbare Klebeverindungen. Patent Number DE 19961940.

Go, T.F, Wahab, D.A., Rahman, M.N.Ab., Ramli, R., and Azhari, C.H. (2011) 'Disassemblability of end-of-life vehicle: a critical review of evaluation methods', Journal of Cleaner Production, 19(13), pp.1536-1546. doi:10.1016/j.jclepro.2011.05.003

Goto, A. and Fukuda, T. (2004) Kinetics of living radical polymerisation, *Progress in Polymer Science*, 29(4), pp.329-385. doi:10.1016/j.progpolymsci.2004.01.002

Grujicic, M., Sellappan, V., Omar, M.A., Seyr, N., Obieglo, A., Erdmann, M. and Holzleitner, J. (2008) 'An overview of the polymer-to-metal direct-adhesion hybrid technologies for load-bearing automotive components', *Journal of Materials Processing Technology*, 197(1-3), pp.363-373. doi:10.1016/j.jmatprotec.2007.06.058

Guillaume, E. and Marechal, L. (2008) 'Weight Reduction with Sandwich Material on Front End Carrier Application', SAE Technical Paper, doi:10.4271/2008-01-0368.

Harton, S.E. and Kumar, S.K. (2007) 'Mean-field theoretical analysis of brush-coated nanoparticle dispersion in polymer matrices', *Journal of Polymer Science Part B: Polymer Physics*, 46(4), pp.351-358. doi:10.1002/polb.21346

Hanley, M. and Kuczynski, J. (2006) Reworkable adhesives containing thermally labile groups, Patent Number US 0014924.

Hansson, S. (2012) ARGET ATRP as a tool for cellulose modification. PhD Thesis. KTH Royal Institute of Technology.

Haydon, D. (2002) 'ElectRelease - electrically disbonding epoxy adhesive', Assembly Automation, 22(4), pp.326-329.

He, W., Jiang, H., Zhang, L., Cheng, Z. and Zhu, X. (2013) 'Atom transfer radical polymerization of hydrophilic monomers and its applications', *Polymer Chemistry*, 4(10), pp.2919-2938.

Hodgin, M.J. (2009) Re-working, removing, and "decapsulating" cured epoxy. Available at: http://www.epotek.com/SSCDocs/whitepapers/Tech%20Paper%2046.pdf. (Accessed 2 May 2012)

Horn, M. Matyjaszewski, K. (2013) 'Solvent effects on the activation rate constant in atom transfer radical polymerization', *Macromolecules*, 46(9), pp.3350-3357.

Hornung, M. and Hajj, M. (2009) Structural bonding for lightweight construction, Material Science Forum, 618, pp.49-56.

Hui, C.M., Pietrasik, J., Schmitt, M., Mahoney, C. et al (2014) 'Surface-initiated polymerisation as an enabling tool for multifunctional (nano-) engineered hybrid materials', *Chemistry of Materials*, 26(1), pp.745-762. doi:10.1021/cm4023634.

International Organization of Motor Vehicle Manufacturers, 2013. Available at: http://oica.net/wp-content/uploads/press-release-press-conference-2013-03-06-_v3b_.pdf. (Accessed: 13 July 2013)

Ishikawa, H., Seto, K., Shimotuma, S., Kishi, N. and Sato, C. (2005) 'Bond strength and disbonding behaviour of elastomer and emulsion-type dismantlable adhesives used for building materials', *International Journal Adhesion and Adhesives*, 25(3), pp.193-199.

Jeyaprakash, J.D., Samuel, S., Dhamodharan, R. and Rühe, J. (2002) 'Polymer brushes via ATRP: role of activator and deactivator in the surface-Initiated ATRP of styrene on planar substrates', *Macromolecular Rapid Communications*, 23(4), pp.277-281.

Jody, B.J., Daniels, E.J., Duranceau, C.M., Pomykala, J.A., and Spangenberger, J.S. (2010) 'End-of-life vehicle recycling: state of the art of resource recovery from shredder residue', Available at: http://www.ipd.anl.gov/anlpubs/2010/01/65969.pdf. (Accessed 5 March 2012)

Jonsson, M., Nyström, D., Nordin, O. and Malmström, E. (2009) 'Surface modification of thermally expandable microspheres by grafting poly(glycidyl methacrylate) using ARGET ATRP', *European Polymer Journal*, 45(8), pp.2374-2382.

Jonsson, M. (2010) Thermally expandable microspheres prepared via suspension polymerisation-suspension polymerisation synthesis, characterisation, and application. PhD Thesis. KTH Royal Institute of Technology.

Kato, M., Kamigaito, M., Sawamoto, M. and Higashimura, T. (1995) 'Polymerisation of Methyl Methacrylate with the Carbon Tetrachloride/Dichlorotris-(triphenylphosphine) ruthenium(II)/Methylaluminum Bis (2, 6-di-tert-butylphenoxide) Initiating System: Possibility of Living Radical Polymerisation', *Macromolecules*, 28(5), pp.1721-1723. doi:10.1021/ma00109a056

Kolbe, J., Kowalik, T., Popp, M. et al (2004) Curable bonded assemblies capable of being dissociated. Patent Number US 20040249037.

Kim, J.B., Bruening, M.L., and Baker, G.L. (2000) 'Surface-initiated atom transfer radical polymerisation on gold at ambient temperature', *Journal of the American Chemical Society*, 122(31), pp.7616-7617. doi:10.1021/ja001652q.

Kim, K., Joung, H., Nam, H., Seo, Y., Hong, J.H., Yoo, T., Lim, B., and Park, J. (2004) 'Management status of end-of-life vehicles and characteristics of automobile shredder residues in Korea', Waste Management, 24(6), pp.533-540. doi:10.1016/j.wasman.2004.02.012

Kuilla, T., Bhadra, S., Yao, D., Kim, N.H., Bose, S. and Lee, J.H. (2010) 'Recent advances in graphene based polymer composites', *Progress in Polymer Science*, 35(11), pp.1350-1375. doi:10.1016/j.progpolymsci.2010.07.005.

LANXESS, (2012) Available at http://techcenter.lanxess.com/ (Accessed: 4 Mar 2012)

Landel, R.F. and Nielsen, L.E. (1993) Mechanical properties of polymers and composites. 2nd Edn. USA: Marcel Dekker.

Leijonmarck, S., Cornell, A., Danielsson, C.O., Akermark, T., Brandner, D.B. and Lindbergh, G. (2012) 'Electrolytically assisted debonding of adhesives: an experimental investigation', International Journal of Adhesion and Adhesives, 32, pp.39-45. doi:10.1016/j.ijadhadh.2011.09.003

Leibson, S. (2011) Future cars: the word from GM at IDC's smart technology world conference. Available at: http://low-powerdesign.com/sleibson/2011/05/01/future-cars-the-word-from-gm-at-idc%E2%80%99s-smart-technology-world-conference/. (Accessed 3 Mar 2012)

Licari, J.J. and Bakhit, G.G. (1991) Reworkable epoxy die-attach adhesive, Patent Number US 5002818.

Lindqvist, J., Nystrom, D., Ostmark, E., Antoni, P., Carlmark, A. et al (2008) 'Intelligent dual-responsive cellulose surfaces via surface-initiated ATRP', *Biomacromolecules*, 9(8), pp.2139-2145. doi:10.1021/bm800193n.

Liu, Y., Klep, V., Zdyrko, B. and Luzinov, I. 'Polymer Grafting via ATRP Initiated from Macroinitiator Synthesized on Surface', *Langmuir*, 20(16), pp.6710-8.

Mangino, E., Carruthers, J. and Pitarresi, G. (2007) 'The future use of structural composite materials in the automotive industry', International Journal of Vehicle Design, 44(3-4), 2007, pp.211-232. doi:10.1504/IJVD.2007.013640

Månson, J.A.E., Wakeman, M.D., Bourban, P.E. and Sunderland, P.W. (2012) 'Driving forces for cost-effective composites: new demands on materials and process', International Conference of Composite Materials.

Manfrè, G. (2005) The Dismantling Glass on ELV Needs Low Cost Technologies, Available at: http://www.glassfiles.com/library/3/article1012.htm. (Accessed 24 April 2013)

Manfrè, G. (2005) The Thermally Expanded Microspheres Debonding Technology and ELV Recycling Glazing. Available at: http://www.glassfiles.com/library/3/article708.htm. (Accessed 24 April 2013)

Marechal, L., 'New metal plastic technology for front end modules', *SAE Technical Paper*, doi:10.4271/2006-01-0728.

Markle, R.A., Brusky, P.L., Cremeans, G.E., Elhard, J.D., Bigg, D.M. and Sowell, S. (1995) Thermally reversible isocyanate-based polymers, Patent Number US 5470945.

Marutani, E., Yamamoto, S., Ninjbadgar, T., Tsujii, Y., Fukuda, T. and Takano, M. (2004) 'Surface-initiated atom transfer radical polymerisation of methyl

methacrylate on magnetite nanoparticles', *Polymer*, 45(7), pp.2231-2235. doi:10.1016/j.polymer.2004.02.005.

Matsumoto Yushi-Seiyaku (no date) Available at: http://www.mtmtys.co.jp/e/product/general/data01_2.html. (Accessed 22 Dec 2014)

Matyjaszewski, K., Miller, P.J., Shukla, N., Immaraporn, B., Gelman, A. et al (1999) Polymers at Interfaces: Using Atom Transfer Radical Polymerization in the Controlled Growth of Homopolymers and Block Copolymers from Silicon Surfaces in the Absence of Untethered Sacrificial Initiator, *Macromolecules*, 32(26), pp.8176-8724. doi:10.1021/ma991146p.

Matyjaszewski, K., Jakubowski, W., Min, K., Tang, W., Huang, J., Braunecker, W.A. and Tsarevsky, N.V. 'Diminishing Catalyst Concentration in Atom Transfer Radical Polymerisation with Reducing Agents', *Proceedings of the National Academy of Sciences of the United States of America*, 103(42), pp.15309–15314. doi: 10.1073/pnas.0602675103

Matyjaszewski, K. (2012) 'Atom transfer radical polymerisation (ATRP): current status and future perspectives', *Macromolecules*, 45(10), pp.4015-4039. doi:10.1021/ma3001719

Mazurowski, M., Gallei, M., Li, M., Li, J., Didzoleit, H., Stühn, B. and Rehahn, M. (2012) Redox-responsive polymer brushes grafted from polystyrene nanoparticles by means of surface initiated atom transfer radical polymerisation, *Macromolecules*, 45(22), pp.8970-8981.

McCurdy, R. (2011) Disassembly methods for automotive structures. PhD thesis. Oxford Brookes University.

Merz, P.W., Wirz, T. and Burchardt, B.R. (2000) Specific adhesive compound suitable for easy removal, Patent Number US 6696124.

Michalos, G., Makris, S., Papakostas, N., Mourtzis, D. and Chryssolouris, G. (2010) 'Automotive assembly technologies review: challenges and outlook for a flexible and adaptive approach', *Journal of Manufacturing Science and Technology*, 2(2), pp.81-91. doi:10.1016/j.cirpj.2009.12.001

Ministry of the Environment Government of Japan (2003) 'Enactment of ministerial ordinances for partially amending the enforcement regulations of the law for the recycling of end-of-life vehicles'. Available at: http://www.env.go.jp/en/press/2003/0808b.html. (Accessed 9 Aug 2012)

Minnicino, M. and Sands, J.M. (2011) Reactive nanocomposites for controllable adhesive debonding, Army Research Laboratory.

Mizutani, A., Kikuchi, A., Yamato, M., Kanazawa, H. and Okano, T. (2008) 'Preparation of thermoresponsive polymer brush surfaces and their interaction with cells', *Biomaterials*, 29(13), pp.2073-2081. doi: 10.1016/j.biomaterials.2008.01.004.

Mortimer, J. (2004) 'Adhesive bonding of car body parts by industrial robot', *Industrial Robot: an International Journal*, 31(5), pp.423-428.

Naini, F.B. and Gill, D.S. Tooth fracture associated with debonding a metal orthodontic bracket: a case report, *World Journal of Orthopedics*, 9(3), pp.78-82.

Naughton, P., Röttger, J., and Bowser, B., 'A new approach to hybrid front-end systems', *SAE Technical Paper*. doi:10.4271/2002-01-1229.

Nishiyama, Y., Uto, N., Sato, C. and Sakurai, H. (2003) 'Dismantlement behaviour and strength of dismantlable adhesive including thermally expansive particles', *International Journal of Adhesion and Adhesives*, 23(5), pp.377-382. doi:10.1016/S0143-7496(03)00067-8.

Obeidat, W.M. (2009) 'Recent patents review in microencapsulation of pharmaceuticals using the emulsion solvent removal methods', *Recent Patents in Drug Delivery Formulation*, 3(3), pp.178-192.

Oliveuxa, G., Bailleula, J.L. and Salle, E.G. (2012) 'Chemical recycling of glass fibre reinforced composites using subcritical water', Applied Science and Manufacturing, 43(11), pp1809-1818. doi:10.1016/j.compositesa.2012.06.008

Oztoprak, M.O., Nalbantgil, D., Erdem, A.S., Tozlu, M. and Arun, T. (2010) Debonding of ceramic brackets by a new, American Journal of Orthodontics and Dentofacial Orthopedics, 138(2), pp.195-200.

Recktenwald, D. (2005) Advanced adhesives foster hybrid structures, Machine Design, 77(21), pp.124-126.

Rossetti, V.A., Palma, D.L., and Medici, F (2006) 'Production of aggregate from non-metallic automotive shredder residues', Journal Hazardous Materials, 137(2), pp.1089-1095.

Rowe, J. (2012) Advanced materials in automotive engineering, (2012), Elsevier.

Sanchis, R., Fenollar, O., García, D., Sánchez, L. and Balart, R. (2008) 'Improved adhesion of LDPE films to polyolefin foams for automotive industry using low-pressure plasma', *International Journal of Adhesion and Adhesives*, 28(8), pp.445-451. doi:10.1016/j.ijadhadh.2008.04.002

Santini, A., Morselli, L., Passarini, F., Vassura, I., Carlo, S.D. (2011) 'End-of-Life vehicles management: Italian material and energy recovery efficiency', Waste Management, 31(3), pp.489-494.

Schmid, A., Sutton, L.R., Armes, S.P., Bain, P.S. and Manfre, G. (2009) Synthesis and evaluation of polypyrrole-coated thermally-expandable microspheres: an improved approach to reversible adhesion, *Journal of Soft Matter*, 5, pp.407-412.

Seeliger, F. and Matyjaszewski, K. (2009) 'Temperature Effect on Activation Rate Constants in ATRP: New Mechanistic Insights into the Activation Process', *Macromolecules*, 42(16), pp.6050-6055. doi:10.1021/ma9010507.

Sethi, S., Ge, L., Ci, L., Ajayan, P.M. and Dhinojwala, A. (2008) 'Gecko-Inspired Carbon Nanotube-Based Self-Cleaning Adhesives', *Nano Letters*, 8(3), pp.822-825. doi:10.1021/nl0727765

Shah, R.R., Merreceyes, D., Husemann, M., Rees, I., Abbott, N.L., Hawker, C.J. and Hedrick, J.L. (2000) 'Using atom transfer radical polymerisaiton to amplify monolayers of initiators patterned by microcontact printing into polymer brushes for pattern transfer', *Macromolecules*, 33(2), pp.597-605.

Shakya, A.K. and Kumar, A. (2013) Recent developments in atom transfer radical polymerisation initiators for development of polymer-protein bioconjugates, *Journal of Bioscience and Biotechnology*, 2(1), pp.1-11.

Shen, Y., Tang, H. and Ding, S. (2004) Catalyst separation in atom transfer radical polymerization, Progress in Polymer Science, 29(10), pp.1053-1078. doi:10.1016/j.progpolymsci.2004.08.002.

Shiote, H., Sato, C. and Ohe, M. (2009) 'Effects of electrical treatment conditions on dismantlable properties of joints bonded with an electrically disbonding adhesive', *Journal of Adhesion Society of Japan*, 45(10), pp.376-381.

Smith, M., Jacobson, J., and Webb, B. (2004) 'Abandoned vehicles in England: impact of the end of life directive and new initiatives, on likely future trends', Resources, Conservative Recycling, 41, pp.177-189. doi:10.1016/j.resconrec.2003.10.001

Smith, B.C. (2011) Fundamentals of Fourier transform infrared spectroscopy, 2nd Ed. Taylor & Francis Group.

Solid waste and emergency response (2008) 'Recycling and reuse: end-of-life vehicles and producer responsibility', Available at: http://www.epa.gov/oswer/international/factsheets/200811_elv_directive.htm. (Accessed: 15 Feb 2013)

Tagliazucchia, M. and Szleifer, I. (2012) 'Stimuli-responsive polymers grafted to nanopores and other nano-curved surfaces: structure, chemical equilibrium and transport', *Soft Mater*, 8, pp.7292-7305. doi:10.1039/C2SM25777G.

Tanaka, K. and Matyjaszewski, K. (2008) 'Copolymerisation of (meth)acrylates with olefins using activators regenerated by electron transfer for atom transfer radical polymerisation (ARGET ATRP)', *MacromolecularSymposia*, 261(1), pp.1-9.

Tang, W. and Matyjaszewski, K. (2007) 'Effects of initiator structure on activation rate constants in ATRP', *Macromolecules*, 40(6), pp.1858-1863. doi: 10.1021/ma062897b.

Tetsuo, K. and Kohichiro, K. (2000) Heat debondable adhesive composition and adhesion structure, Patent Number WO 0040648.

Toncelli, C., Reus, D.C.D., Picchioni, F. and Broekhuis, A.A. (2012) 'Properties of reversible diels–alder furan/maleimide polymer networks as function of crosslink density', *Macromolecular Chemistry and Physics*, 213(2), pp.157-165. doi:10.1002/macp.201100405.

Tsarevsky, N.V. and Matyjaszewski, K. (2007) '"Green" atom transfer radical polymerization: from process design to preparation of well-defined environmentally friendly polymeric materials', *Chemical Reviews*, 107(6), pp.2270-2299. doi: 10.1021/cr050947p.

Tsuruoka, T., Namura, Y. and Shimizu, N. (2007) 'Development of an easy-debonding orthodontic adhesive using thermal heating', *Dental Materials Journal*, 26(1), pp.78-83.

Tunius, M. (2011) Switchable Adhesives. Patent Number US 2011/0224593 A1.

Vargün, E. and Usanmaz, A. (2005) 'Polymerization of 2-hydroxyethyl acrylate in bulk and solution by chemical initiator and by ATRP method', *Journal of Polymer Science Part A: Polymer Chemistry*, 43(17), pp.3957-3965.

Vasani, R.B., McInnes, S.J., Cole, M.A., Jani, A.M., Ellis, A.V. and Voelcker, N.H. (2011) 'Stimulus-responsiveness and drug release from porous silicon films ATRP-grafted with poly(N-isopropylacrylamide)', *Langmuir*, 27(12), pp.7843-7853. doi: 10.1021/la200551g.

Vasilash, G.S. (1997) The Lotus Elise -- a technological tour de force. Available at: http://www.autofieldguide.com/articles/the-lotus-elise-a-technological-tour-de-force. (Accessed: 10 Mar 2013)

Vermeulen, I., Caneghem, V., Block, C., Baeyens, J., and Vandecasteele, C. (2011) 'Automotive shredder residue (ASR): reviewing its production from end-of-life vehicles (ELV) and its recycling, energy or chemicals' valorisation', Journal of Hazardous Materials, 190(1-3), pp.8-27. doi:10.1016/j.jhazmat.2011.02.088.

Viganò, F., Consonni, S., Grosso, M., and Rigamonti, L. (2010) 'Material and energy recovery from Automotive Shredded Residues (ASR) via sequential gasification and combustion', Waste Management, 30(1), pp.145-153.

Wang, J. and Matyjaszewski, K. (1995) 'Controlled/"living" radical polymerization. atom transfer radical polymerization in the presence of transition-metal complexes', *Journal of the American Chemical Society*, 117(20), pp.5614-5615.

Wong, C.P. and Wu, J. (2002) Reworkable high temperature adhesives, Patent Number US 6380322.

Wijmans, C.M. and Zhulina, E.B. (1993) 'Polymer brushes at curved surfaces', *Macromolecules*, 26, pp.7214-7224.

Wu, T., Efimenko, K., Vlc, P., Sÿubr, V. and Genzer, J. (2003) 'Formation and Properties of Anchored Polymers with a Gradual variation of grafting densities on flat substrates', *Macromolecules*, 26(7), pp.2448-2453.

Xu, F.J., Zhao, J.P., Kang, E.T., Neoh, K.G. and Li, J. (2007) 'Functionalization of Nylon Membranes via Surface-Initiated Atom-Transfer Radical Polymerization', *Langmuir*, 23(16), pp.8585-8592. doi:10.1021/la7011342.

Yao, F., Fu, G.D., Zhao, J., Kang, E.T., Neoh, K.G. (2008) 'Antibacterial effect of surface-functionalized polypropylene hollow fibre membrane from surface-initiated atom transfer radical polymerization', *Journal of Membrane Science*, 319(1-2), pp.149-157. doi:10.1016/j.memsci.2008.03.049.

Yasuhiro, O. and Kensho, S. (1976) Adhesive bonding method allowing nondestructive separation of bonded materials, Patent Number US 3993524.

Yuan, S.J., Pehkonen, S.O., Ting, Y.P., Neoh, K.G. and Kang, E.T. (2009) 'Inorganic−Organic Hybrid Coatings on Stainless Steel by Layer-by-Layer Deposition and Surface-Initiated Atom-Transfer-Radical Polymerization for Combating Biocorrosion', *ACS Applied Materials and Interfaces*, 1(3), pp.640-652.

Zhao, Q. and Chen, M. (2011) 'A comparison of ELV recycling system in China and Japan and China's strategies', Resources, Conservative Recycling, 57, pp.15-21. doi:10.1016/j.resconrec.2011.09.010

Zheng, G. and Stover, H.D.H. (2003) 'Living/Controlled grafting from polymer microspheres', *Chinese Journal of Polymer Science*, 21(6), pp.639-651.

Zhu, B. (2012) Surface initiated polymerisation for applications in materials science. PhD Thesis. Loughborough Univerisity.

Zhu, B. and Edmondson, S. (2011) 'Polydopamine-melanin initiators for Surface-initiated ATRP', *Polymer*, 52(10), pp.2141-2149. doi:10.1016/j.polymer.2011.03.027

Zhulina, E.B. and Borisov, O.V. (1996) 'Polyelectrolytes Grafted to Curved Surfaces', *Macromolecules*, 29(7), pp.2618-2626. doi:10.1021/ma9515801.

Zoppi, C. and Lai, S. (2010) 'Assessment of the regional landscape plan of Sardinia (Italy): A participatory-action-research case study type', Land Use Policy, 27(3), pp. 690-705. doi:10.1016/j.landusepol.2009.09.004

Zorpas, A.A. and Inglezakis, V.J. (2012) 'Automotive industry challenges in meeting EU 2015 environmental standard', Technology in Society, 34(1), pp.55-83. doi:10.1016/j.techsoc.2011.12.006

Appendix

Expancel grades of TEMs

Specification

Product Specification for Expancel microspheres

Issue 2014.12 (replaces 2014.03)

AkzoNobel

Expancel DU

Expancel	Particle Size µm[1] D(0.5)	Thermomechanical Analysis[2] Tstart, °C	Tmax, °C	Density kg/m³	Solvent Resistance[3]
551 DU 40	10–16	94–99	141–149	≤ 17	3
461 DU 20	6–9	100–106	137–145	≤ 30	4
461 DU 40	9–15	98–104	142–150	≤ 20	4
051 DU 40	9–15	108–113	142–151	≤ 25	4
031 DU 40	10–16	80–95	120–135	≤ 12	3
053 DU 40	10–16	96–103	138–146	≤ 20	3
093 DU 120	28–38	120–130	188–203	≤ 6.5	5
909 DU 80	18–24	120–130	175–190	≤ 10	5
920 DU 40	10–16	123–133	168–178	≤ 17	5
920 DU 80	18–24	123–133	180–195	≤ 14	5
920 DU 120	28–38	122–132	194–206	≤ 14	5
930 DU 120	28–38	122–132	191–204	≤ 6,5	5
950 DU 80	18–24	138–148	188–200	≤ 12	5
951 DU 120	28–38	133–143	190–205	≤ 9	5
980 DU 120	25–40	158–173	215–235	≤ 14	5
New product					
920 DU 20	5–9	120–145	155–175	≤ 25	5

Expancel DU = Dry Unexpanded Expancel microspheres

Delivered in fibre drums, net weight 50 kg or in big-bags 500 kg

Use the product within three years after production date, if unopened.

Not all grades available in all locations. Check local sales office for availability.

(1) "Particle size of Expancel Microspheres"
(2) "Thermomechanical analysis of Expancel MS"
(3) "Chemical resistance of Expancel MS"

Expancel
The art of microspheres

Expancel 930 DU 120

SECTION 3: COMPOSITION/INFORMATION ON INGREDIENTS

3.2 Mixtures

Hazardous substance

Chemical Name	PBT vPvB OEL	CAS-No. EC-No. REACH No.	Classification (REGULATION (EC) No 1272/2008)	Classification (67/548/EEC)	Concentration [%]
2,2,4-Trimethylpentane		540-84-1 208-759-1	Flam. Liq. 2; H225 Asp. Tox. 1; H304 Skin Irrit. 2; H315 STOT SE 3; H336 Aquatic Acute 1; H400 Aquatic Chronic 1; H410 M-Factor (Acute): 1	F; R11 Xn; R65 Xi; R38 R67 N; R50-R53	15 - 20
isobutane		75-28-5 200-857-2	Flam. Gas 1; H220 Press. Gas H280	F+; R12	5 - 10

For the full text of the H-Statements mentioned in this Section, see Section 16.

For the full text of the R-phrases mentioned in this Section, see Section 16.

Candidate List of Substances of Very High Concern for Authorisation

Candidate List of Substances of Very High Concern for Authorisation : This product does not contain substances of very high concern (Regulation (EC) No 1907/2006 (REACH), Article 57).

Non-hazardous substance

Chemical Name	CAS-No. EC-No. REACH No.	Concentration [%]
Copolymer	38742-70-0	60 - 100
Magnesium hydroxide	1309-42-8 215-170-3	0 - 20

SECTION 4: FIRST AID MEASURES

4.1 Description of first aid measures

General advice : No hazards which require special first aid measures.

If inhaled : Remove to fresh air.
Keep patient warm and at rest.
Rinse nose and mouth with water.

Expancel 930 DU 120

In case of skin contact	:	Take off contaminated clothing and shoes immediately. Wash the skin immediately with soap and water.
In case of eye contact	:	Rinse with plenty of water. Remove contact lenses. Protect unharmed eye. Keep eye wide open while rinsing. If eye irritation persists, consult a specialist.
If swallowed	:	Clean mouth with water and drink afterwards plenty of water. Never give anything by mouth to an unconscious person. If symptoms persist, call a physician.

4.2 Most important symptoms and effects, both acute and delayed

Symptoms	:	No information available.
Risks	:	No information available.

4.3 Indication of any immediate medical attention and special treatment needed

Treatment	:	No information available.

SECTION 5: FIREFIGHTING MEASURES

5.1 Extinguishing media

Suitable extinguishing media	:	Water spray Foam

5.2 Special hazards arising from the substance or mixture

Specific hazards during firefighting / Specific hazards arising from the chemical	:	Do not allow run-off from fire fighting to enter drains or water courses. Risks of ignition followed by flame propagation or secondary explosions shall be prevented by avoiding accumulation of dust, e.g. on floors and ledges.

5.3 Advice for firefighters

Special protective equipment for firefighters	:	In the event of fire, wear self-contained breathing apparatus.
Further information	:	Collect contaminated fire extinguishing water separately. This must not be discharged into drains. Fire residues and contaminated fire extinguishing water must be disposed of in accordance with local regulations.

SECTION 6: ACCIDENTAL RELEASE MEASURES

6.1 Personal precautions, protective equipment and emergency procedures

Personal precautions	:	Avoid dust formation.

6.2 Environmental precautions

Environmental precautions	:	Do not flush into surface water or sanitary sewer system. If the product contaminates rivers and lakes or drains inform respective authorities.

Expancel 930 DU 120

6.3 Methods and materials for containment and cleaning up

Methods for cleaning up / Methods for containment	:	Pick up and arrange disposal without creating dust. Keep in suitable, closed containers for disposal.

6.4 Reference to other sections

Additional advice	:	For personal protection see section 8.

SECTION 7: HANDLING AND STORAGE

7.1 Precautions for safe handling

Advice on safe handling	:	For personal protection see section 8. Open container in a well ventilated area. Allow enough time to permit escape of harmful and flammable vapours before emptying. Maintain adequate ventilation when preparing mixtures and during the expansion process. The release of blowing agent is increased during expansion. Avoid creating dust. Keep away from heat/sparks/open flames/hot surfaces. - No smoking. Dispose of rinse water in accordance with local and national regulations.
Advice on protection against fire and explosion	:	Provide appropriate exhaust ventilation at places where dust is formed. No sparking tools should be used.
Dust explosion class	:	St2

7.2 Conditions for safe storage, including any incompatibilities

Requirements for storage areas and containers	:	Store at room temperature in the original container. Keep container tightly closed in a dry and well-ventilated place.
Maximum storage temperature:	:	50 °C
Other data	:	No decomposition if stored and applied as directed.

7.3 Specific end use(s)

Specific use(s)	:	No information available.

SECTION 8: EXPOSURE CONTROLS/PERSONAL PROTECTION

8.1 Control parameters

Components with workplace control parameters

Components	CAS-No.	Value	Control parameters	Update	Basis	Form of exposure
Dust		TWA	4 mg/m3	1997-01-01	GB EH40	Total dust

SEKISUI

Thermoexpandable Microspheres

ADVANCELL® EM

● Outline of product

Expansion mechanism

ADVANCELL EM are tiny thermo-expandable microspheres, containing a low boiling point liquid hydrocarbon inside a thermoplastic polymer shell.

When heated, ADVANCELL EM microspheres expand greatly in size; the heat softens the thermoplastic shell while the hydrocarbon boils and expands the shell.

The expanded micro-balloons form a uniform, closed-cell structure. The expansion start temperature and the cell size, etc. can be optimized by selecting appropriate grade.

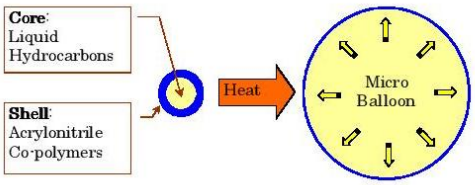

	Before expansion	After expansion
Avg. Diameter	15 - 40mm	40 - 150mm
Density	1.00 - 1.20g/cm3	0.02 - 0.04g/cm3

● Application / Process

Uses of ADVANCELL EM

ADVANCELL EM can be used as blowing agents for ink and paints.

Wallpaper, Structural foam, etc,
Various foams (Acrylic, PVC, Epoxy, Rubber, Silicon, etc.)

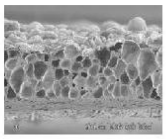

Wall paper
(Cross section)

Applicable process

ADVANCELL EM can be used in extrusion and injection molding as well as other forming methods.

- Extrusion molding
- Injection molding
- Coating
- Press molding
- Blow molding

Example <Injection molding>

● Test condition
Quantity: 1.5wt% (weight of particle)
Resin: PP
Process: Core back molding
*added as MB
(particle density:50%)

● Result
Expansion ratio: 150% (thickness)
Weight saving: 30% off
Surface : Flat and fine

	No expansion	Expansion
Cross section		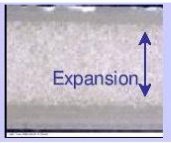
Density	0.91g/cm3	0.61g/cm3

● Benefits
- Weight saving
- Reduction of resin
- Uniform cell
- High foaming
- Flat surface

● Comparison with chemical blowing agent

When expanding, ADVANCELL EM becomes a very low density hollow micro-balloon, with the following characteristics:

- Fine, uniform, closed-cell structure
- Expandable even in low-viscosity compositions
- No surface pinholes
- Cell size can be controlled by selecting the appropriate grade.

	Cross section	Surface
ADVANCELL ・Fine expanded cells ・Closed-cell structure		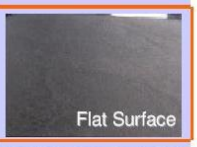
CBA ・Large expanded cells ・Open-cell structure ・Surface pinholes		

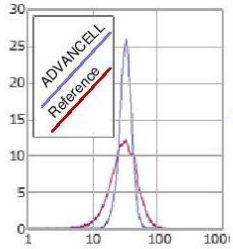

ADVANCELL
Sharp particle size distribution results in uniform expansion.
・Uniform cell structure
・Better expansion efficiency
・Uniform expansion allows consistent physical properties
・Easier to control expansion start temperature

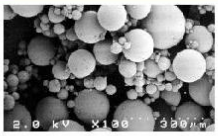

Reference
Wide spread of particle sizes results in uneven foam structure.
・Foams with non-uniform cells
・Expansion loss caused by unexpanded particles
・Difficult to control expansion start temperature

● Physical properties

Grade

Code	Diameter	Start of Exp.	Max of Exp.	TMA-density	Application
EML101	14-20μm	120-130℃	160-170℃	＜21	Wallpaper, leather, expandable ink, etc
EMH204	38-44μm	115-125℃	165-175℃	＜12	
EHM301	22-28μm	130-140℃	160-170℃	＜18	
EHM302	18-24μm	130-140℃	160-170℃	＜23	Wallpaper, gloss reduction additives, Molding additives, etc
EHM303	26-34μm	130-140℃	160-170℃	＜16	
EM304	23-29μm	135-145℃	170-185℃	＜20	
EHM401	26-34μm	140-150℃	180-190℃	＜11	

	Code	Diameter	Start of Exp.	Max of Exp.	TMA-density	Molding temp.
Powder	EHM401	26-34μm	140-150℃	180-190℃	＜11	160-190℃
	EM403	26-34μm	150-170℃	200-220℃	＜7	180-210℃
	EM501	22-28μm	160-180℃	210-230℃	＜14	190-220℃
Masterbatch	P403M1	26-34μm	150-170℃	200-220℃		180-210℃
	P501M1	22-28μm	160-180℃	210-230℃		190-220℃
	P501E1	22-28μm	160-180℃	210-230℃		190-220℃

Expansion *

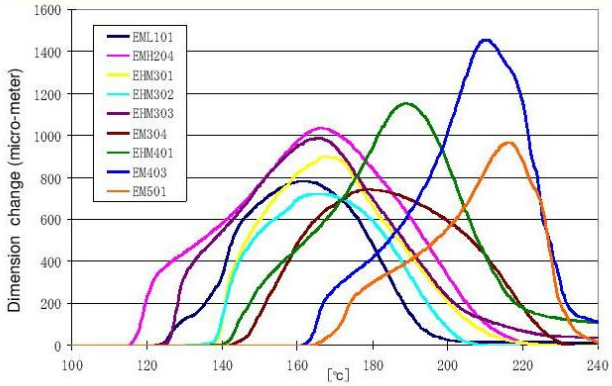

[Condition]
Method: TMA
Loading: 0.1N
Ramp rate: 5℃/min from 80 to 220℃

*Expansion tested using dry microspheres in air only. Actual expansion properties depend on the composition and processing parameters

● Sekisui Chemical GmbH – Cantadorstr. 3
D-40211 Düsseldorf Phone: +49 211 36977-0
info@advancell.info

● SEKISUI CHEMICAL CO., LTD
High Performance Plastics Company Functional Resins Sales Branc
Tel. 03-5521-0672 Fax. 03-5521-0673 HP : http://www.sekisui.co.jp/cs

MATERIAL SAFETY DATA SHEET TOKUYAMA SEKISUI Co., Ltd.

ISSUE DATE: 2011/10/1

1. CHEMICAL PRODUCT & COMPANY IDENTIFICATION

- PRODUCT NAME: ADVANCELL EM501
- NAME OF MANUFACTURER: TOKUYAMA SEKISUI Co., Ltd.
- ADDRESS: Kaisei-cho4560,Shu-nan city,Yamaguchi 746-0006 Japan
- TELEPHONE No.: +81-(0)834-63-0188
- FAX No.: +81-(0)834-64-2081
- EMERGENCY TELEPHONE No.:+81-(0)834-63-0192
  Technical Section
  Polymer Production Dept.
  TOKUYAMA SEKISUI CO., LTD.

2. COMPOSITION/INFORMATION ON INGREDIENTS

- DISTINCTION OF MONOMERIC PRODUCT OR MIXED SUBSTANCE:
  Mixed product
- CHEMICAL NAME:
  Thermal expansion microcapsule

  Acrylonitrile Methacrylonitrile copolymer (encapsulating agent)
  Hydrocarbon (blowing agent)
- COMPOSITION AND CONTENT:
  Encapsulating agent : > 70 wt %
  Blowing agent : 10 - 30 wt %
  Residual monomer :
  Acrylonitrile (cas.107-13-1) – < 0.05 wt %
  Methacrylonitrile (cas.126-98-7) – < 0.3 wt %

3. HAZARDS IDENTIFICATION

- HAZARDS: Has possibility of dust explosion. When stored in closed containers, a flammable atmosphere within the containers develops.
- HAZARDOUSNESS TO HUMAN BODY: There is no data of hazardousness of the polymer, but acrylonitrile, one of the residual monomers, is readily absorbed in the body when the vapor is inhaled or comes into contact with the skin or the liquid is ingested, and develops acute toxicity. Further, methacrylonitrile is high in cutaneous absorbency and is toxic. When stored in closed containers, the concentration of residual monomer in the vapor phase may reach such a level that inhalation is harmful.

1.Matsumoto Microsphere®F and FN Series(unexpanded) Characteristics of grades

	Average particle size (μm)	Shell polymer	Tstart (DC)	Tmax (DC)	Solvent resistance
Chlorinated Grades					
Low-temperature-expansive products					
F-30	10-18	VCl_2 -AN copolymer	70-80	110-120	☆
Chlorine-free Grades					
Low-temperature-expansive products					
F-36	10-16	AN copolymer	70-80	110-120	☆
F-36LV	13-19	AN copolymer	75-85	110-120	☆
F-48※1	9-15	AN copolymer	90-100	125-135	☆☆
FN-80GS※1	6-10	AN copolymer	100-110	125-135	☆☆
F-50※1	10-18	AN copolymer	95-105	125-135	☆☆
Medium-temperature-expansive products					
F-65※1	12-18	AN copolymer	105-115	145-155	☆☆
FN-100SS	6-11	AN copolymer	120-130	145-155	☆☆☆☆☆
FN-100S	10-20	AN copolymer	125-135	150-160	☆☆☆☆☆
F-100M	17-23	AN copolymer	115-125	155-165	☆☆☆
High-temperature-expansive products					
FN-100M	20-30	AN copolymer	125-135	165-180	☆☆☆☆☆
FN-100	25-35	AN copolymer	120-135	170-180	☆☆☆☆
FN-105	35-45	AN copolymer	120-135	175-185	☆☆☆
FN-180SS	15-25	AN copolymer	135-150	165-180	☆☆☆
FN-180S	25-35	AN copolymer	145-155	175-185	☆☆☆
FN-180	35-45	AN copolymer	140-155	175-185	☆☆☆
Extremely high-temperature-expansive products					
F-190D※2	30-40	AN copolymer	160-170	210-220	☆☆☆
F-230D※2 (trial product)	20-35	AN copolymer	180-190	220-240	☆☆☆
F-260D※2	20-35	AN copolymer	190-200	250-260	☆☆☆
F-2800D※2	20-35	AN copolymer	200-210	255-270	☆☆☆☆
F-2830D※2 (trial product)	20-35	AN copolymer	220-230	260-275	☆☆☆☆

F-2860D※2 (trial product)	20-35	AN copolymer	250-260	270-285	☆☆☆☆

Dry types excluded, the products contain about 70 % of solid. Dry type products containing 95 % or more of solid are also available being identified with the final letter "D" of their name.

※1 Types of low content of ionic substances

※2 Dry type or Master Batch products are available.

Solvent resistance scale： Higher number of ☆ means better resistance to solvent.

Tstart, Tmax: TMA (Thermo Mechanical Analysis) value

2.Expandability of Matsumoto Microsphere®F and FN (unexpanded)

The expansion curves in an EVA binder shown below represent one of basic performances of microcapsules. The tested microcapsules and EVA were blended in 1 to 9 ratio based on the weight of solid content. The mixture was heated for 2 minutes at each temperature level.

< Low-temperature-expansive products >

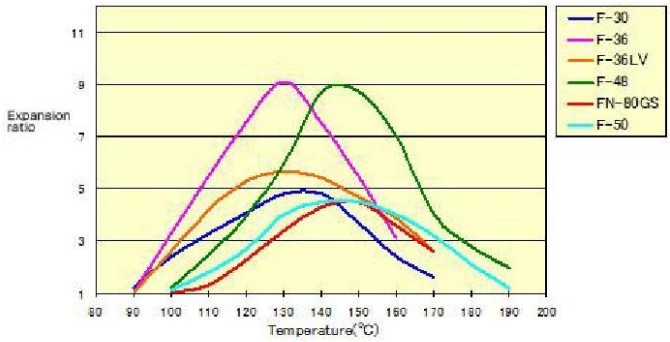

< Medium- and High- temperature-expansive products >

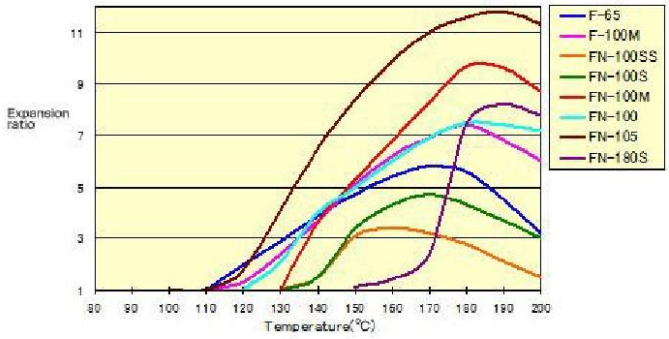

< Extremely high-temperature-expansive products >

Expansion behavior of extremely high-temperature products （By TMA with gradual increase of temperature at the rate of 10 degrees Celsius /min ）

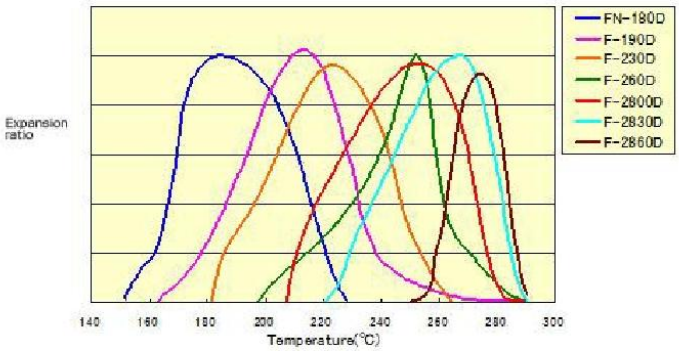

*The data refer to thermo expandable microcapsule expanded alone and not mixed with resin. Therefore, when in actual use with resins, the thermo-expansion behavior may be different.

3.Expanded Microcapusule; Plastic microballoon

Matsumoto Microsphere® F-E (Expanded Wet powder)

	Average particle size(μm)	Shell polymer	Specific gravity	Solid Content(%)	Solvent resistance
F-30E	30-60	VCl_2-AN copolymer	0.025±0.005	9-13	☆
F-50E	40-60	AN copolymer	0.030±0.010	11-16	☆☆
F-65E	40-60	AN copolymer	0.025±0.005	9-13	☆☆

Matsumoto Microsphere ®F-DE (Expanded Wet powder)

	Average particle size(μm)	Shell polymer	Specific gravity	Solid Content(%)	Solvent resistance
FN-80SDE	20-40	AN copolymer	0.025±0.005	97%min.	☆☆
F-65DE	40-60	AN copolymer	0.030±0.005	97%min.	☆☆
F-80DE	90-130	AN copolymer	0.020±0.005	97%min.	☆☆☆

Aerospace Technical Data Sheet

3M™ Scotch-Weld™ EC-9323 B/A Two Part Structural Adhesive
https://multimedia.3m.com/mws/media/820936O/3m-scotch-weld-ec-9323-2-b-a.pdf

Automotive and Aerospace Solutions DivisionEuropean Aerospace Laboratorywww.3m.eu/aerospaceReference: 224

Copyrighted material removed from electronic version